

UiT

THE ARCTIC  
UNIVERSITY  
OF NORWAY

Department of Geology

# The occurrence of flow transformations within sandy submarine fans:

*A case study from the Eocene on Spitsbergen*

—  
**Elliot Alessandro Broze**

*Master thesis in Sedimentary Geology ... May 2017*





## **Abstract**

The Van Keulenfjorden transect on Spitsbergen offers valuable insight into submarine processes, with well exposed seismic scale clinoforms of Paleocene and Eocene age, which show the distribution of sediments from deltaic to basin floor environments. Several progradational submarine fans are preserved as cliffs on Hyrnestabben. They serve as an analogues to coarse grained submarine fans in provinces of the Barents Sea margin. The architecture of submarine fan bodies is of importance to petroleum exploration, as the distribution of sand prone lobes impact fluid migration reservoir compartmentalization, and the presence or absence of baffles. Gravity flow processes emplace different deposits affecting deep sea fans that change according to both allogenic and autogenic factors, at scales below the limits of seismic detection.

Detailed sedimentological and stratigraphic study was conducted on three shelf proximal submarine fans, of the Frysjaodden Formation, to record and characterize flow transformations as they occur in the deep sea environment. The fans had similar overall stacking patterns, with thin bedded heterolithic deposits overlain by thick sandy amalgamated lobes. The progradational sandy submarine fans were exposed in an area less than 3km in length, and contained deposits from hybrid flows, turbulent gravity flows, and debris flows. Evidence for flow transformations occurred as linked debrites both proximal to the slope and in distal locations, the result of abrupt slope changes and down flow changes flow process. The occurrence of sandy lobes, heterolithic sheets, and mixed debrites did not follow a well-defined systems tract, rather they were interbedded, expressions of local lateral changes in topography and sediment supply.

**Keywords:** Frysjaodden Formation, linked debrites, flow transformations, submarine fans, Spitsbergen

## **Acknowledgments**

The list of those who deserve acknowledgement for their support throughout this process, is too long to be included its entirety. The present study was conducted as part of the ARCex project (Research Centre for Arctic Petroleum Exploration) funded by the Research Council of Norway (grant number (228107), without whose support none of this would be possible. Sten-Andreas Grundvåg, whose guidance throughout the thesis process is apparent in the finished product, deserves all the thanks in the world. Thank you also to the external sensor Michal Janocko. The unbelievable inspiration in the writing process provided by the music of Beyoncé cannot be understated. Also invaluable were the University Centre in Svalbard (UNIS) who provided logistical support, and Governor of Svalbard for providing helicopter support. A big thank you to the field help and bear watch, Joel Schiffer and Cal Bachell. Thanks Dad.

**Elliot Broze**

**Tromsø, May 2017**

## Contents

1. Introduction .....	1
1.1 The influence of submarine gravity flows in marine sediment deposition .....	1
1.2 Objectives .....	3
1.3 Terminology .....	4
2. Geological Setting.....	7
2.1 Tectonic Framework.....	7
2.1.1 Tectonic setting .....	7
2.1.2. The west Spitsbergen fold-and-thrust belt (WSFTB).....	8
2.1.3. The Central Tertiary Basin (CTB).....	11
2.2 Lithostratigraphy of the Central Tertiary Basin: .....	13
2.2.1. Paleocene Lithostratigraphy .....	15
2.2.2. Eocene Lithostratigraphy: .....	16
2.2.3. Eocene climate .....	20
2.3 The Van Keulenfjorden transect.....	22
2.3.1 Clinoformal Trends within The Battfjellet Formation and association with the Frysjaodden Formation:.....	23
2.3.2. Shelf Edge Deltas.....	27
2.3.3. Slope segments .....	27
2.4. Basin Floor Fans:.....	28
3. Methods .....	31
3.1 Study area - Clinoform 14 and 15:.....	31
3.2 Sedimentary Logging .....	33
4. Results .....	37
4.1. Bed Types .....	37
4.1.1. Bed Type 1 (BT 1):.....	44
4.1.2. Bed Type 2 (BT 2):.....	44
4.1.3. Bed Type 3 (BT 3):.....	45
4.1.4. Bed Type 4 (BT 4):.....	46
4.1.5. Bed Type 5 (BT 5):.....	47
4.1.6. Bed Type 6 (BT 6):.....	48
4.1.7. Bed Type 7 (BT 7):.....	49
4.1.8. Bed Type 8 (BT 8):.....	50

4.1.9. Bed Type 9 (BT 9):.....	51
4.1.10. Bed Type 10 (BT 10):.....	52
4.1.11. Bed Type 11 (BT 11):.....	53
4.1.12. Bed Type 12 (BT 12):.....	54
4.1.13. Bed Type 13 (BT 13):.....	57
4.1.14. Bed Type 14 (BT 14):.....	58
4.1.15. Bed Type 15 (BT 15):.....	59
4.1.16. Bed Type 16 (BT 16):.....	61
4.1.17. Bed Type 17 (BT 17):.....	62
4.1.18. Bed Type 18 (BT 18):.....	63
4.2 Facies Associations.....	64
4.2.1. FA1- Background Basinal .....	65
4.2.2 FA2- Lobe Fringe Deposits.....	65
4.2.3 FA 3 - Off axis Lobe Deposits- .....	66
4.2.4. FA4 On axis lobe deposits- .....	67
4.2.5. FA5-Channel deposits:.....	69
4.3 Depositional Architecture .....	71
4.3.1 Lobe stacking pattern of C12:.....	82
4.3.2. Lobe Stacking Pattern of C14a:.....	83
4.3.3 Lobe stacking pattern of C14b: .....	84
4.3.4. Lobe Stacking Pattern of C15: .....	86
4.3.5. Comparison of the lobes C12, C14a, C14b, and C15: .....	87
5. Discussion .....	91
5.1. Origin of Bed Types.....	91
5.1.1. Deposits emplaced by surge type turbidites.....	91
5.1.2. Deposits deposited by sustained flows or hyperpycnites .....	92
5.1.3. Beds deposited by Debris Flows and Slumps:.....	94
5.1.4. Beds deposited by Hybrid Flows.....	95
5.2 Depositional elements in Sand Rich submarine fans.....	98
5.2.1. Lateral and Frontal Splays .....	100
5.2.2. Distributary Channels .....	101
5.3. Controls on Submarine fans and Lobe Hierarchy: .....	101
5.3.1. Fan Trends .....	103

5.4. Occurrences of and mechanisms for linked debrites in the study area.....	105
5.5. Importance of hyperpycnal flows in the study area:.....	108
5.6 Offshore analogues.....	111
6. Conclusions: .....	115
7. References.....	117
8. Appendix .....	125



# 1. Introduction

## 1.1 The influence of submarine gravity flows in marine sediment deposition

Submarine gravity flows are the primary means for continent derived sediment to reach the deep ocean, and exist on a continuum of sediment concentrations with a mixture of fluid support processes (Shanmugam, 2000). One type of submarine gravity flow, termed turbidity currents are generally characterized by low sediment concentrations and turbulent flow. Sediment concentration, and type, within submarine gravity flows effect the flow characteristics and their resulting deposits. Turbidity currents in which fluid turbulence dominates transport (Lowe, 1982) have sediment concentrations between 1% and 23% (Shanmugam, 2000). Fluidized flows and liquefied flows transport sediment primarily by hindering particle settling (Lowe, 1982). These types of flows, sometimes referred to as high density turbidity currents can consist of 6 to 44% sediment (Shanmugam, 2000). Resulting deposits, are referred to as turbidites, and have received a considerable amount of attention in literature (Keunen and Migliorini, 1950; Bouma, 1962; Normark, 1970; Middleton and Hampton, 1973; Mutti and Ricci-Lucchi, 1978; Lowe, 1982). Turbidity currents occurring in the deep ocean are difficult to monitor and investigate, thus their exhumed deposits offer us an opportunity to investigate flow processes. Turbidites accumulate into thick sand-rich submarine fan successions with reservoir potential in many prolific sedimentary basins. Depending on the dominant depositional process, turbidites beds may exhibit dramatically different porosity and permeability, with implications on reservoir potential. Large sand-rich lobes serve as

excellent hydrocarbon reservoirs, whereas muddy intervals can act as migration barriers. The internal architecture and characteristics of single turbidite beds within submarine fans are difficult to study using commercial seismic techniques. Sediment core data provide detailed facies information at bed-scale, but wells are expensive to drill and commonly lateral correlation is hampered by the lack of well coverage. The facies architecture is vital to understand both reservoir prediction and increased production. The facies distribution and architecture of submarine fans effecting fluid migration, reservoir compartmentalization, and the occurrence of flow barriers and baffles is strongly determined by the presence of fine-grained, mud-rich intervals (Hodgson, 2009; Prélat et al. 2009). Therefore, outcrop studies of exhumed submarine fans are important for establishing dominant processes acting on submarine gravity flows in those environments, as well as mapping detailed changes within flows. Outcrops which offer walkable bed boundaries add much more detail to the picture of deep sea fans than cores and seismic studies alone. The character of bed boundaries are readily traceable and the lateral changes in sediment distribution within fans, is well exposed.

Some recent work on sediment gravity flows has focused on the conditions for hybrid flow events, which display a range of flow rheologies within a single flow event (Kneller and Buckee, 2000; Baas and Best, 2002; Haughton et al., 2003; Johannessen and Steel, 2005; Amy et al., 2006; Talling et al., 2007; Barker et al., 2008; Haughton et al., 2009; Jackson et al., 2009). Hybrid flows with intermediate sand to clay content (Barker et al., 2008) and unsteady flow density result in bipartite beds, termed co-genetic turbidites and debrites. The upper of these two beds is termed a linked debrite (Jackson et al., 2009).

Linked debrites are noted to have down-slope wedged architecture, in which the finer grained cohesive upper flow portion thickens distally, while the lower, cleaner, sandy partition thins away from the flow source. (Haughton et al., 2003; Amy and Talling, 2007; Ito, 2008; Davies et al., 2009; Hodgson, 2009). There is variation throughout deposits due, in part, to hydraulic jumps, local topography, and confinement; but the mechanisms for emplacing linked debrites are potentially multitudinous and very much under debate still (Amy and Talling, 2006; Haughton et al., 2009; Jackson et al., 2009). Allogenic changes in a fan system can result in an overall reduction of coarse-grained sediment flux into a basin, and potentially result in sandy lobes being separated by discreet muddy units (Prélat et al., 2010). Longitudinal increases in fine grained sediments from slope changes or sediment filtering through sediment gravity processes (Prélat et al., 2010), differences in erosive potential (Zavala et al., 2006; Haughton et al., 2009) as well as cyclic stepping of sub and super critical flow (Postma and Cartigny, 2014) along submarine gravity flows as they develop, can have additional impacts on sediment distribution within submarine fans. Change in flow energy effect flow efficiency, with drops in energy preferentially depositing coarser grains, and increased energies having more erosive potential (Kneller, 1996). The increase in the fine grained portion within co-genetic turbidite beds reduce the reservoir potential of distal or off axis fan deposits.

## 1.2 Objectives

The Central Tertiary Basin (CTB) on Spitsbergen, the largest island in the Svalbard Archipelago, Arctic Norway, represents an exhumed, small (70 x 30 km) foreland basin

(Spencer et al., 1984) that formed in response to seafloor spreading in the Norwegian Greenland Sea, in the Paleocene.(Müller and Spielhagen, 1990) Sediments remaining within the CTB span the Paleocene and Eocene (Steel et al., 1985; Müller and Spielhagen, 1990) and represent basinal to continental depositional environments (Steel et al., 1985; Helland-Hansen, 1992). It offers unparalleled insights into the sediment distribution and regional history of the Barents Sea, an area of economic interest. Svalbard represent the uplifted and exposed NW corner of the Barents Shelf and offers a window into the subsurface regional geology at a level of detail not possible to achieve by seismic studies alone. Complete shelf clinoforms outcrop along Van Kuelenfjorden (Helland-Hansen, 1992), with linked deep sea fans (Steel and Olsen, 2002) Detailed outcrop studies of sand rich beds in the Eocene submarine fan succession in the CTB offer insight into the conditions which lead to flow transformations and the deposition of linked debrites in small fans.

### 1.3 Terminology

The study was conducted on the submarine fans corresponding to clinoforms 12, 14, and 15 (*sensu* Steel and Olsen, 2002; Johannessen and Steel, 2005). The term submarine fan is used to describe the thick sandy accumulations occurring distally to the shelf break as the term basin floor fan which others have used (Crabaugh and Steel, 2004) implies sediment delivered by sediment gravity flows during low stand conditions. The submarine fans outcropping on Hyrnestabben are referred to as C12, C14a, C14b, and C15. C12, corresponds to the ‘green’ fan body of Crabaugh and Steel (2004). The submarine fan of clinoform 14, is composed of two fans, the lower C14a corresponds to

the 'orange' fan body (Crabaugh and Steel, 2004), and upper C14b ('yellow' from Crabaugh and Steel, 2004). C15, corresponds to the "pink" fan body from Crabaugh and Steel (2004). The submarine fan lobes are built internally of individual packages of sediment, beds, which represent single flow events. Successive flow events form lobe elements (Prélat et al., 2009) genetically linked beds are termed bed-types. Bed types are separated into Facies Associations, which are defined by their position along a grouped assemblage of lobe elements termed composite lobes (*sensu* Deptuck et al., 2008). Bed assemblages are groupings of bed-types indicative of process. Processes that are commonly referred to be: turbidites, depletive sediment flows primarily acted upon by turbulent flow processes; hybrid flows displaying intermediate rheological characteristics, and debris flows which are dominated by grain on grain interactions and display plastic behavior. Bi-partite beds result from flows which underwent mixed flow processes depositing beds with turbidite basal members and debris flow deposit upper members (Jackson et al., 2009)



## 2. Geological Setting

### 2.1 Tectonic Framework

#### 2.1.1 Tectonic setting

The Svalbard archipelago represents an uplifted and exposed corner of the Barents Shelf and has undergone multiple tectonic phases since pre-Cambrian times (Faleide et al., 1984; Nøttvedt, 1985; Blythe and Kleinspehn, 1998, Piepjohn et al., 2016). Major structural lineaments; the Lomfjorden/Agardbukta, Billefjorden, Inner Hornsund and Paleo-Hornsund fault zones have seen persistent structural movement since pre-Caledonian times (Faleide et al., 1984, Steel and Worsley, 1984; Nøttvedt, 1985). The western margin of Spitsbergen, is dominated by the West-Spitsbergen Fold and Thrust Belt (WSFTB), a 300km long and less than 50 km wide feature (Steel et al., 1985) which developed in Paleogene times (Steel and Worsley, 1984).

Large scale Cretaceous continental break-up was driven regionally by the northward propagation of the Atlantic spreading ridge (Talwani and Eldholm, 1977, Faleide et al., 1984) that separated Svalbard from Laurasia (Blythe and Kleinspehn, 1998). The Paleogene structural setting of Svalbard was strongly influenced by the Eureka Orogeny with the movement of Greenland relative to Svalbard (Piepjohn et al., 2016), and resulting formation of the WSFTB (Steel et al., 1985; Braathen and Bergh, 1995; Blythe and Kleinspehn, 1998). Counterclockwise rotation of Greenland in conjunction with clockwise rotation of Svalbard and the Eurasian plate initiated during the Late Cretaceous (Steel et al., 1985; Lundin and Doré, 2002 ) in response to spreading in the Labrador and Norwegian Greenland seas (Johannessen et al. 2011). There were two distinct phases of tectonic development; the first began around 58 Ma (Eldholm et al., 1984) when

Greenland moved north-northwesterly and the second commenced 37 Ma, when plate movement shifted to be west-north westerly. The tectonic regime off Svalbard evolved from several phases of rifting, as sea floor spreading progressed northward (Steel et al., 1985). The isochronous tectonic action resulted in compressional and strike-slip tectonics, which Piepjohn et al. (2016) suggest occurred between 53 – 34 Ma.

The western Barents Shelf margin runs roughly 1000 km to the NNW, and is comprised into three distinct segments: a sheared margin along the Senja Fracture Zone in the south, a central volcanic rift segment, and a sheared and rifted margin along the Hornsund Fault Zone in the north (Ryseth et al., 2003). For the focus of this study, only the northern section of this system is important, the subsequent section summarizes Paleogene tectonic history, and the most important structural elements that influenced the Central Tertiary Basin (CTB).

#### 2.1.2. The west Spitsbergen fold-and-thrust belt (WSFTB)

In Svalbard, the Caledonian basement, as well as the Devonian to Late Paleozoic and Mesozoic platform succession were affected by the Eurekan deformation, which occurred from the Late Cretaceous through the Eocene (Braathen and Bergh, 1995; Piepjohn et al. 2016). The opening of a rift between North America and Greenland initiated in the Late Cretaceous approximately 100 Ma (Srivastava, 1978). Some onshore rift related magmatic activity is associated with this event between 124.7 Ma and 123.3 Ma (Steel and Worsley, 1984; Piepjohn et al., 2016). At the same time rifting, without evidence of seafloor spreading, occurred in the Norwegian and Greenland Seas (Srivastava, 1978).

The Eurekan Orogeny began in earnest between 53 Ma and 47 Ma (Eldholm et al., 1984; Steel et al., 1985; Piepjohn et al., 2016) in concert with the onset of seafloor spreading in Baffin-Bay, the sinistral Wegner fault zone, and Norwegian-Greenland seas (Steel and Woorsley, 1984; Steel et al., 1985;), with the dextral De Greer fracture zone. Greenland was moving north east as a separate plate from the North American plate, while undergoing counter clockwise rotation (Steel et al., 1985; Lundin and Doré, 2002; Johannessen et al., 2011). The plate movements resulted in the transpression of the West Spitsbergen fold and thrust belt (Kellogg, 1975; Myhre et al., 1982). Three main phases of tectonism occurred during the opening of the Greenland-Norwegian Sea (Vagnes, 1987; Eldholm et al., 1987; Bergh et al., 2011). First a continent-continent transform zone in the early Eocene (Steel and Woorsley, 1984); then an ocean continent transform margin while the Mid-Atlantic ridge propagated northward (Eldholm et al., 1984). Finally the passive margin regime that lacks in large-scale shear developed (Braathen and Bergh, 1995), and persisted since the early Oligocene (Steel and Woorsley, 1984; Piepjohn et al., 2016).

A tectonic regime shift is also associated with the change in transport direction noted in Paleogene sedimentary rocks of the CTB (Braathen and Bergh, 1995). Around 47 Ma Greenland began drifting more northwest, perhaps due to the northward migration of the Mid-Atlantic Rift (Vagnes, 1997). This change initiated the second, dextral transpressional, tectonic stage of the Eurekan Orogeny in the WSFTB. The second stage

occurred as the gradual transition from oblique convergence to oblique divergence (Piepjohn et al., 2016).

Shallowing took place in the Paleocene to middle Eocene and is evident through sedimentary analysis of the Paleogene succession along the western margin of the Barents Shelf (Ryseth et al., 2003). The change as one from trans-tensional to pure tectonic subsidence (Ryseth et al., 2003; Safronova et al., 2014). This subsidence was a regional event, with other basins along the margin, undergoing synchronous increases in accommodation space (Safronova et al., 2014). Piepjohn et al. (2016) define the final, post-Eurekan stage of tectonic activity as initiating after 34 Ma; with the end of spreading in the Labrador Sea, the establishment of passive margin tectonics (Faleide et al., 1984; Ryseth et al., 2003) and seafloor spreading between North America and the Eurasian plate occurring east of Greenland.

The WSFTB was sub-divided into four sections by Braathen et al. (1999). The farthest western hinterland, was affected by extensional deformation, and is bounded to the east on-land by a basement fold-and-thrust complex (fig. 1). East of the thick-skinned fold-and-thrust belt, the central zone, is defined by thin-skinned fold and thrust tectonism with several décollements along Permian planes of weakness in the Gipshuken evaporates (Leever et al., 2011). The eastern foreland province is characterized by thick-skinned structural inversion of Billefjorden and Lomfjorden fault zones, which bound Carboniferous and Devonian grabens, and caused folding (Leever et al. 2011). Kinematic analysis of faults in the WSFTB support a history marked by crustal

shortening and uplift and subsequent extension and collapse (Braathen et al., 1999). 20–40km of crustal shortening occurred margin perpendicular to the WSFTB, during the Paleocene–Eocene break-up of the northern Atlantic (Leever et al. 2011). The Eureka orogeny shows pre-folding shortening of the strata. Syn-folding buildup and thickening of the crust, related to thrusting. As well as post folding West to East and West-South-West to East-North-East structures associated with extension (Braathen et al., 1999). In the early Eocene, transform shifted to the east, connecting nascent spreading centers in the Norwegian-Greenland Sea and the Eurasian Basin (Blythe and Kleinspehn, 1998). The latest kinematic episode in the region is of Eocene age and can be related to extensional collapse in the hinterland of the WSFTB (Braathen et al., 1999).

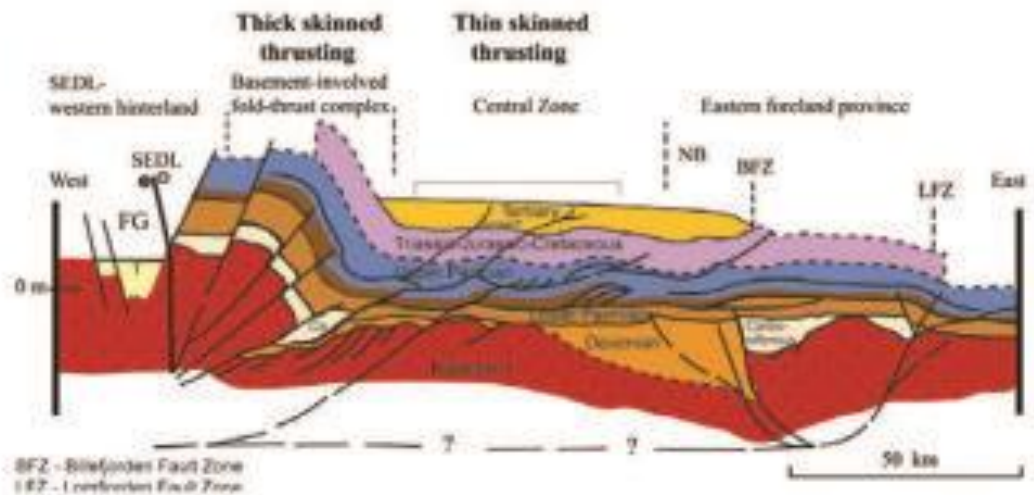


Figure 1: Generalized west to east cross section of the Spitsbergen Basement from Johannessen et al. (2011). BFZ= Billefjorden Fault Zone, LFZ= Lomfjorden Fault zone

### 2.1.3. The Central Tertiary Basin (CTB)

In Spitsbergen, a small foreland basin referred to as the Central Tertiary Basin (CTB) developed to the east of the WSFTB (Steel et al., 1985; Helland-Hansen, 1992; Leever et al., 2011; Grundvåg et al., 2014a,). It has also been proposed that the CTB is a piggy-back basin by Blythe and Kleinspehn (1998). The change in transport direction, 47 Ma (Vagnes, 1977), suggests a change in source areas of fill for the basin (Steel et al., 1981; Steel et al., 1985). Paleocene successions are sourced from the east-north-east (Bruhn and Steel, 2003), while latest Paleocene and Eocene sediments in the CTB were deposited from rivers draining the fold and thrust belt to the west (Steel et al. 1985; Harland, 1997). With continued tectonic activity throughout the period in question the depocenter in the basin moved eastward and southward, shown in the changing geometries of deposited sediments (Grundvåg et al., 2014b) and in tectonic loading (Pónten & Plink-Björklund, 2009).

Both the change in fault kinematics of the Eureka Orogeny to the west and a peripheral bulge to the east have been proposed as possible solutions to the change in transport directions (Bruhn and Steel, 2003). The timing of the deformation of the WSFTB, likely changed the source of sediments into the CTB, gradually shifting from the east, to north, to west (Leever et al., 2011). Bruhn and Steel (2003) suggest the entire Paleocene-Eocene basin fill was incorporated into a foreland basin fill scenario which switched drainage directions. This interpretation classifies parts of the Central Basin as an eastward migrating, landward stepping peripheral bulge succession. Transgressions and regressions were overprinted on it due to the adjustment of the foreland basin to thrust sheet loading and sediment supply (Bruhn and Steel, 2003). The CTB fill rests on a

regional unconformity that corresponds to a northward increasing hiatus which extends across the northwest Barents Shelf, and spanned most of the Late Cretaceous (Bruhn and Steel, 2003; Safronova et al., 2014). Steel and Worsley (1984) as well as others (Faleide et al., 1993) attributed this unconformity to thermal doming north of Svalbard, associated with the high arctic large igneous province (Maher, 2001) or initial transpression along the shelf (Nøttvedt et al., 1988). The theory presented by Bruhn and Steel. (2003) suggests that the hiatus was also influenced by the presence of the peripheral bulge. Sediment fill from the north is only seen in the lowermost unit of the Paleocene fill (Bruhn and Steel, 2003), confounding the gradual shift hypothesis of sedimentary source filling from eastward to westward by the WSFTB (Braathen and Bergh, 1995; Leever et al., 2011). The shape of a foreland basin is a result of thrust wedge buildup and plate flexure; thus, the depositional character and accommodation space of the basin is controlled by the thrust wedge heights and potentially the height of the peripheral bulge. It is proposed that the bulge was a factor in the westward transport of sediments in the CTB, as well as the transgressive episodes in an otherwise regressive sequence (Bruhn and Steel, 2003). The peripheral bulge migrated away and was eroded in the evolution of a margin supplying decreasing sediment to a progressively lower gradient basin. The thrust belt, foreland basin, and peripheral bulge likely migrated 10's of kilometers as well (Bruhn and Steel, 2003). Müller and Spielhagen (1990), suggest that the north-south drainage pattern in the region occurred due to a controlling factor of lithospheric shortening on the orders of tens of kilometers.

## 2.2 Lithostratigraphy of the Central Tertiary Basin:

The CTB fill is primarily composed of the Van Milenfjorden Group, which covers an area roughly 60 km by 200 km, with 2.3 km of infill (Steel and Worsley, 1984; Steel et al., 1985; Harland et al., 1997). The CTB is a foreland basin that formed in response to dextral compression on the WSFTB, where a mega sequence of more than 1500 m preserving westward progressive basin fill (Helland-Hansen, 1990; 1992; Blythe and Kleinspehn, 1998; Bruhn and Steel, 2003; Helland-Hansen, 2010). Coal vitrine reflectivity data suggests that the CTB has lost 1 km of sediment overburden since its last depositional hiatus (Marshall et al., 2015); making the total overburden deposited in the tertiary 2km or greater. Igneous intrusions are cited as complicating factors to the thickness estimates of overburden in the CTB (Manum and Throndsen, 1984). Ages derived from coal vitrine reflectivity show extreme lateral variation from the center to the margin of the basin (Marshall et al., 2015) The Billefjorden Fault Zone and the WSFTB bound the basin to the east and west, respectively. (Harland, 1997). The Van Milenfjorden Group has been broken into a Paleocene and a lower Eocene successions by Steel et. al. (1985) and Blythe & Kleinspehn (1998). This study deals with the Eocene succession, but a brief overview of the Paleocene stratigraphy is included.

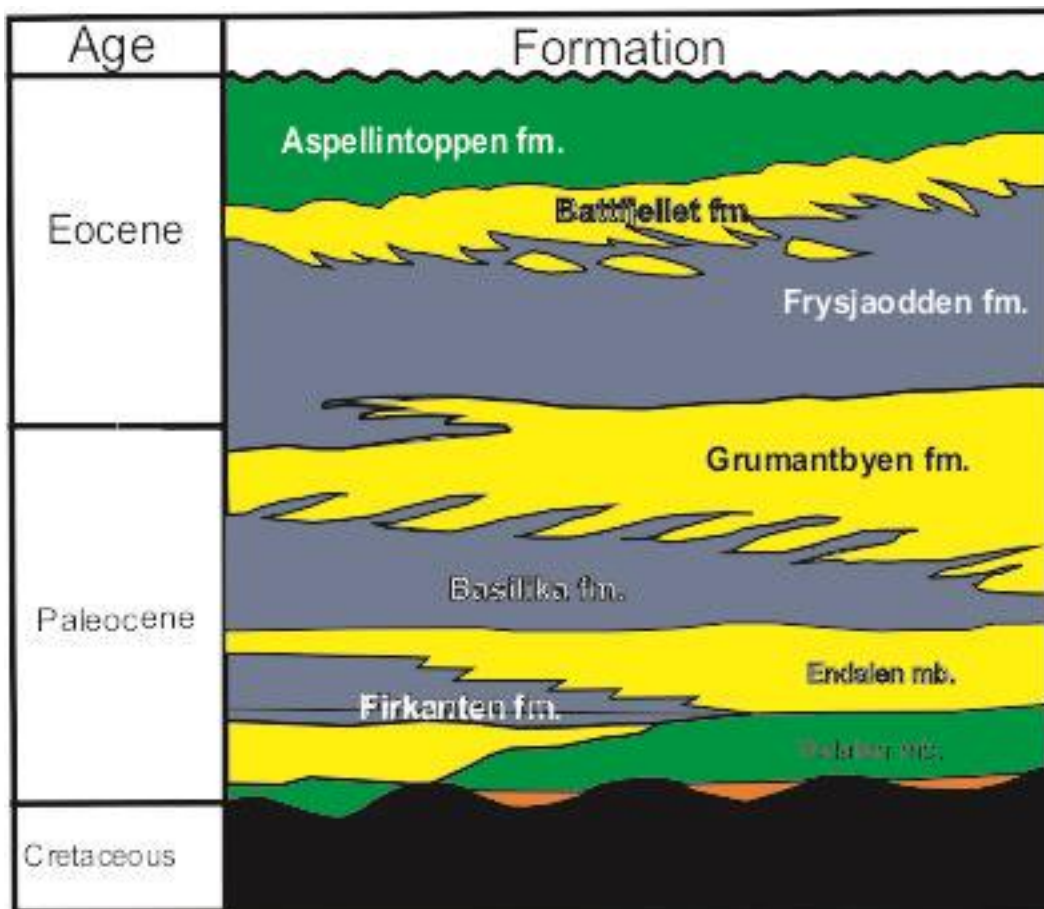


Figure 2 Stratigraphy of the Central Basin adapted from Mørk et al. (1999), the orange is the Grønfjorden bed of the Todalen member.

### 2.2.1. Paleocene Lithostratigraphy

The lower Paleocene succession is comprised of the Firkanten Formation, Basilika Formation, and Grumantbyen Formation (Steel et al., 1981; Nøttvedt, 1985; Steel et al., 1985; Helland-Hansen, 1992). It was fed from the east (Dypvik et al., 2011; Bruhn and Steel, 2003).

The Firkanten Formation rests on top of the regional unconformity and thickens westward (Faleide et al., 1984). The Firkanten Formation is comprised of: the Grønfjorden Bed, local basal conglomerates (Nøttvedt., 1985; Harland et al., 1997;

Dallmann et al., 1999); delta plain deposits of the Todalen Member (Harland et al., 1997; Dallmann et al., 1999); and the Endalen Member which interfingers the upper portion of the Todalen (Harland et al., 1997; Dallmann et al., 1999; Bruhn and Steel, 2003; Dypvik et al. 2011). Pollen, mollusks, spores and macro-fauna place the Firkanten Formation generally in the Paleocene (Steel et al., 1981; Nøttvedt, 1985; Steel et al., 1985; Dallmann et al., 1999; Bruhn and Steel, 2003). The transgressive portions of the Firkanten Formation are represented by the Todalen Member and lower Endalen Member (Harland et al., 1997; Dallmann et al., 1999; Bruhn and Steel, 2003). The transgressive units display sheet like geometry, stepping eastward, transgressing and on lapping their underlying units (Bruhn and Steel, 2003).

The Basilika Formation and Grumantbyen Formation represent 200 m to 500m a coarsening upward sequence of deep-water marine sediments from the late Paleocene (Blythe and Kleinspehn, 1998), with basinal settings in the east (Harland et al., 1997; Bruhn and Steel, 2003; Dallmann et al., 2009; Dypvik et al., 2011) The Grumantbyen Formation consists of five major sandstone sheets denoting the same number of small-scale systems (Bruhn and Steel, 2003), it inter-fingers the Basilika Formation and Frysjaodden Formation (Steel et al., 1985). The uppermost Grumantbyen Formation consists of upward coarsening sandstone intervals, inferred by Steel et al. (1985) to be a regressive surface or shallow marine ridge. The Grumantbyen Formation deposit consists of shoreline to shelf deposits during its regressive portion (Dallmann et al., 1999).

#### 2.2.2. Eocene Lithostratigraphy:

The Eocene succession consists of continental Aspelintoppen Formation and the basinal Frysjaodden Formation that link to each other through a series of shelf to shelf-edge and slope clinothems, the Battfjellet Formation (Helland-Hansen, 2010). The whole Eocene succession thickens to the west and south from the north and east (Grundvåg et al. 2014a) and was sourced from the west. (Braathen and Bergh, 1995; Dypvik et al., 2011; Vagnes, 1997).

The Frysjaodden Formation is comprised of gravity flow deposits emplaced in offshore to prodelta settings (Steel 1977, Steel et al 1981; Dalland et al., 1999). The lower Frysjaodden Formation are largely marine shales with large amounts of silt, and contain a surface of maximum transgression. Dinocyst assemblages gathered from the mid and lower Frysjaodden Formation indicate the formation is of a late Paleogene age (Blythe and Kleinspehn, 1998). The Paleocene-Eocene temperature maximum (PETM) can be identified in the shale prone Frysjaodden Formation. U/Th ratios in the distal Frysjaodden Formation kaolinites suggest high rates of chemical weathering, consistent with the PETM (Dypvik et al., 2011). The upper Frysjaodden is largely composed of siltstones and sandstones with upward coarsening silts to sands in its upper reaches. The upper and lower portions of the Frysjaodden Formation together have 450 m of thickness.

The Battfjellet Formation consists of multiple stacked upward coarsening and shallowing siltstone to sandstone parasequences of Eocene age (Steel, 1977; Steel et al., 1981; Helland-Hansen, 1990; Petter and Steel, 2006; Helland-Hansen, 2010). It represents shoreline tongues that locally can be traced into shelf margin delta successions and slope

clinothem, which dip eastward into the basin floor (Helland-Hansen, 2010; Grundvåg et al. 2014a). The formation inter-fingers down-dip with the basinal Frysjaodden Formation (Blythe and Kleinspehn, 1998) and up-dip with the continental Aspelintoppen Formation (Helland-Hansen, 1990; 1992; Helland-Hansen, 2010). The Battfjellet Formation records a largely regressive sequence of basin infilling phase (Løseth et al., 2006). Clinothem in the Battfjellet Formation roughly represent 210-300 kyr time intervals (Løseth et al., 2006). The shoreline and depositional process have been controlled by deltaic and tidal influence (Helland-Hansen, 2010; Grundvåg et al., 2014a). The deltas were flood dominated and prograded mainly when the rivers feeding them were at high discharge (Plink-Björklund and Steel, 2004). Aided by the high rates of sediment supply, the deltas repeatedly managed to prograde across the shelf during a period otherwise characterized by a long-term rise in relative sea-level (Petter and Steel, 2006; Helland-Hansen, 2010; Grundvåg et al. 2014a).

The long-term rise in sea-level was the result of high rates of tectonic subsidence, compaction of sediments and the Eocene eustatic high stand (Petter and Steel, 2006; Helland-Hansen, 2010; Grundvåg et al. 2014a). In eastern locations, clinothem stack aggradationally, compared with normal progradational trends in the west (Helland-Hansen, 2010; Grundvåg et al., 2014b). Seaward stepping and stratigraphically climbing parasequences describe the regional trend within the Battfjellet Formation, separated by marine flooding surfaces. The clinotherm trajectory angle is between  $1.2^\circ$  and  $0.88^\circ$ , showing that the Battfjellet Formation was deposited in a time of relative sea-level rise (Helland-Hansen, 1992; Helland-Hansen and Martinsen, 1996; Grundvåg et al., 2014b).

The Battfjellet Formation is composed of near-tabular parasequences lacking shelf breaks. Parasequences vary in number and thickness and partly overlap throughout the region (Grundvåg et al, 2014b). In a 15 to 20 km section in the west and central part of the CTB, the parasequences can be traced down-dip into the shelf-edge delta deposits and slope wedges forming a clinothem zone. East of this zone, both slope wedges and submarine fans are lacking (Steel and Olsen, 2002; Grundvåg et al., 2014b). The shoreline of the Battfjellet Formation was broadly deltaic without great transport potential, based on the limited lateral extent of the sand-bodies (Helland-Hansen, 1992). The delta stacking structure shows frequent delta-lobe switching (Grundvåg et al., 2014a). Depositional styles in the lower part of the Battfjellet Formation show more gravity influence in the near shore environment, while wave-base is a controlling factor in them in the upper sequence (Pónten and Plink Björklund, 2009; Helland-Hansen, 2010). The Battfjellet Formation in nearshore locations, such as Nordenskiöld Land is composed of several smaller overlapping parasequences of variable lateral extents. The variability in number does not follow a trend laterally, suggesting that the shingled delta deposits are variable laterally and longitudinally (Helland-Hansen, 2010). The individual parasequences are likely on the scale of a few kilometers to 10 km in any one direction. Well-developed clinothems tend to occur where the parasequence stacks are thickest and progradation occurred directly on top of deep water deposits of the Frysjaodden Formation. The deltas that built out in inner Van Kuelenfjorden area faced deep waters causing a slower advance of the system and the building up of the system (Helland-Hansen, 2010).

The Aspelintoppen Formation is comprised largely of fluvial, floodplain and delta-plain heterolithic deposits (Steel et al., 1981; Helland-Hansen, 1990; 1992). It is characterized by a succession of grey or greenish sandstones alternating with grey brownish siltstones. Calcareous horizons and thin coal beds are also present (Dallmann et al. 1999). Soft sediment deformation is common in the unit (Steel et al., 1985). The lower l is synchronous with the easternmost Battfjellet clinofolds (Helland-Hansen, 2010). The Aspelintoppen Formation shows an eastward shoreline advance (Steel et al., 1985; Helland-Hansen, 1990; 1992). In some locations its thickness exceeds 1 km (Steel et al., 1985). Abundant plant debris is present in the strata (Steel et al., 1985), recording a warmer than present climate in the Eocene, at high latitudes (Dypvik et al., 2011).

### 2.2.3. Eocene climate

The climatic conditions present in the Eocene were warmer than they are today (Schweitzer, 1980), with implications on depositional styles. The late Paleocene, and Eocene were climatically unstable times, with rapid shifts in temperature and climate in the northern latitudes. This period is referred to as the Paleocene Eocene Temperature Maximum (PETM) (Dypvik et al., 2011). Anoxic and stratified ocean conditions were likely present during this time as well. (Slujs et al., 2006; Dypvik et al., 2011). Land temperatures are recorded as higher throughout the Eocene; conifer analysis places the annual mean temperature at 15–18°C (Schweitzer, 1980). Ocean surface temperatures were significantly higher than they are today as well (Slujs et al., 2006). The rapid jump of mean annual temperatures, from -18°C to 23 °C, is associated with stratified and

anoxic oceanic conditions (Slujs et al., 2006). Terrestrial fauna from Aspelintoppen Formation and other locales in Svalbard from latest Paleocene to Oligocene ages commonly contain large deciduous leaves.



*Figure 3 Leaf fossil from Aspelintoppen Formation on Hyrnestabben*

Ice rafted debris is common in marine sediments around the area (Dalland, 1976), suggesting cooler winter temperatures. Paleomagnetic data places Spitsbergen at 71-72°N (Dalland, 1976) while Irving (1975) placed it between 65-70° N, nearer to present day Tromsø. Current climatic conditions in Tromsø are slightly cooler than the PETM conditions on Svalbard, and a higher rate of erosion has been assumed by various authors (Dypvik et al., 2011; Nøttvedt, 1985). U/Th ratios in the distal Frysjaodden Formation kaolinites suggest high rates of chemical weathering, consistent with the PETM (Dypvik et al., 2011)

### 2.3 The Van Keulenfjorden transect

A complete Eocene section crops out on Pallfjellet, Brognarfjellet, Storvola, and Hyrnestabben on the north side of Van Keulenfjorden (Johannessen and Steel, 2005). The clinofolds show the progressive eastward (Plink-Björklund and Steel, 2004; Grundvåg et al., 2014b) development of a passive margin (Johannessen et al., 2011). More than 20 Eocene clinofolds are exposed along Van Keulenfjorden in the span of 35 km (Plink-Björklund and Steel, 2004; Johannessen and Steel, 2006). Clinofold 14, from widely adopted (Crabaugh and Steel, 2004; Clark and Steel, 2006; Johannessen and Steel, 2005; Henriksen et al., 2010) nomenclature introduced by Steel and Olsen (2002) is exposed on Storvola, showing a complete succession from lower slope channels to shelf edge delta. Connected submarine fan deposits are visible on Hyrnestabben, and are the focus of this study. A well, drilled at the same paleo-shelf break 15 km away, brought up only slope shales (Johannessen et al., 2011), suggesting slope channels and shelf-edge deltas are the exception, not the rule. Slope environments on Pallfjellet are also shale dominated (Johannessen et al., 2011). Frequent distributary switching from the delta growth, switching, and embayment, is inferred to have occurred on the shelf and shelf margin during the Eocene period (Helland-Hansen, 1992; Helland-Hansen, 2010; Grundvåg et al., 2014a). Shelf accretion rates are estimated at 1 km per 100 kyr. Below clinofold 14, are thick basinal shales, on Storvola, as well as some slope shales, and a 20m thick basin floor fan (fig.4) (Johannessen et al., 2011). Above the slope portions of clinofold 14 are thick shales that thin westward into shelf shales and eventually pinch out between the

sandy delta and shore sections of clinoforms 14 and 15 (fig. 4) (Johannessen and Steel, 2005; Johannessen et al., 2011).

### 2.3.1 Clinoformal Trends within The Battfjellet Formation and association with the Frysjaodden Formation:

Stacked clinoform geometries are well exposed longitudinally along Van Keulenfjorden, documenting the basinal and orogenic history of the Paleocene to Eocene central tertiary basin (Helland-Hansen, 1992; Crabaugh and Steel, 2004; Clark and Steel, 2006; Johannessen and Steel, 2005; Henriksen et al., 2010). Clinoforms, represent the coeval deltaic through basin floor sediments (Johannessen and Steel, 2005). They are the basic building block of the system and show how sediment supply to the basin was budgeted as well as tectonic and climatological influence, over a short timespan (Johannessen and Steel, 2005). The clinothems composing a clinoform, are roughly equivalent to a parasequence, and clinothem sets are comparable to systems tracts (Pónten & Plink-Björklund, 2009). In the basinal setting, transgressive surfaces are often only noted by a lack of sedimentation, the deepest water facies (Petter and Steel, 2006) or siderite horizon. The maximum flooding surface of the clinothems is usually demarcated as where the deepest water facies reach their most shore proximal extents (Johannessen and Steel, 2005). The bottom boundary of a clinothem is marked by an erosional surface on the slope, which becomes conformable on the basin floor. The basin floor fan is partial a product of shelfal erosion and sediment by-pass. However, it is usually linked with the continued discharge from a shelf edge delta, making it broadly co-eval with the shelfal sequence boundary (Johannessen and Steel, 2005).

Process changes in a given clinothem do not necessarily represent basinal changes, but rather changes in local conditions (Pónten & Plink-Björklund, 2009). The shingled clinothems (Plink-Björklund and Steel, 2004) have durations of a few hundred thousand years, and link up-dip with coastal plains, and down-dip with coeval deep water deposits (Helland-Hansen, 1990; Steel and Olsen, 2002, Løseth et al., 2006; Helland-Hansen, 2010). Clinothems are supposed to go through four stages when built (Johannessen and Steel, 2005). First, a regressive shelf transit of the sediment supply system, near shore (Johannessen and Steel, 2005); next, the delivery and accumulation of slope and basin-floor sediment gravity flows. The slope segment in this type of situation can be mud-prone or sand prone (Johannessen and Steel, 2005). Where it is sandy, sheet like turbidites tend to dominate (Plink- Björklund et al. 2001). Third, a re-establishment of the sandy depocenter on the shelf edge occurs congruent with shoreline retreat. Sometimes early sand-prone channels are overlain by back-stepping muddy channel levee systems (Johannessen and Steel, 2005). The slope break deposits often include a re-established shelf edge delta, which represents much of the volume of prograded sediments in Clinoform 14 (Johannessen and Steel, 2005). The transgressive transit of the shoreline across the shelf is the final stage in a clinothem's development.

Individual clinoforms can be considered fourth order features. Shale prone intervals separate them on the slope, shelf edge and outer shelf (Johannessen and Steel, 2005). The clinoforms along Van Kuelenfjorden have compacted thicknesses of 200–400 m. Similar thicknesses on Van Milenfjorden were observed by Mellere et al. (2002). Three third

order systems are contained within the Battfjellet Formation, identified largely by the development of basin-floor fan complexes, transgressive surfaces, and shelf trajectories (Johannessen and Steel, 2005) that indicate different phases of thrusting from the west. The overall geometry of the Battfjellet clinoforms become flatter, with a wider shelf, in the upper forms (15-18) (Johannessen and Steel, 2005; Helland-Hansen, 2010). Steel and Olsen (2002) attribute this change in geometry to shallowing of the basin away from the fore-deep.

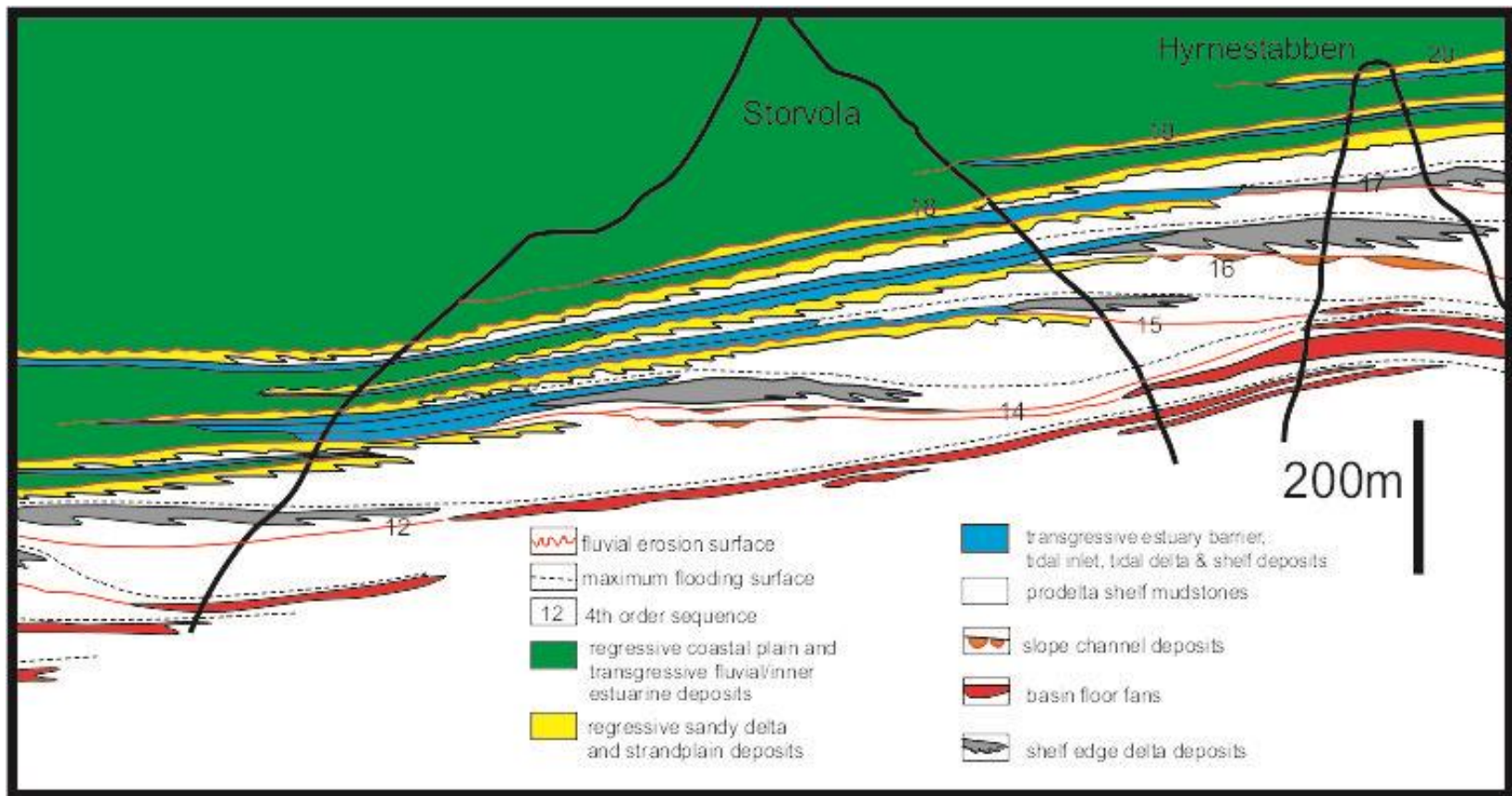


Figure 4 : Clinoformal schematic of the study area, adopted from Steel and Olsen (2002).

### 2.3.2. Shelf Edge Deltas

Fluvial processes are documented as the most common means for sand delivery onto the outer shelf and shelf edge in the Battfjellet, (Crabaugh and Steel, 2004; Henriksen et al., 2010). A case can be made for transgressions and regressions mostly influenced by sedimentation related to uplift of the WSFTB and increased erosion due to Eocene climate, recognized by the migration of deltas toward the shelf edge, (Steel and Olsen., 2002; Helland-Hansen, 2010). Clinofolds, including 14 and 15, preserved in the Battfjellet Formation and Frysjaodden Formation document shore trajectories that place deltas on or near the shelf break (Steel and Olsen, 2002; Crabaugh and Steel, 2004; Helland-Hansen, 2010). Sand prone shelves were present when clinofold trajectory was falling slightly or relatively flat (Johannessen and Steel, 2005). The shelf edge delta wedge can lie largely below the older shelf edge (Johannessen and Steel, 2005). Løseth et al. (2006) measured the pinch-out angle of the shelf/shore of clinothem 15, noting a  $0.8^\circ$  pinchout angle, with a high degree of aggradation. The high angle suggests that during the regression to transgression turn-around point, a large amount of aggradation occurred (Løseth et al., 2006), implying a steepened slope.

### 2.3.3. Slope segments

Slope segments on Storvola are generally mud prone. Sand prone segments can be found usually feeding basin floor sands, emplaced early in the fall to rise (Petter and Steel,

2006). Depocenters shift slope-ward or deeper, with base level fall below the shelf edge and the associated shelf incisions (Crabaugh and Steel, 2004; Petter and Steel, 2006).

Incised systems with low base levels are a means for sandy sediment to reach the basin floor fans (Steel et al. 2000; Mellere et al., 2002; Steel and Olsen, 2002; Posamentier and Kolla, 2003).

Substantial sheets of turbidite sands develop on the upper and middle slope of clinoform 14 (Crabaugh and Steel, 2004). Slopes are likely to be sandier when relative sea-level is low (Steel et al., 1985; Mellere et al., 2002; Petter and Steel, 2006). However high sediment rates (Burgess and Hovius, 1998) and narrow shelves (Mulder et al., 2003) can still produce sediment bypass of the shelf with high sea levels. There are large, abundant and well-preserved organic clasts within these deposits, that continue into the basin floor fan (Crabaugh and Steel, 2004; Clark and Steel, 2006, this study). Well preserved progradational shelf edge delta architecture and smooth draped slope clinoform profiles are indicative stable shelf margin deltas (Porębski and Steel, 2006).

#### 2.4. Basin Floor Fans:

Crabaugh and Steel, (2004) as well as Clark and Steel (2006) studied the basin floor fan of Clinoform 14, as it records sediment basin bypass on the slope. The extent of the basin floor fan, and slope clinoform demonstrate the prevalence of quasi-steady hyperpycnites in the system. Hyperpycnites can initiate turbidity flows, which have been referred to as hyperpycnal flows. Depositional models do not often take into account shelf-edge and slope system that feed basin floor fans (Petter and Steel, 2006).

Hyperpycnal flows generated from the shelf-edge are likely to continue farther downslope by inertia (Clark and Steel, 2006). The attachment of the basin floor fan to the shelf sediments within clinoform 14, demonstrates that sand bypasses the slope, to some degree.

Cliniform 12, 14 and 15 are associated with extensive sandy basin floor fans (Steel and Olsen, 2002; Crabaugh and Steel, 2004). The basin floor fan deposits of clinoform 14 were described as relatively clean and relatively thick medium to fine-grained sandstone beds. They are found at the distal end of the system extending out from the toe of the slope onto the basin floor (Clark and Steel, 2006). The segments show compensational bed stacking on top of each other, in the case of clinoform 14 (Johannessen and Steel, 2005). Johannessen and Steel (2005) note that scours and erosion caused by the thick sands are minor. Pinchouts are inferred to be the effect of sidelap (Hodgson et al., 2006; Pr lat et al., 2009) No channels deeper than 1.5 m were encountered (Johannessen and Steel 2005, this study). The thick sandy beds can be interpreted as fans or lobes (Crabaugh & Steel, 2004; Petter and Steel, 2006).

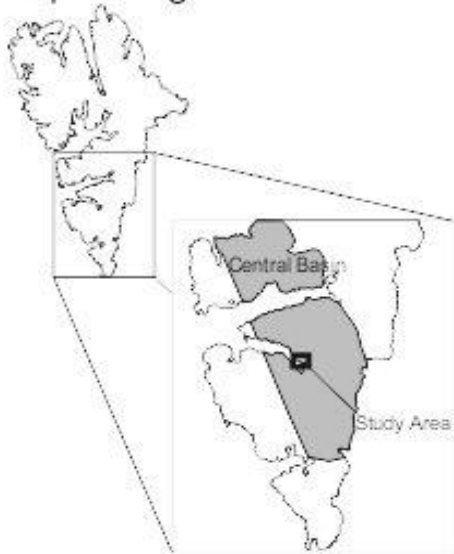


### 3. Methods

#### 3.1 Study area - Clinoform 14 and 15:

The studied outcrops are exposed along cliff faces on the northern, southern and eastern faces of Hyrnestabben, approximately 80 km SSE of Longyearbyen, on the north shore of Van Keulenfjorden (fig.5). Distal slope and basinal settings were encountered in the study area, in accordance with findings by Steel and Olsen (2002) and Crabaugh and Steel (2004). Sandy deposits emplaced in a basin floor setting (Steel and Olsen, 2002; Crabaugh & Steel, 2004), belonging to clinoform 14, comprise the major outcrop belt visible on the south and southeast faces of Hyrnestabben. Thinner, sandstone units form C15. The top elevations of the studied sections range from 390 m toward the western end, to 420 m at the extreme eastern faces, the ascending basinward geometry has been attributed to minor tectonic warping of the deep basin both syn and post depositionally, creating a distal shallowing (Helland-Hansen, 1990). Various authors (Crabaugh and Steel, 2004; Clark and Steel, 2006) note the sandy fans are genetically linked to slope and shelf clinoforms to the west, which are well exposed on the southern face of Storvola.

# Spitsbergen



## Study Area

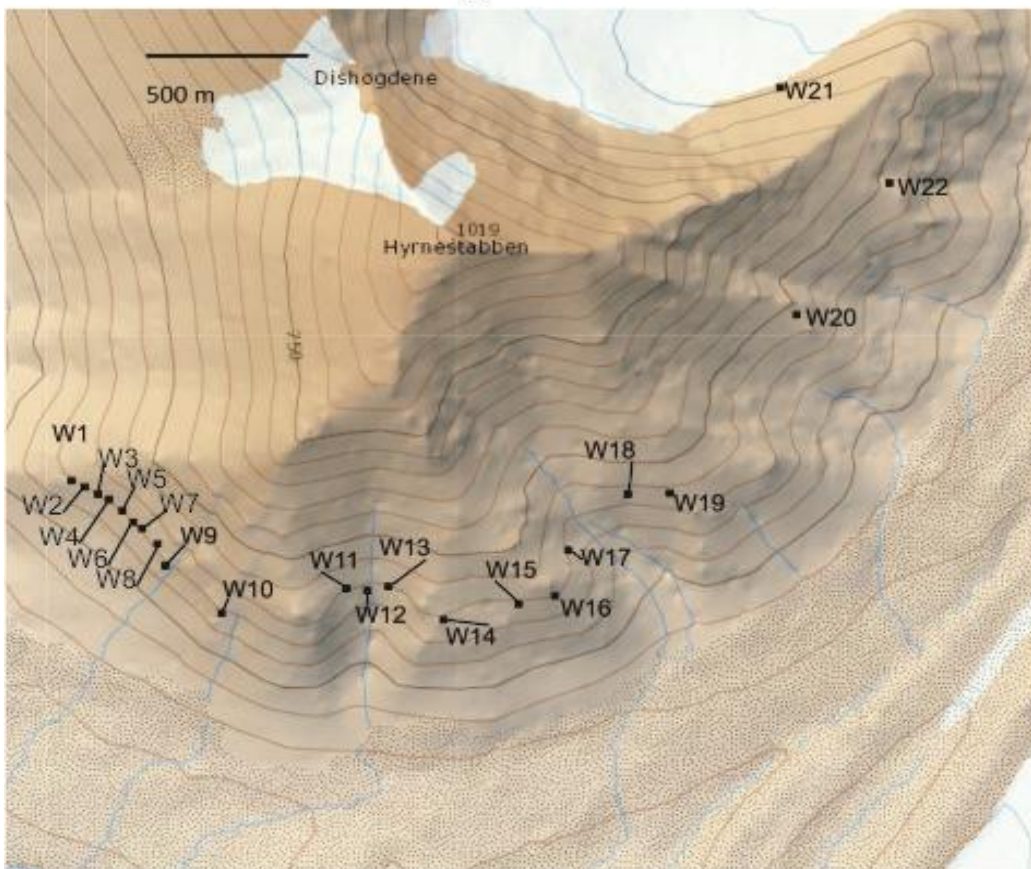


Figure 5: Study Area with logs called out.

### 3.2 Sedimentary Logging

Sedimentary logs were measured bed by bed, at a 1:20 centimeter scale on the North, East, and South face of Hyrnestabben (Figs. 5, 6, 7, 8). Twenty-two logs, out of the twenty six recorded, are included in the report (figs. 47 to 61). The locations of excluded logs were later determined to be landslide affected. Information on lithology, grainsize, structures, paleocurrent, sorting, body and trace fossils were noted in the field logs.

Presentation logs are in 1:100 scale. The logs were collected from outcrops out on the south, east, west and north sides of the mountain. The 22 included logs are named W1 through W22. They pass through portions of C12, C14a, C14b, and C15 (figs.33, 34, 35, and 36). Most logs are from C14b, however four sections (W2, W10, W12, W21 and W22) pass through clinoform 15. Two logs (W10 and W12) contained C12, C14a, C14b, and C15, separated by several meters of basinal shales.

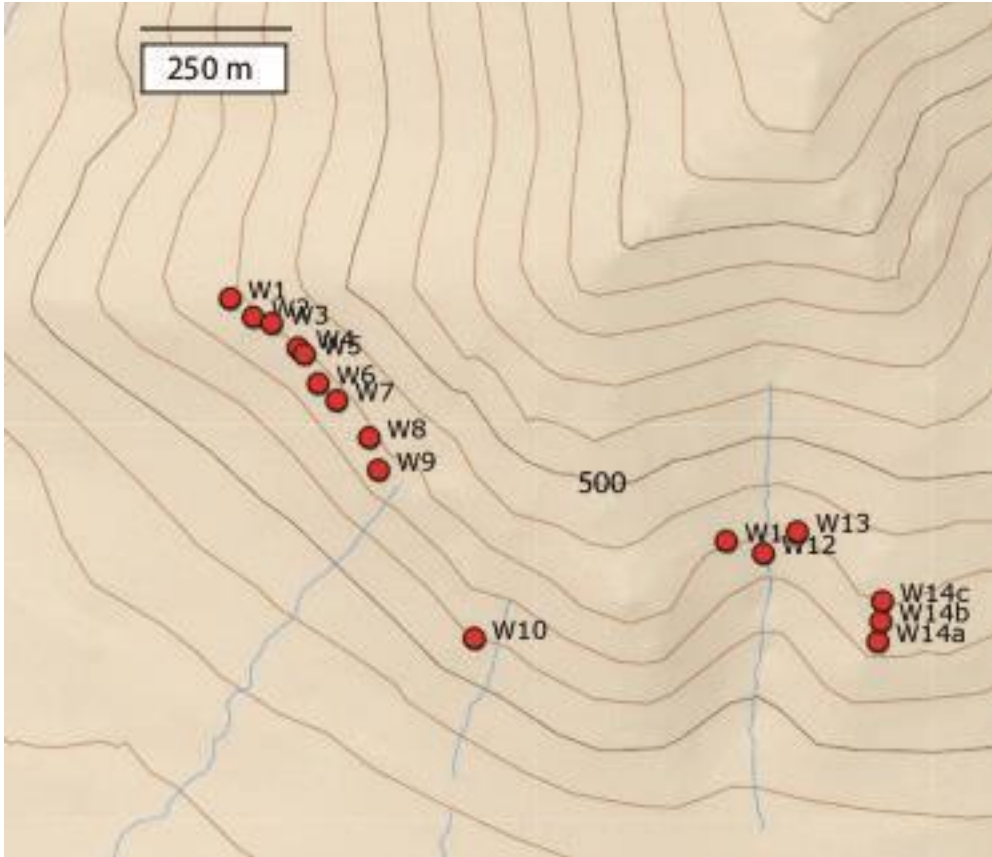


Figure 6: Logged locations on the Southwest face of Hyrnestabben, comprising the most proximal, and medial submarine fan environments.

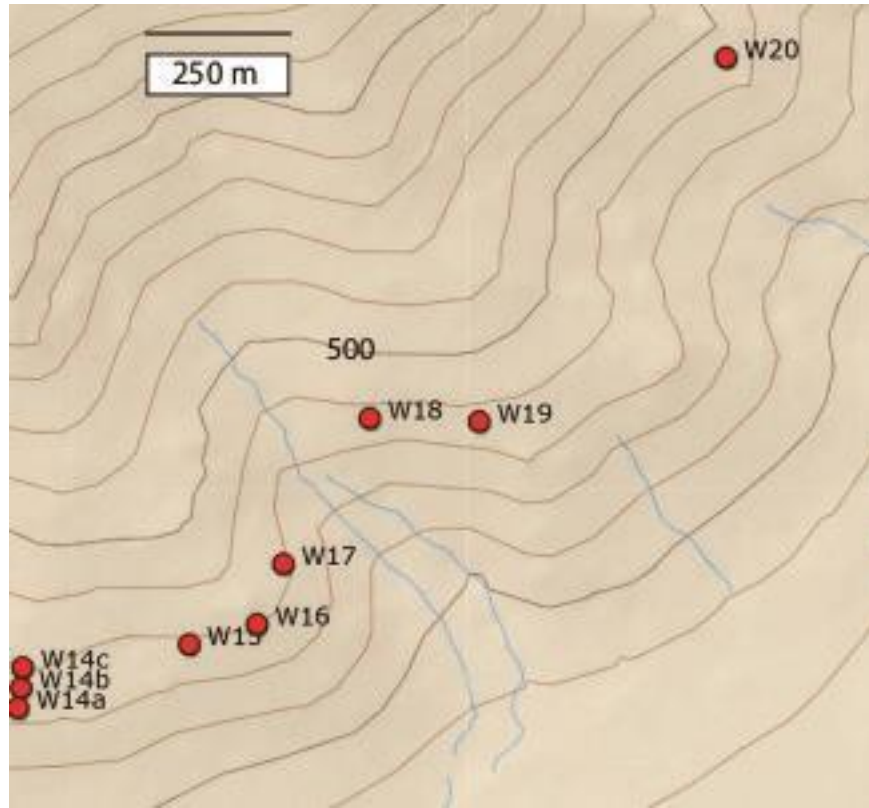


Figure 7: Logged sections from medial fan locations on the south and southeast face of Hyrnestabben.

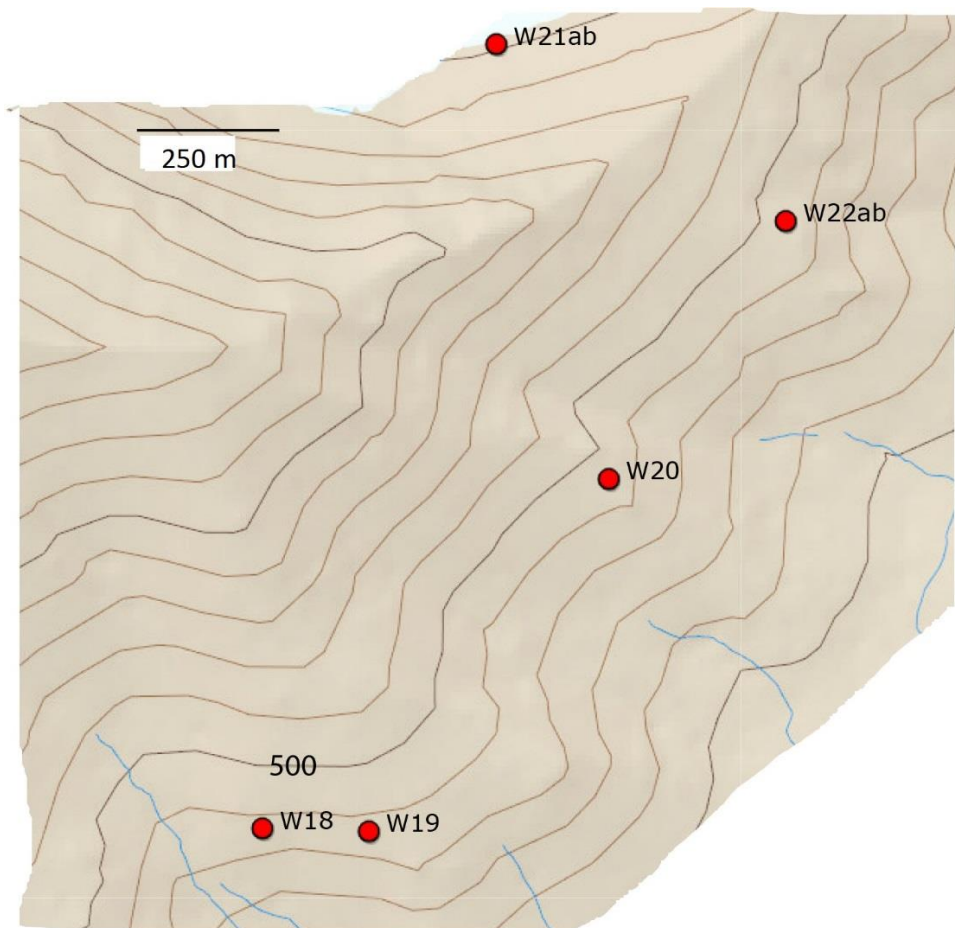


Figure 8: Distal logged locations on eastern and northern faces of Hyrnestabben

## 4. Results

### 4.1. Bed Types

From the logged sections eighteen bed types were recognized (summarized in Table 1).

The bed types are broadly organized into five facies associations (FAs): background basinal (FA 1), distal heterolithic lobe deposits (FA 2), thin bedded sandstone sheets (FA 3), thick bedded amalgamated deposits (FA 4), and channel or slump deposits (FA 5).

The main facies associations are differentiated by degree of amalgamation, prevalent structures, dominant grain size, and bed thicknesses. Although much of the difference in facies architecture can be explained by relative position within a fan system, flow processes also factors into the vertical facies trends within the overall system.

*Table 1: Summary of Bed types (BT). ms= medium sand grainsize fs=fine sand grainsize, vfs= very fine sand grainsize*

Bed Types	Lithology and grainsize	Structures	Thickness (m)	Geometry	Interpretation
1 (Fig. 9)	Mudstone Occasional very fine-sand (vfs) sandstone	Laminated beds, normal grading	< .005 beds	Thin sheets, wavy or planar bed boundaries	Background basinal sedimentation, with occasional spillover type turbidites
2 (Fig. 10)	Fine sand (fs) and vfs sandstone and/or siltstone	Fining upwards, laminated beds, or climbing asymmetric ripples.	Beds <.03 Units 20 cm or less.	Tabular with wavy bed boundaries	Bouma type C and D deposits
3 (Fig. 11)	Siltstone, and sandstone vfs to fs grainsizes	Coarsening upwards beds, from silty bases to fs tops.	Beds 0.015-0.03	Thin tabular sheets	Accumulative flows, in distal lobe or channel mouth settings
4 (Fig. 12)	Mudstones with interbedded vfs sandstones.	Interbedded complex or convolute laminations of mudstones. No discernible grading.	Beds <0.02	Tops of these units often have flame structures, and/or erosional features.	DBackground sedimentation processes that underwent post depositional deformation.
5 (Fig. 13)	Sandstones with vfs to fs grainsizes sometimes a silty top	Normal grading, sharp erosive bases	0.05<0.1beds	Tabular, sharp based	Sheet sandstones conforming to Bouma type A and B beds

6 (Fig. 14)	Fs sandstone	Normal grading, with asymmetric ripples in the bases planar top, wavy erosive bases	Beds 0.05-0.1	Sheet like geometries	Deposits from long lived tractive flows
7 (Fig. 15)	Sandstones of fs grainsizes, and mudstones	Interbedded clean fs sandstone and mudstone beds. Grainsize decreases upwards. Normal grading, flame structures at the top boundary of siltstone beds, overlain by sandstone beds	Sandstone beds < 0.03 series 0.5-1	Tabular thin sandstones, and massive silt stone with clay.	Thin bedded heterolithic deposits from progressively decreasing energy turbidity flows.
8 (Fig. 16)	Sandstone with vfs to fs, plentiful organic detritus	Reverse graded sand with plentiful organic clasts throughout, bases can show high or low degrees of erosion	Beds 0.1-1.0	Unit often overlain by an erosive contact and a normal graded sandstone bed-type.	C Accumulative sediment gravity flow.
9 (Fig. 17)	Sandstone of fs and vfs grainsizes	Normal grading, with laminations coarser grained laminations towards the top of the assemblage, ripples and erosional contact in some beds <i>Arenituba</i> and <i>Planolites</i> trace fossils at bed boundaries.	Laminations <0.02 Beds 0.01-0.1	Planar laminated fining upwards assemblage, beds decrease in laminae thickness with upward progression in assemblage.	O Low energy depletive submarine gravity deposits.

10 (Fig. 18)	Siltstone and sandstone of vfs and fs	Upwards coarsening laminated silts and vfs sandstones, usually erosional upper contact	Laminations <0.01, units <0.10	Thin beds with broad lateral extent.	Heterolithic deposits, increasing sand content indicated depositional axis shifting towards location
11 (Fig. 19)	Sandstone of fs and vfs.	Grain sizes decrease upwards, and structurally the unit changes from basal structureless fine sand, through laminated sand, and into convolutedly bedded fine sand to very fine sand.	Total bed thickness 0.60 to 1.0. Faint laminations < 0.02.	Sharp base, and wedge shaped geometry.	Terminal debris or slurry flow deposit, flow bulking and freezing.
12 (Fig. 20)	Sandstone of Medium sand (ms) and fs, organic clasts, and silty rip ups	Normal grading, sometimes ripples in the tops, or bases of beds. Rip up clasts occasionally present near flow bases, often in conjunction with silty organic rich lenses. Organic detrital clasts can occur in thin aligned layers at flow bases or thick unaligned bands in upper bed portions. Flame structures, and pillows frequently occur. Thicker units show some dish structures.	Beds 0.1 to 0.5	Rapid changes in thickness over a short (meters) distance. Erosive or non-erosive bases. Beds often pinch out rapidly, into silty lenses with silty interclasts.	Rapidly deposited, and sediment rich submarine flows, perhaps from flow collapse.
13 (Fig. 22)	vfs to fs, sandstone	Reverse graded clean sand	Beds 0.1<0.3	Unit overlain by erosional contact and normally graded bed	Accumulative flow from long lived quasi-steady current.
14 (Fig. 23)	Sandstone of fs grainsize fractions with plentiful	Massive, or with some normal grading in the very upper section, lower contact heavily erosive, or planar upper contact also wavy.	Beds 0.05-0.30	Beds can cut aggressively into underlying bed.	Transitional or slurry flow,

	organic clasts throughout				
15 (Fig. 24)	Sandstone composed of ms and fs.	Low angle cross stratification in sandy beds that have a higher proportion of medium grains in their bases. Flame structures occur in the base.	Stratification 0.005 to 0.02 Beds 0.05 to 0.10	The lower contact is often erosive, and/or shows flame structures from underlying beds. The upper contact grades upward into asymmetric ripples, and occasionally laminated bedding.	Bed emplaced by higher energy semi-steady sustained flow hyperpycnal, or simple high density flow
16 (Fig. 25)	Sandstone with ms, fs, and vfs grainsizes, interclasts and large organic fragments	Structureless or normally graded sandstone, with interclasts, and organic fragments concentrated near bed bases. Basal scours occur.	Beds 0.1 to 0.3 Organic clasts 0.01 to 0.05	Thick accumulations, tend to show convex bases, cutting into underlying beds. Scours can be several meters in cross section.	CConfined turbiditic flows
17 (Fig. 26)	Siltstones, and sandstones of vfs and fs grainsize fractions	Unit coarsens upward from silt, through very fine sand and into fine sand before grading back to very fine sand in upper portion of the bed. Bedding is convolute throughout. Scours at the base of the flow.	Units 0.20 to 1.0	Irregular base, unit thick units show wedge shaped geometries.	Terminal debris or slurry flow.

18 (Fig. 27)	Fs sandstone	Convolutely bedded sands. Normal or reverse grading apparent in the original beds. Clean sand.	0.05-0.10	Thick assemblages made up of thinner fine sand beds	Slumps or debris flows
--------------------	-----------------	--	-----------	---	------------------------

#### 4.1.1. Bed Type 1 (BT 1):

*Description:* Dark thinly laminated mudstones with occasional very fine sand sheets which display wavy or planar bed boundaries. The individual mudstone beds are normally graded, and thinner than 5 mm.

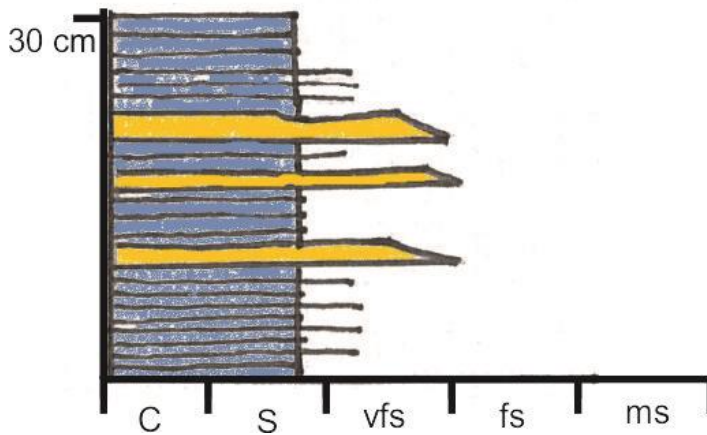


Figure 9: Block Diagram of BT 1

*Interpretation:* Background basinal or slope sedimentation with occasional surge type turbidites *in sensu*. (Jackson et al., 2009; Grundvåg et al., 2014b).

#### 4.1.2. Bed Type 2 (BT 2):

*Description:* Thin tabular fining upwards very fine to fine-grained sandstone beds with wavy tops and bottoms. Beds often contain climbing ripple cross-lamination or thin

planar laminations, and are less than 3 cm thick. Units of this bed type are generally less than 20 cm.

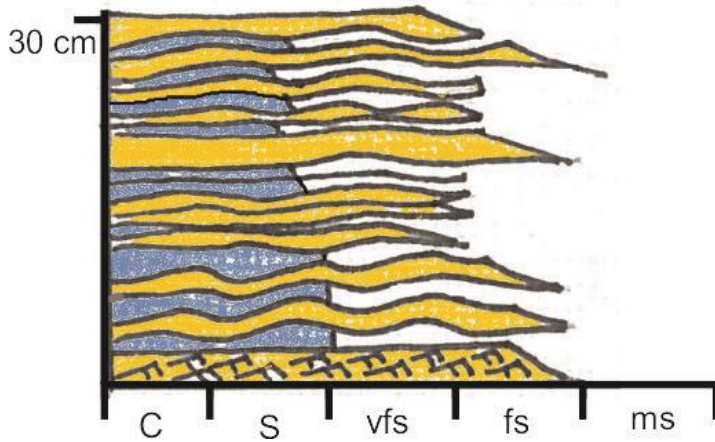


Figure 10: Block Diagram of BT2

*Interpretation:* Type 2 facies is interpreted to be similar to these Bouma T<sub>c</sub> and T<sub>d</sub> beds. Which result from surge type turbidites (Bouma, 1962). The Bouma T<sub>c</sub> division is defined as rippled, and wavy, while Bouma T<sub>D</sub> beds are very fine sand and silt in planar parallel laminae.

#### 4.1.3. Bed Type 3 (BT 3):

*Description:* 1.5 to 3 cm sandstone beds which coarsen upwards from silty bases, through very fine sand mid-sections, and fine sand tops, beds are 1.5 to 3 cm thick.

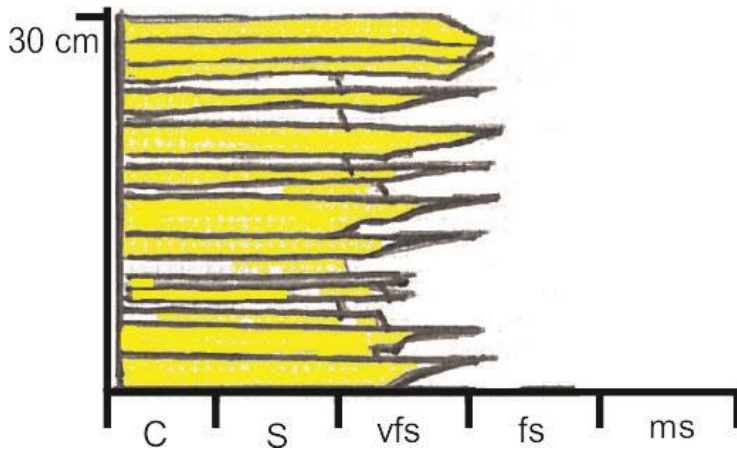


Figure 11: Block Diagram of BT 3

*Interpretation:* Inversely graded beds can be emplaced by a variety of flow processes but based on bed scale and distal locations in the study area, BT 3 is interpreted to be deposited by hyperpycnal or distal accumulative flows (Kneller, 1996) with a basal grain flow component (Mellere et al., 2002). Waxing depletive flow (Kneller, 1996; Kneller and Buckee, 2000) in hyperpycnal flows can emplace inversely graded beds, if there is a highly concentrated basal flow layer. Inverse grading and lack of fossils can be indicative of debris flow deposits (Shanmugam, 1996) or a sandy density underflow (Mellere et al., 2002).

#### 4.1.4. Bed Type 4 (BT 4):

*Description:* Mudstones with interbedded very fine sandstones, beds display convolute laminated beds. Grading is not discernible and beds are less than 2cm thick. BT 4 is often overlain by thicker sandstone deposits, and upper beds can sometimes display flame structures.

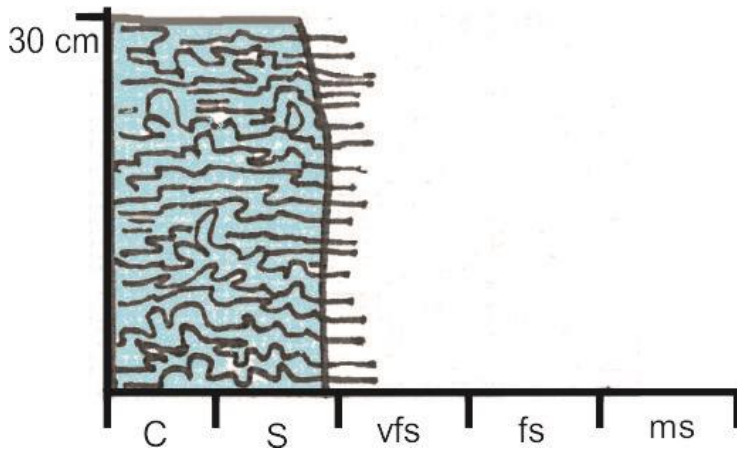


Figure 12: Block Diagram of BT 4

*Interpretation:* Given the association with thicker sandstone beds, and small grainsize BT 4 is interpreted to be background sedimentation which has undergone post-depositional deformation from overlying beds.

#### 4.1.5. Bed Type 5 (BT 5):

*Description:* Tabular sandy sheet sandstones composed of very fine and fine sand grains, with a sharp erosive base. BT 5 bed's thicknesses are between 1 cm and 10 cm, and show normal grading. Commonly they have a silty bed on top.

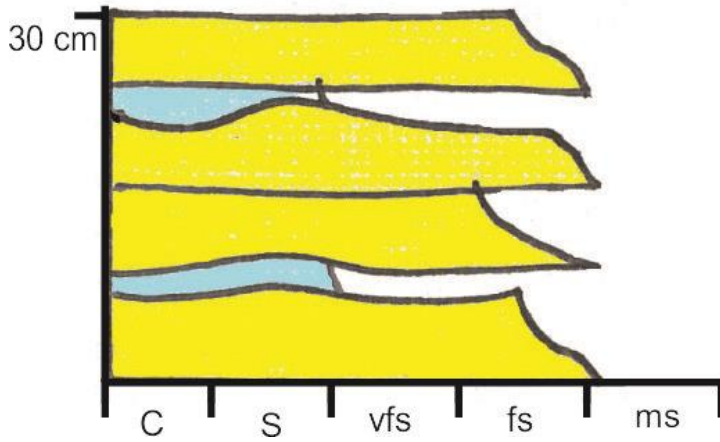


Figure 13: Block Diagram of BT 5

*Interpretation:* BT 5 conforms to  $T_a$  and  $T_b$  beds that (Bouma 1962) are defined as massive graded sands with rip-ups and occasional flame structures ( $T_a$ ) and fine sand with plane parallel laminae, and generally planar or wavy bases.

#### 4.1.6. Bed Type 6 (BT 6):

*Description:* Normal graded fine sand sandstone beds that display sheet like geometries, with planar bases, and asymmetric ripples in their lower sections which give way to structure less sand. The beds are between 5 and 10 cm thick.

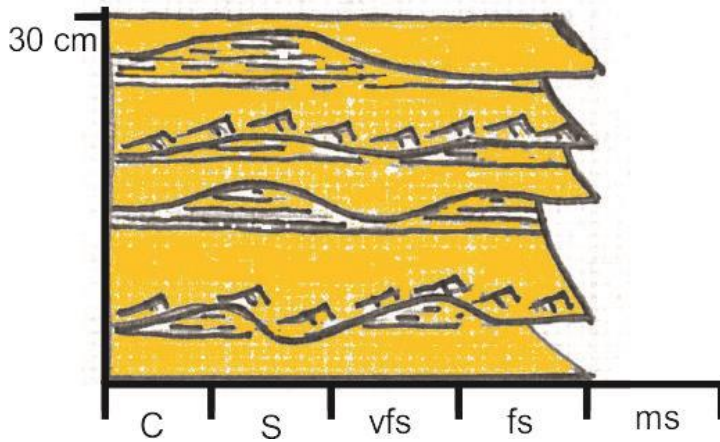


Figure 14: Block Diagram of BT 6

*Interpretation:* Due to the general sheet geometry, and normal grading of these deposits, BT 6 are interpreted as spill over or distal sandy turbidites from long lived quasi-steady flows. Kneller and Branney (1995) note that turbidites are not associated with tractive based deposits. Current ripples can indicate traction at the terminus of a surging turbulent flow according to Jackson et al. (2009).

#### 4.1.7. Bed Type 7 (BT 7):

*Description:* Thin, normally graded, tabular, clean, fine sand, sandstone beds with interbedded structureless mudstones. Beds are less than 3 cm, and the assemblages are between 50 cm and one meter thick. The assemblage becomes more dominated by fines upwards. Flame structures often occur in the muddy beds.

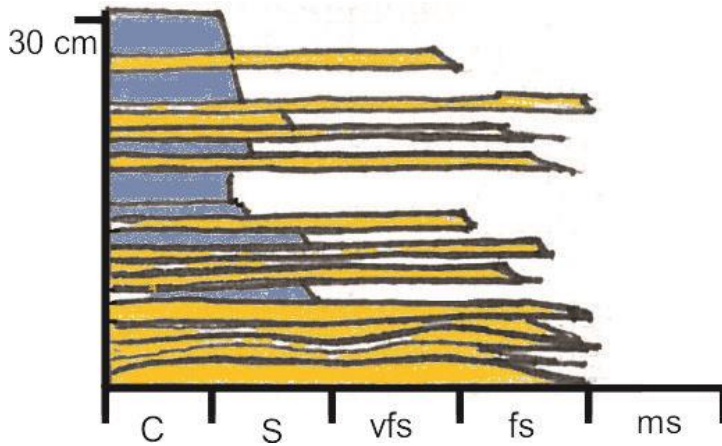


Figure 15: Block Diagram of BT 7

*Interpretation:*

BT 7 facies is interpreted as emplacements by distal turbulent flow emplacement.

It has been proposed that the fine grained heterolithics encountered on Hyrnestabben represent distal and off axis deposition, the general trend of these deposits underlying thicker sandy units is evidence of basin floor fan progradation (Crahaugh and Steel 2004). Jackson et al. (2009) attribute thin bedded upward fining sandy sheets to surge-like low density flows.

4.1.8. Bed Type 8 (BT 8):

*Description:* Reverse graded very fine to fine sand with plentiful organic clasts throughout, bases can be erosive. Top contact can also be eroded. Beds are between 10 cm and one meter thick.

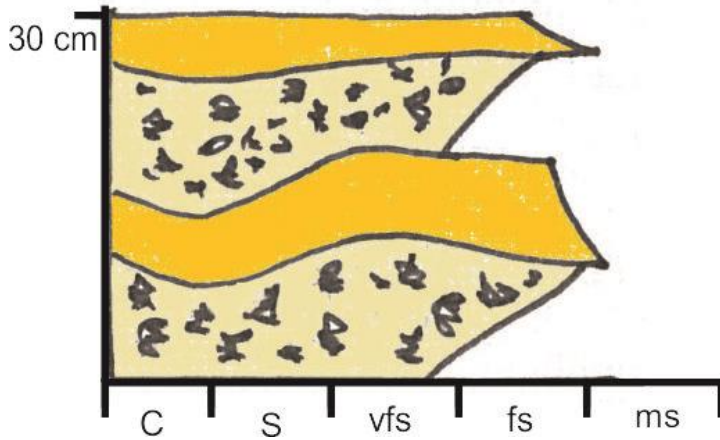


Figure 16: Block diagram of BT 8

*Interpretation:* BT 8 is interpreted to be deposited from a long lived quasi steady flow; or a flow, which deposited most of its load in a short space and time suppressing erosion and fabric development. Rapid fallout from suspension has the effect of turbulence and fabric suppression (Duller et al., 2010). Organic clasts are a good indicator of fluvial terrestrial sourcing of sediments in basin floor fans (Mulder et al., 2003; Plink Björklund and Steel, 2004; Nakajima, 2006; Zavala et al., 2006). Reverse grading is also indicative of waxing sub-critical flow conditions (Kneller and Branney, 1995).

#### 4.1.9. Bed Type 9 (BT 9):

*Description:* Laminated fine and normally graded very fine sand sandstone. Beds are less than 2 cm thick. The beds of the facies become progressively more thin and fine grained upwards. Ripples and erosional contacts are present in some beds, *Arenituba* and *Planolites* traces at bed boundaries.

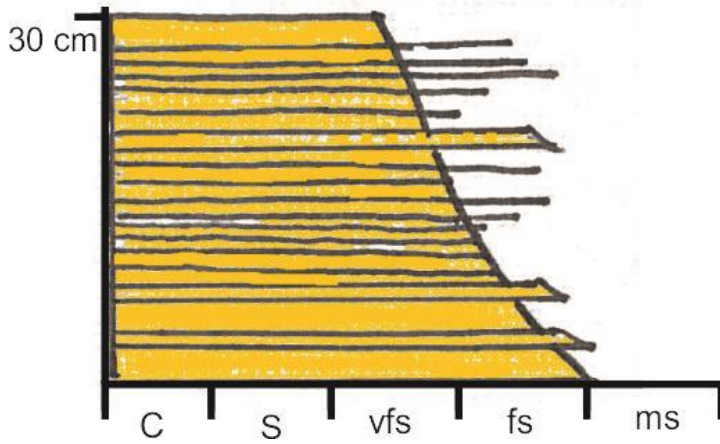


Figure 17: Block Diagram of BT 9

*Interpretation:* Off axis or distal sheet sandstones with a low sedimentation rate. (in *sensu* Grundvåg et al, 2014b) with some terminal or thin turbidite sheets. The facies is located predominately below or above thick amalgamated facies.

#### 4.1.10. Bed Type 10 (BT 10):

*Description:* upwards coarsening laminated siltstones and very fine sand sandstones, unconformably overlain by massive or normally graded very fine sand to fine sand sandstone bed. Laminations are less than 1cm thick, sandy beds are typically 2 to 5 cm thick. Beds have broad lateral extents.

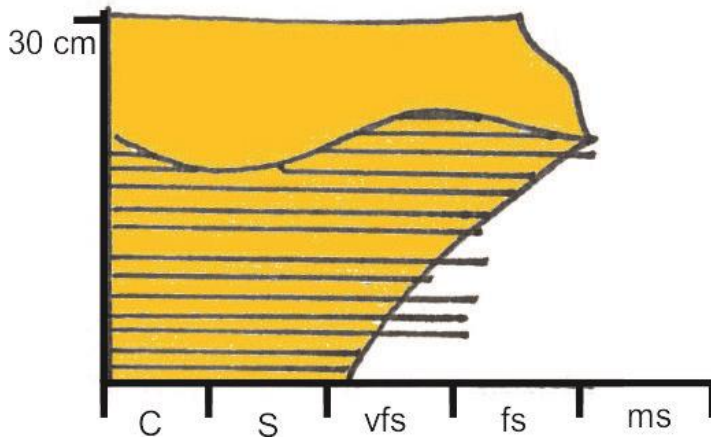


Figure 18: Block diagram of BT 10

*Interpretation:* BT 10 facies is analogous to what Crabaugh and Steel (2004) inferred coarsening upwards heterolithic within the Frysjaodden Formation as the initial deposits in a channel mouth or lobe-front setting, of prograding lobes. Clark and Steel (2006) note the presence of late lowstand wedge complexes, comprised of heterolithic deposits. The increasing grainsize of BT 10 deposits suggests a greater depositional energy, either from progradation or lateral migration toward the location.

#### 4.1.11. Bed Type 11 (BT 11):

*Description:* Thick sandstone deposits of fine sand to very fine sand, which grade normally, from a base of structureless sand, through laminated sand and into convolutedly bedded fine to very fine sand. Laminations in the unit are less than 2 cm, and total bed thicknesses are 60 cm to 1 meter. Units have tabular to wedge shaped geometry.

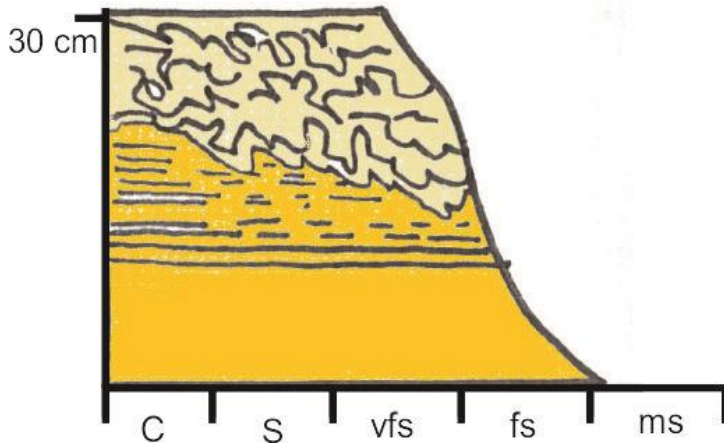


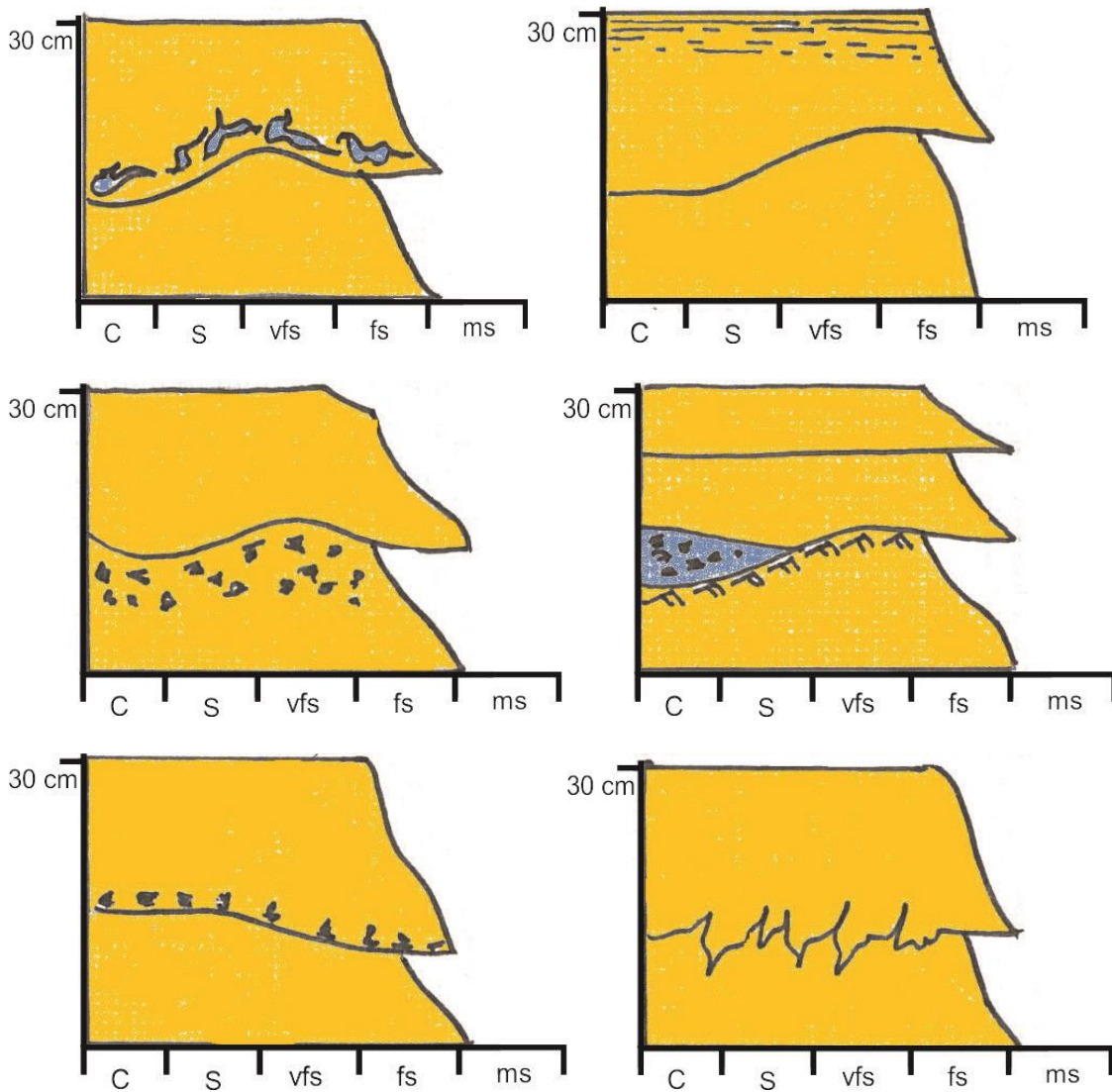
Figure 19: Block diagram of BT 11.

*Interpretation:* The transition of BT 11 from structureless to laminated sand, indicative of Bouma T<sub>a</sub> and T<sub>b</sub> beds into convolute bedding is inferred to be the result of flow bulking within a turbidite or mixed debris flow. Haughton et al. (2003) noted some hybrid beds to show syn-depositional upward dewatering of sandy, silty, and occasionally clast rich flows, overriding a slurry flow. Talling et al. (2013) noted the occurrence of flow freezing directly above Bouma T<sub>a</sub> type beds. The gradual fining and obfuscation of bedding planes can also be attributed to flow bulking, where by sandy turbidite type flows transition into debris flows by the addition of eroded fines (Haughton et al., 2009). The proportion of debris flows to turbidite flows in distal fan settings, increases with distance from flow initiation (Haughton et al., 2009).

#### 4.1.12. Bed Type 12 (BT 12):

*Description:* Medium sand or fine-grained sandstone beds, which display normal grading, and rapid changes in thickness over short distances. Individual beds can be between 10 and 50 cm thick; whole assemblages can be 20 m thick. Commonly the beds contain

organic detrital clasts, clay rip ups, asymmetric ripples, faint laminations, flame structures, dish and pillow structures. Bases of individual lobes are mostly wavy or planar. Organic detritus occur usually as distinct thin aligned bands in the bed bases, or in wider belts at the flow tops. Occasionally organics can occur throughout an entire lobe. Pillow and dish structures are more common in thicker units. Faint laminations indicate bed boundaries in heavily amalgamated sections. Silty rip ups can be often traced to thicker silty lenses or interbeds.



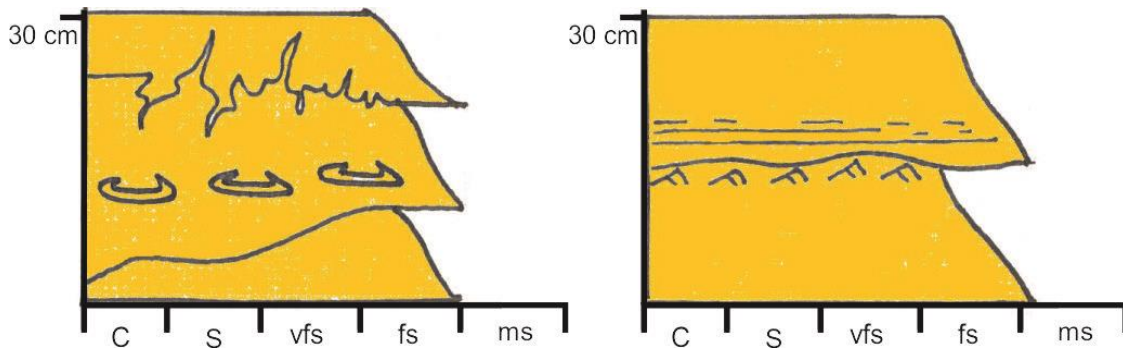


Figure 20: Block diagrams of bed-type 12



Figure 21: Beds Type 12, sandy bed with plentiful organics in the upper portion, border called out between organic rich upper portion, and lower sandy portion.

*Interpretation:* Bed type 12 is interpreted as thick toe of slope units, deposited from high density turbidites. Ryseth et al. (2003) encountered similar beds in a sandstone unit in the Sørvestnaget basin, which they interpreted as stacked high density turbidite deposits. The alternating thick beds with ungraded and plane-parallel laminated intervals is

suggestive of sustained turbidity current deposition (Kneller and Branney, 1995; Kneller, 1996). Abundant coal clasts and woody debris are indicative of a direct link to shelf edge deltas and continental fluvial sourcing (Mellere et al., 2002; Crabaugh and Steel, 2004). The considerable thickness and variability within the sandy units (Mellere et al., 2002) suggest long-lived and quasi-steady turbidity flows, commonly associated with hyperpycnal flows (Kneller and Branney, 1995; Zavala et al., 2006). Frequent lobe switching and compensational stacking within hyperpycnal fans (Mellere et al., 2002; Bourget et al., 2009; Grundvåg et al., 2014b) result in difficult to trace beds. Gradual or abrupt upward fining is likely due to waning flows. Current ripples are evidence of tractive deposition toward the end of the flow event. Mud clasts were interpreted by Jackson et al. (2009) to be emplaced from upstream erosion of underlying sediment.

#### 4.1.13. Bed Type 13 (BT 13):

*Description:* Reverse graded, clean very fine to fine sand sandstone beds 10 to 30 cm thick. The upper contact is erosional, and unit is typically overlain by a normally graded unit.

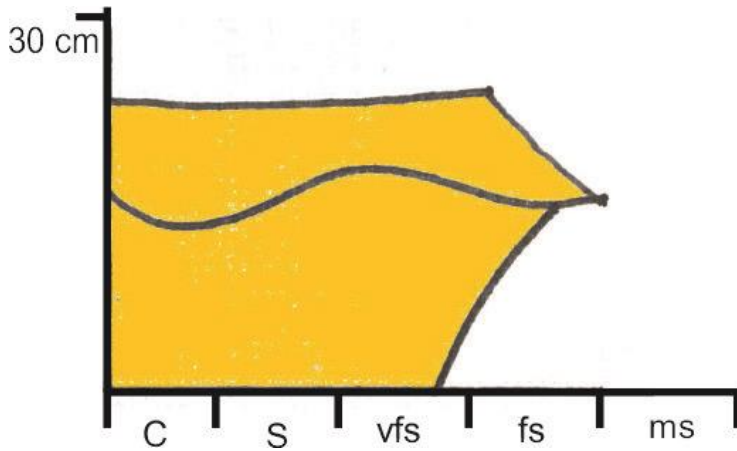


Figure 22: Block diagram of BT 13

*Interpretation:* BT 13 deposits are inferred to be the result of the waxing flow conditions. Pónten and Plink-Björklund (2009) attributed coarsening upward sequences in mouth bar deposits on Storvola to Hyperpycnal flows, which source slope and basin floor deposits of the Battfjellet (Crabough and Steel, 2004; Petter and Steel, 2006). Hyperpycnally sourced deposits were described as coarsening upwards sandstone and mudstone deposits (Pónten and Plink-Björklund, 2009). Most facies under traction plus fallout conditions, according to Zavala et al. (2006), are structureless or display low angle cross-stratification, parallel lamination or climbing ripples, until a critical velocity is met.

#### 4.1.14. Bed Type 14 (BT 14):

*Description:* Massive and structureless fine sand sandstone beds that are 5 to 30 cm thick with plentiful organic clasts throughout. The facies sometimes shows normal grading in the upper reaches of the individual beds. The lower contacts are heavily erosive or planar. The upper contacts are usually wavy.

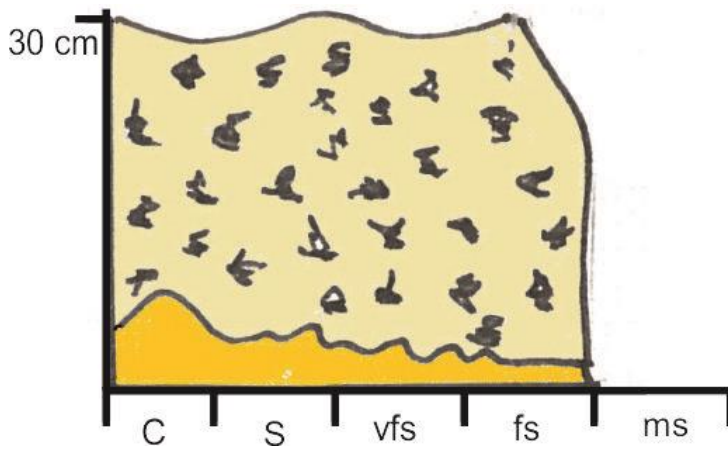


Figure 23: Block Diagram of BT 14

*Interpretation:* Rapid deposition of high density terrestrially or near terrestrially sourced sediments from long-lived, quasi steady hybrid currents is inferred to be the cause of BT 14. Rapid sedimentation rates can dampen flow structures (Talling et al., 2012) until the sediment load decreases at the end of the flow. Lowe (1982) observed turbulence intensity decreasing with depth within a flow. Shanmugam (2000) notes grain on grain interactions in dense underflows results in higher than usual support of large clasts. Kneller and Branney (1995) observed the occurrence of thick beds deposited from quasi-steady currents, whereby their thicknesses are functions of flow duration. Deposits emplaced by long-lived quasi steady high density flows lack traction structures (Kneller and Branney, 1995) The large down flux of grains, corresponding to the lowest portion of a flow, is continuously replaced by less dense more turbulent flow from above, resulting in a basal liquefied zone which includes the flow boundary (Kneller and Branney, 1995).

#### 4.1.15. Bed Type 15 (BT 15):

*Description:* BT 15 is defined by medium and fine grained sandstone with low angle cross stratification. The basal contact of the facies often shows flame structures, or fills scours in underlying beds. The bed often grades upwards into asymmetrical ripples and planar bedding.

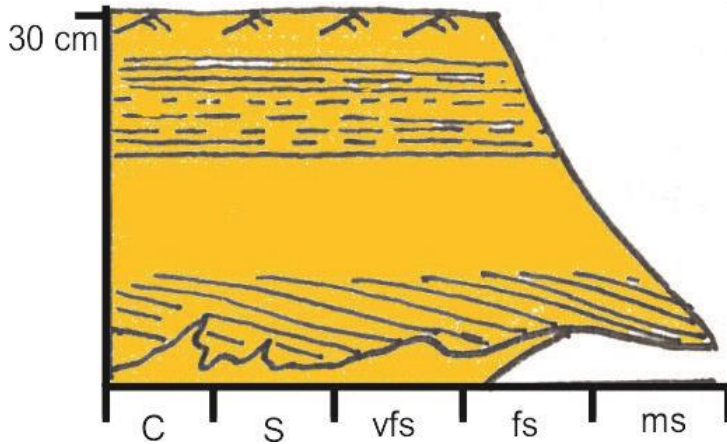


Figure 24: Block Diagram of BT 15

*Interpretation:*

BT 15 is interpreted as a deposit emplaced by hyperpycnal underflows. Mounds and smaller truncating laminations point toward a variable rates of super critical flow, over space (Lang and Winsemann, 2013). Zavala et al. (2006) describe tractive structures such as ripples and low angle cross bedding in hyperpycnal flows. The amalgamated beds do not display the broad change in grainsizes one would expect from a deposit resulting from a changing flood hydrograph, however Petter and Steel (2006) observed hyperpycnal deposits to not follow typical patterns. Lang and Winsemann (2013) note

that cyclic jumps related to flow thinning in deep sea fan settings can occur in mid-fan settings, resulting in patterns of laterally extensive humpback dunes.

There is debate whether cross bedding can occur in turbidite beds (Lowe, 1982; Shanmugam, 2002). Lowe (1982) noted that high density sandy turbidites have a tractive sedimentation phase of deposition. Stating, however, that flow dynamics producing them; standing waves and antidunes, were uncommon except in local instances (Lowe, 1982). The tractive sedimentation phase of deposition resulted in crude horizontal laminations and oblique cross bedding (Lowe, 1982). Cross bedding resulting from hyperpycnal flows occurs initially after flow velocities fall below the critical boundary ( $Fr=1$ ) (Zavala et al., 2006). Due to the relatively small scale of the basin floor fan, as well as its proximity to shelf edge deltas (Petter and Steel, 2006), hyperpycnal flow is interpreted to have emplaced the deposit.

#### 4.1.16. Bed Type 16 (BT 16):

*Description:* Structureless or normally graded medium, fine and very fine-grained sandstone, with basal lags of large interclasts, and plentiful terrestrial organic fragments.

BT 16 presents commonly with meters scale convex downward geometries.

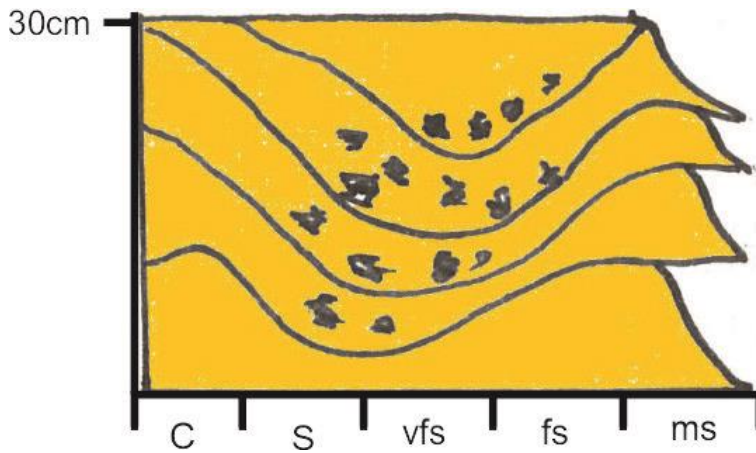


Figure 25: Block diagram of BT 16

*Interpretation:* BT 16 are interpreted to be channel filling deposits of cut and fill channels. Channels are not noted to be long lived in sand prone submarine fans (Bourget et al., 2009) who observed them to become rapidly bathymetrically indecipherable from fan lobes. The short lived basin floor fan channels do not develop into large scale bypass features. Mellere et al. (2002) interpreted units with basal shaley rip up pavements and convex geometries on the slope environment of the Battfjellet Formation, to be channel filling deposits. While slope channels observed by Mellere et al. (2002) were broad, others (Zavala et al., 2006; Bourget, 2009) note hyperpycnally related basin floor fan channels often are smaller. BT 16 was observed in the study area to be less than 4m thick, and less than 20 m wide. Their locations mid fan, near the tops of the sandy assemblages of clinofolds 14 and 15 can indicate that they developed in the later stage of the fan, or that high sedimentation rates (Plink-Björklund and Steel; 2004; Zavala et al., 2006; Bourget et al., 2009) resulted in rapid cut and fill channels (Grecula et al., 2003).

#### 4.1.17 Bed Type 17 (BT 17):

*Description:* Convolutely bedded upward coarsening then fining silt, very fine sand and fine sand. Basal silt gives way to very fine, then fine sand, which then grades back into very fine sand. Scours at the base of the flow denote erosion at deposition. The units are 20 cm to 1 m thick, and have tapering geometries.

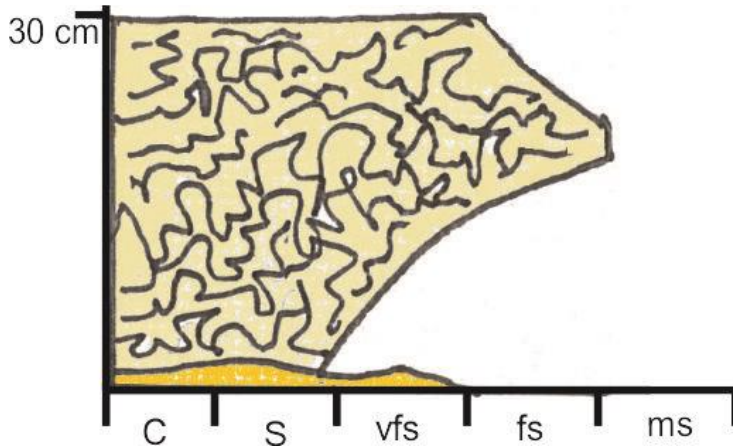


Figure 26: Block Diagram of BT 17

*Interpretation:* BT 17 represents distal debris flows. Incorporation of clay into flows resulting in flow bulking, can cause flow to behave more plastically, leading to settling impedance (Baas and Best, 2002; Amy et al., 2006) and eventual flow freezing (Haughton et al., 2009). BT 17 displayed a higher proportion of basal fines, a tapering geometry, and convolute bedding consistent with dewatering and hindered flow.

#### 4.1.18. Bed Type 18 (BT 18):

*Description:* convolutely bedded fine sand sandstones, normal or reverse grading apparent in the original clean sand beds. Individual beds are 5 to 10 cm thick.

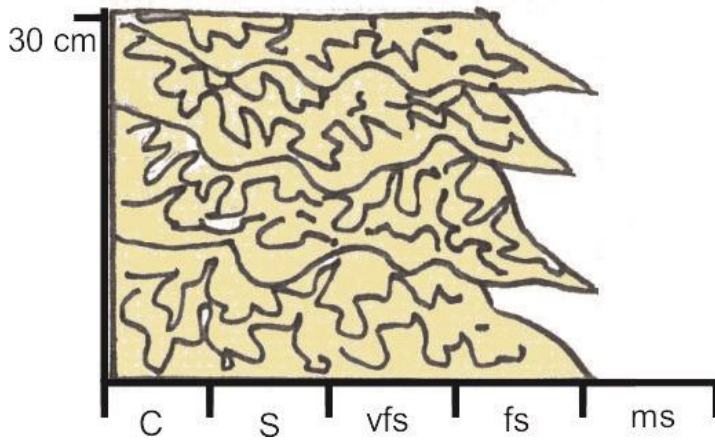


Figure 27: Block diagram of BT 18

*Interpretation:* Cryptic bedding of can be attributed to secondary mobilization of previously deposited sediments. In this case they are inferred to be the results of slumping. Flows are not inferred to be from terrestrially sourced massive flows, due to the lack of organics in the facies 18, and preservation of original bedding.



Figure 28: Convolutely bedded fine sands part of BT 18

#### 4.2 Facies Associations

Facies associations are composed of the previous bed types (table 1), and are divided according to their locations along the fan system. FA 1 represents background or basinal deposits. FA 2 are composed of lobe fringe deposits, FA 3 are off axis lobe deposits. FA 4 deposits are interpreted as on axis lobe deposits. FA 5 are channel or slump deposits.

#### 4.2.1. FA1- Background Basinal

Thin, (less than 1 cm.) fine grained, and dark laminated mudstones, typify the background basinal facies association. Infrequent isolated fine sand to very fine sand normally graded and thin (less than 3cm) sandstone beds are sometimes present. Pr elat et al. (2009) noted fine grained inter-units in the Karoo basin, while Lien et al. (2003) refer to basal mudstones in the Ross fan which are equivalent to FA 1. Frequent distributary switching has been inferred in the delta deposits within the Battfjellet Formation (Helland-Hansen, 2010; Grundv ag et al., 2014a). As a result very local transgressions and regressions, from changes in sediment pathways are present in shelf, slope, and basinal sediments. Some sediments in FA 1 show wavy or convolute bedding, when overlain by thick sandy assemblages. BT 1 (fig. 9), or BT 4 (fig. 12), are representative of background sedimentation. BT 4 is generally overlain by an amalgamated or thick surge type turbidite facies.

#### 4.2.2 FA2- Lobe Fringe Deposits

Thin (less than 3 cm) bedded heterolithic facies show reverse, normal, and no grading, and high silt content in the form of interbeds. Sandstone beds are predominantly very fine sand, with some fine sand as well. Climbing ripples are present in the silt to very fine sand grain size fractions. This facies association is interpreted as off axis and distal sedimentation in a lobe fringe settings. The higher proportion of sandy beds shows the increased influence of sediment gravity flows. FA 2 is similar to a heterolithic lithofacies described by Pr elat et al. (2009) in the Karoo basin, which was interpreted to result from dilute turbidity flows. Lobe fringe deposits in the present study are most frequently the result of low density surge type turbidites, evidenced by the predominance of normal grading. Deposits present as BT 2 (fig. 10), BT 3 (fig. 11), and BT 7 (fig.15) are part of FA 2.

#### 4.2.3 FA 3 - Off axis Lobe Deposits-

Off axis lobe deposits are recognized on their bed thicknesses (2–15cm). They are composed of very fine sand to fine sand grain sizes, in laminated beds without many silt inter-beds. Lower flow energies and longer intervening periods between events are inferred from this facies association. Pr elat et al., (2009) noted a medium bed thickness sandstone lithofacies, which they interpreted as off fringe axis deposition. The Ross sandstone contains thin bedded turbidite packages with 5cm thick sandy beds, separated by siltstones (Lien et al., 2003). Bed types contained within FA 3 on Hyrnestabben are: BT 5 (fig. 13), BT 6 (fig. 14), BT 9 (fig. 17), and BT 10 (fig. 18). These display structures congruent with Bouma surge type turbidites. The grain sizes within BT 10 coarsen upwards, suggesting lobe migration towards the location, in contrast with BT 9 in

which the normal graded laminated beds become more dominated upwards by fine grains. BT 5 and BT 6 correspond closely to lateral splay turbidites.

#### 4.2.4. FA4 On axis lobe deposits-

On axis lobe deposits are composed of thicker (15 to 60 cm) bedded units, showing high degrees of amalgamation high sediment input, or rapid deposition is inferred. These deposits are represented by BT 8 (fig. 16), BT 11 (fig. 19), BT 12 (figs. 20, 21), BT 13 (fig. 22), BT 14 (fig.23), BT 15 (fig. 25), and BT 17 (fig. 26) (table 1). On axis lobe deposits display dish structures, pillows, flame structures, massive grading, and poor grading indicating high sedimentation rates, as well as erosion. Debris flows are included in this facies association. Prélat et al. (2009) describe an on axis thick bedded highly amalgamated units, resulting from high density flows, to which FA 4 is genetically similar. Bipartite beds were contained within the thick bedded lithofacies of (Prélat et al., 2003). Thick bedded amalgamated facies were described in the Ross Sandstone, typified by rapidly changing bed thicknesses, with thicknesses ranging between 23 and 612 cm (Lien et al., 2003)

Normal graded bed types with highly amalgamated boundaries were determined by the presence of abrupt grainsize changes, planar or erosive margins, truncated structures, rip up mudstone clasts, silty lenses, organic bands, flame structures, and ripples. BT 12, in particular, is defined most by boundary structures. Flame structures are indicative of high rates of deposition deforming the underlying bed while rip ups in the system indicate some degree of erosion. Pinching out silty lenses indicate also either the degree of

erosive forces in the overlying flow or its rapid deposition, causing deformation. Rip ups were interpreted by previous workers to indicate basal surfaces of thick sandy beds (Crabaugh and Steel, 2004; Plink-Björklund and Steel, 2004; Mellere et al., 2002). Well defined organic clast rich horizons, showing good alignment are inferred to be deposited from the bottom of the flow consistent with Plink-Björklund and Steel (2004) (Mellere et al. 2002). Thicker but less dense bands of coals clasts, showing less alignment are more likely the result of the tail of a flow losing energy and depositing the more buoyant organic clasts (in. sensu Crabaugh and Steel, 2004). The slope toe is a typical environment to encounter reductions in flow energy. Structures within the bed types in FA 4 are indicative of a variety of processes. Normal grading is suggestive of a waning flow or a depleting flow energy (Kneller, 1995); BT 12 and in some cases BT 14. BT 8 and BT 13, show reverse grading, while BT 11 and BT 17, have convolute bedding, which often indicate plastic flow rheologies (Baas et al., 2011).

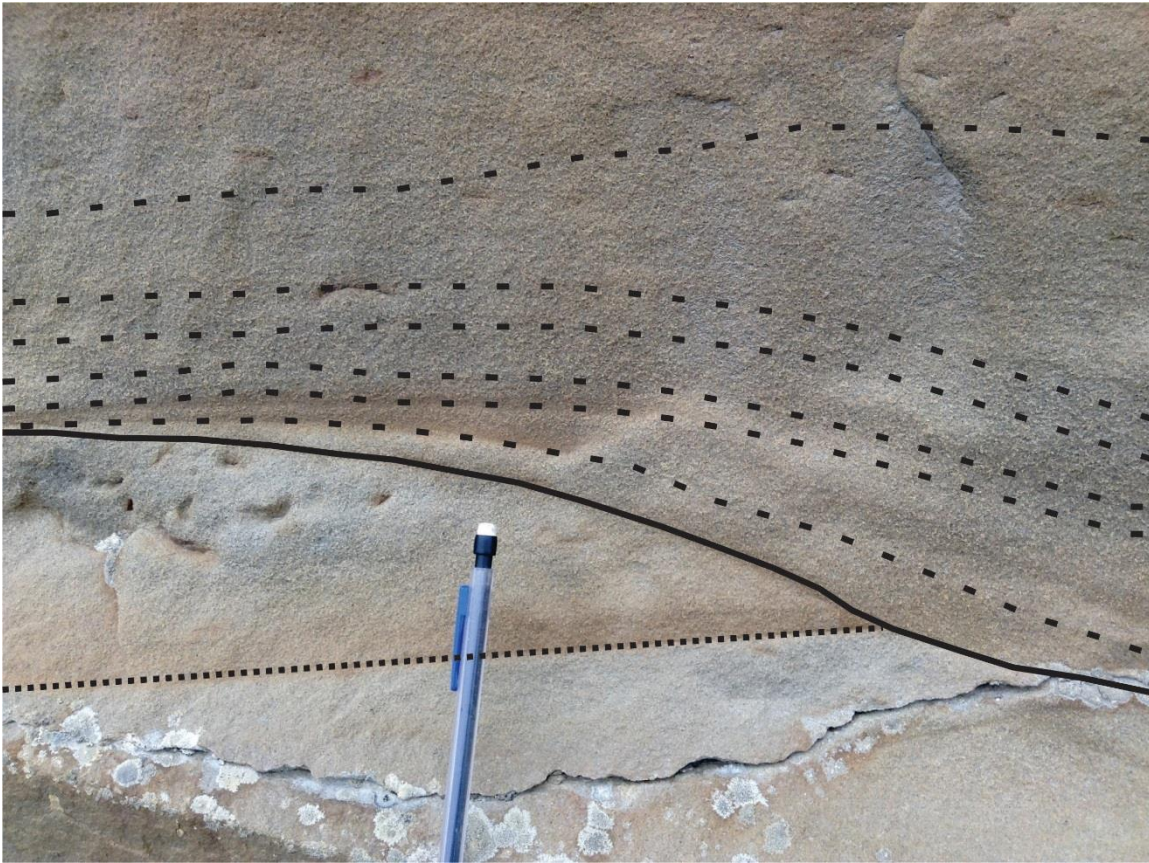


*Figure 29: Truncating Mounds of BT 15, low angle bedding gives way to massive sand.*

#### 4.2.5. FA5-Channel deposits:

In the upper portion C14b, some channel features are visible (fig.30). Bed types BT 16 (fig. 25) and BT 18 (figs. 27, 28) comprise FA 5. Convex downward geometries, coarse grainsizes, and large organic detritus in fine grained to medium grained sandstone beds. With an exposed lateral cross sections less than 20 m, and a total depth of assembly less 4 m, the feature resembles cut and fill type channels. Well exposed, individual, channel fill features in the Permian Laingsburg Formation, had between 3 and 10 m of down-cutting

(Grecula et al., 2003). BT 18, convolutedly bedded fine sandstone deposits occur in limited areas, also in the upper portions of the fan bodies. Thickest slumps are in the middle of the exposed section (W10 to W14) (figs. 52, 56). Over steepening, and resultant channelized debris flows have been linked broadly to late wedge debris flows (Posamentier and Kola, 2003, Clark and Steel, 2006). Within the system there is debate whether the driving factor in deposition is sedimentation rate (Helland-Hansen, 2010; Grundvåg et al., 2014a), or sea level rise and fall (Crabaugh and Steel, 2004). Over steepening can result from either condition, either eastward progression of the system, caused by high sedimentation rates, or from sea level changes steepening the source to sink gradient.



*Figure 30: Channel cross section with Backpack and rifle for scale in lower right hand corner.*

### 4.3 Depositional Architecture

Description: The investigated succession at Hyrnestabben has over 100 m of sediment gravity flow deposits stacked in four wedge-shaped sandstone bodies, separated from each other by between 3 and 12 m thick mudstone units. The longest section collected, passes through C12, C14a, C14b, and C15 with a total length of 104 m. Comparing deposits between the lobes in this section reveals system progradation occurred in the system during the deposition of the fans. Some have noted the sandstone dominated lobes in the Frysjaodden Formation to be compensationally stacked (Mellere et al., 2002; Johannessen and Steel, 2005). The lowermost cliff-forming turbidite sandstone (figs. 31, 32, 33) belongs to clinoform 12 (Steel and Olsen, 2002; Crabaugh and Steel, 2004). The submarine fan sections of clinoform 14 and 15 on Hyrnestabben have been well characterized (Steel and Olsen, 2002; Crabaugh and Steel, 2004; Plink-Björklund and Steel, 2004; Johannessen and Steel, 2005; Clark and Steel, 2006). The submarine fans show a two-fold architecture (fig. 31). The lower part is heterolithic and thin bedded facies which in the present study are characterized by FA 2 and FA 3. The heterolithic units grade upward into thicker bedded coarser grained deposits (Crabaugh and Steel, 2004, FA 2, FA 3, FA 4 or FA 5 in this study).



*Figure 31: Twofold fan architecture, at W21, with thin bedded heterolithics overlain sharply by amalgamated sandy beds.*

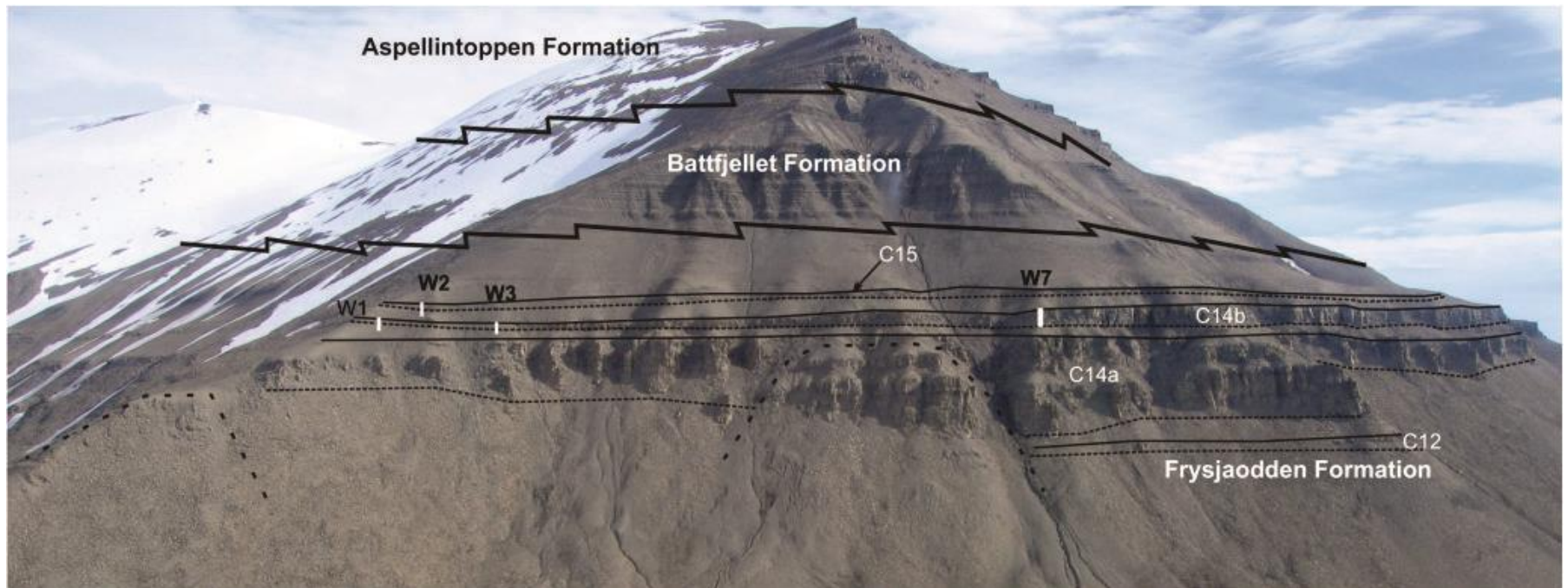


Figure 32: The Western proximal reaches of the basin floor fans, with W1, W2, W3, and W7 called out.



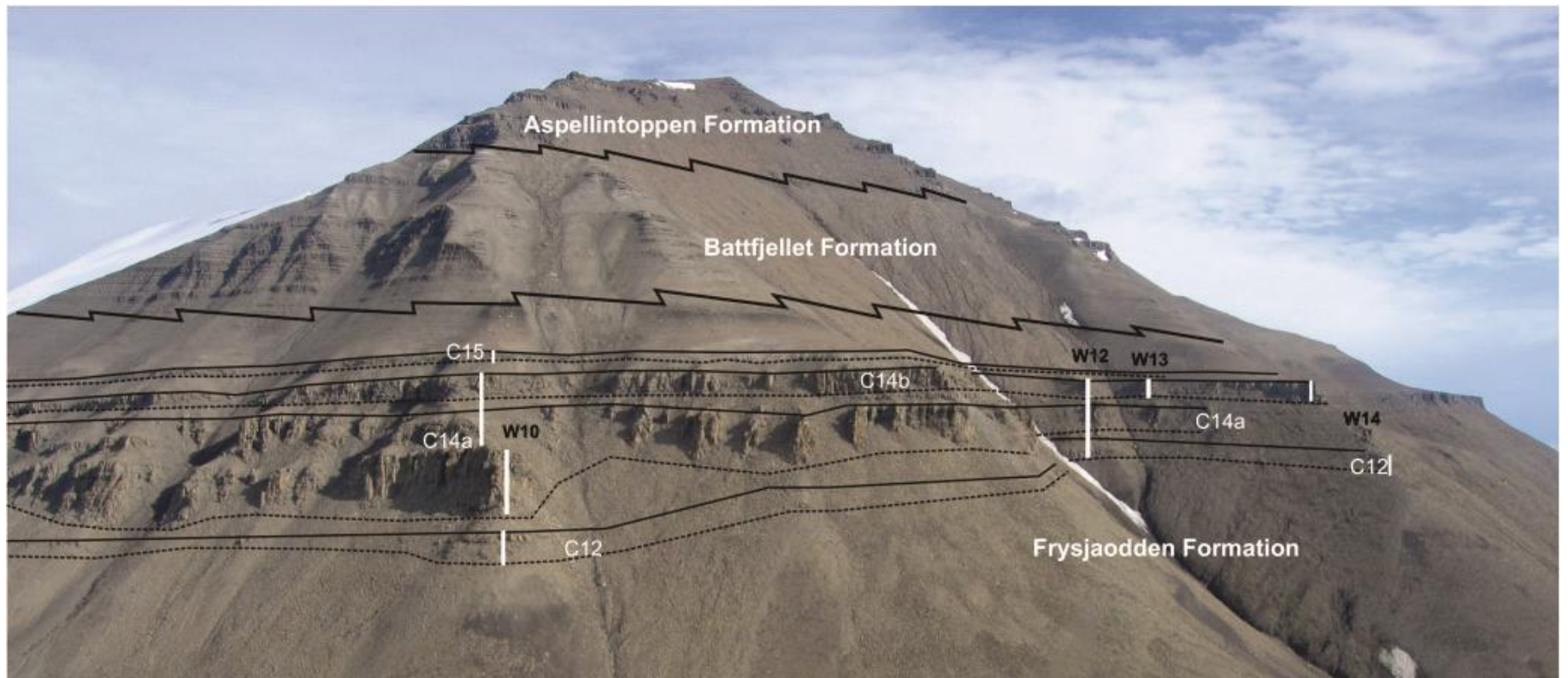


Figure 33: Aerial photo of the medial lobes, with call outs of W10, W12, W13, and W14 called out.



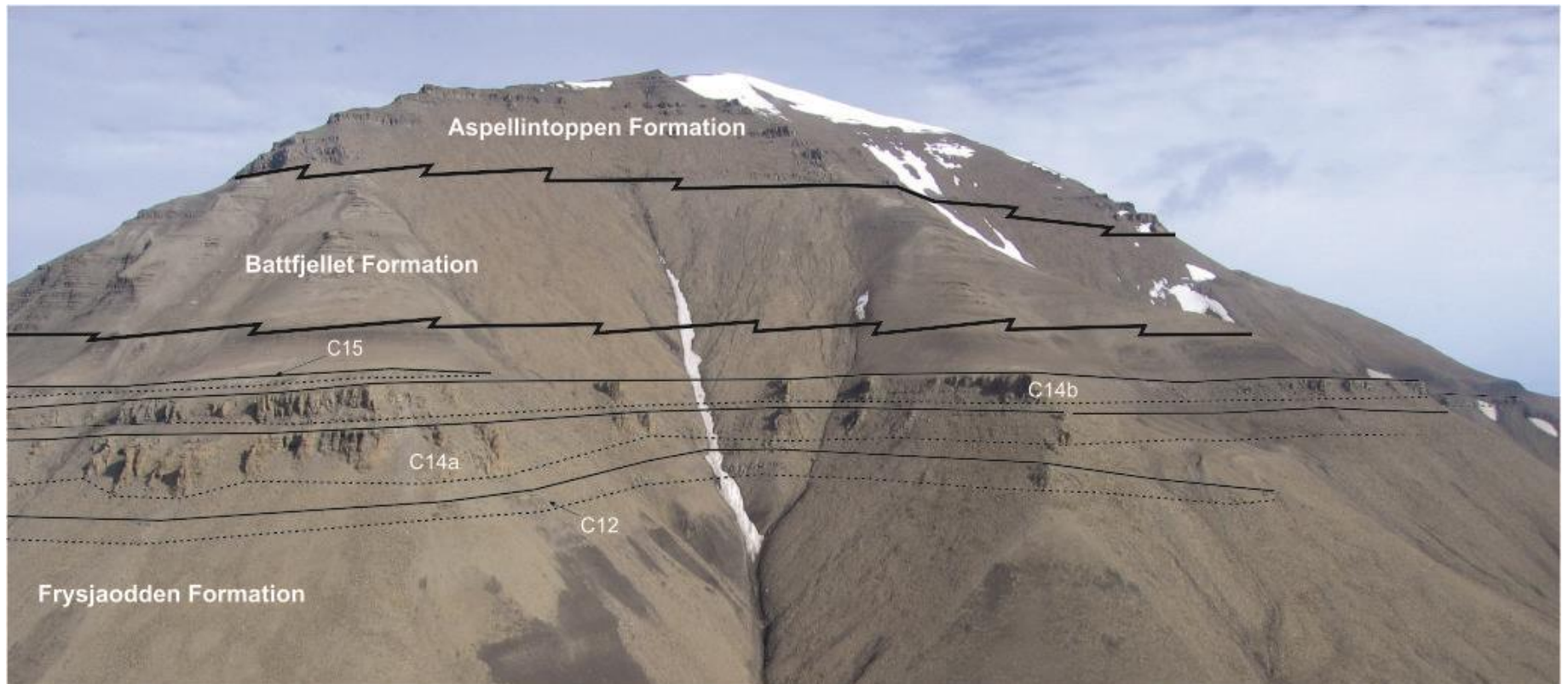


Figure 34: Medial fan with submarine fan lobes called out



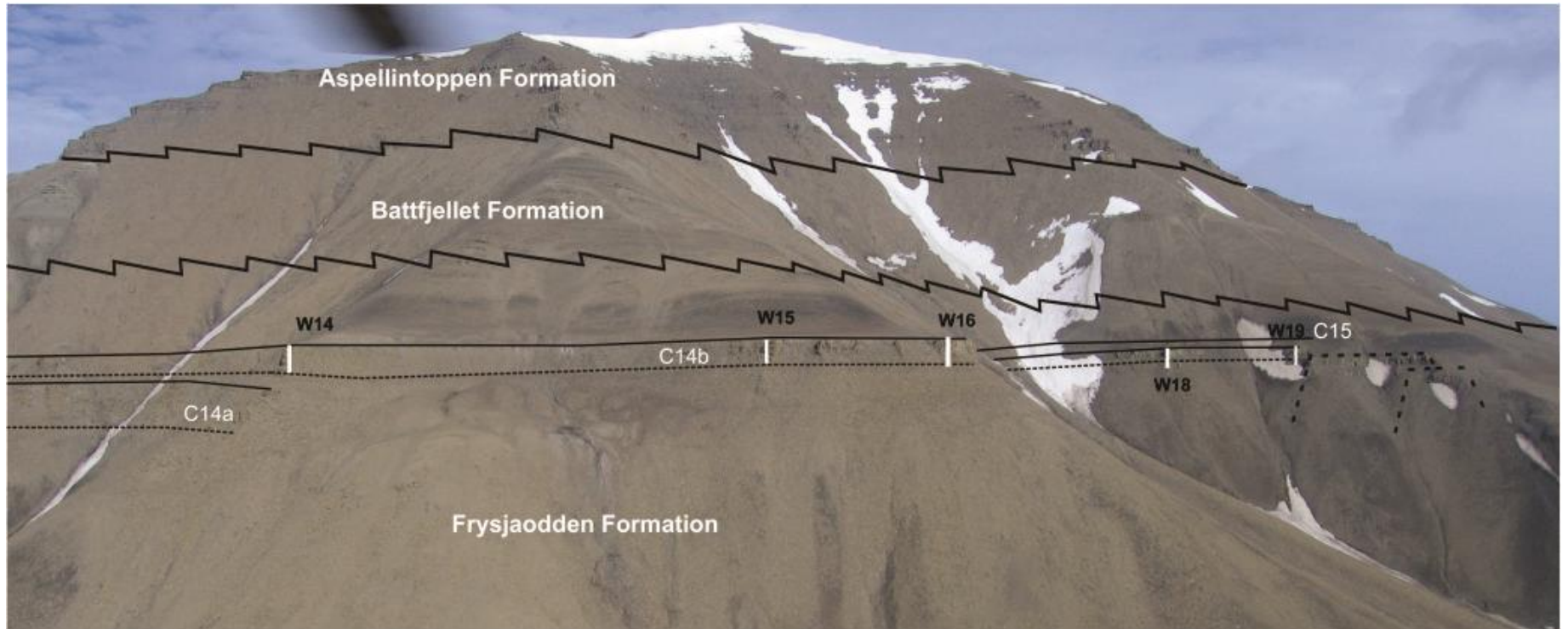


Figure 35: Medial to Distal fan locations, with W14, W15, W16, W18, and W19 called out.



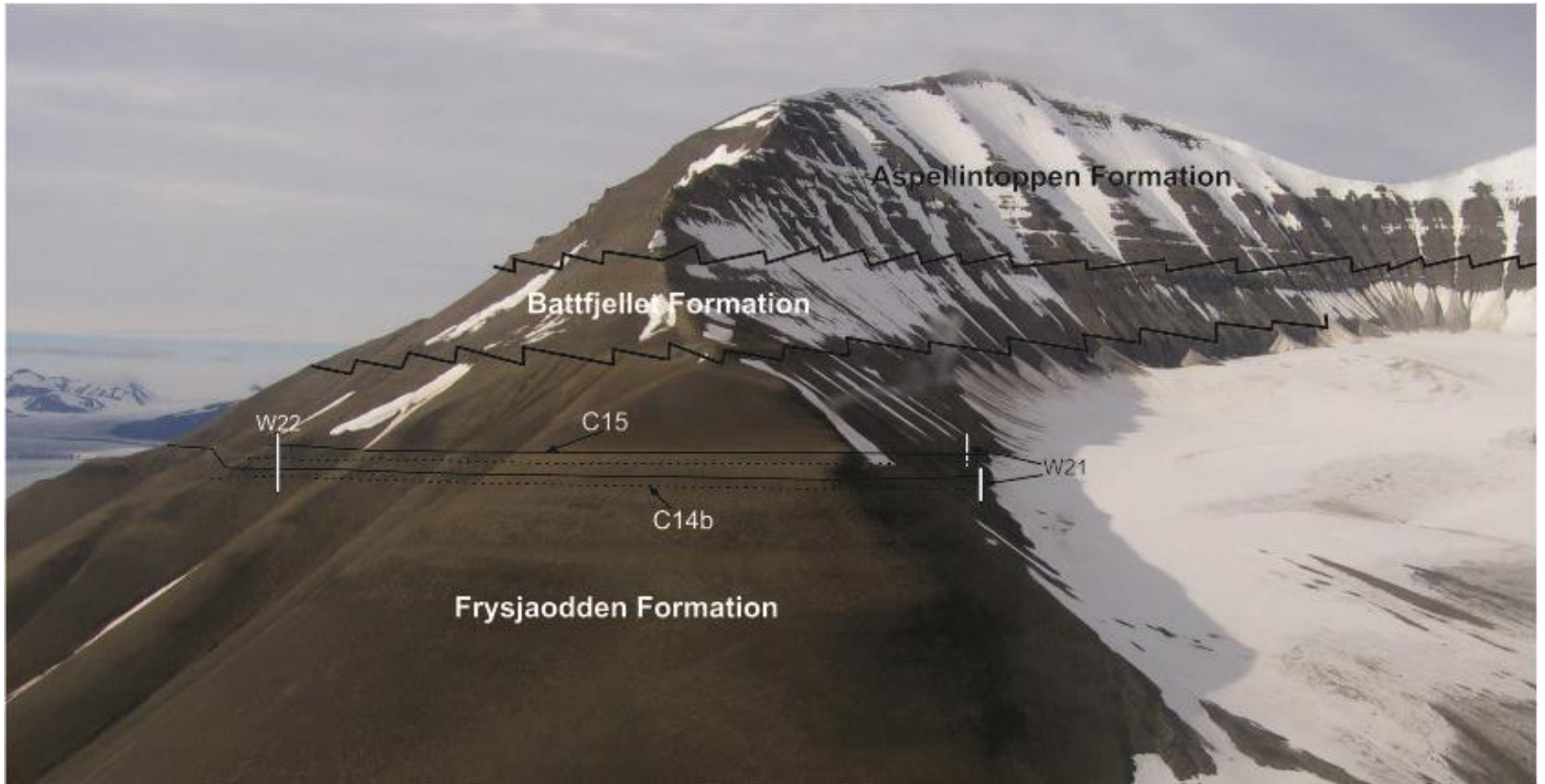


Figure 36: The backside of Hyrnestabben, distal outcrops W21 and W22 called out

#### 4.3.1 Lobe stacking pattern of C12:

The two logged sections intersecting lobe C12 (W10, and W12) (figs. 52, 54) are medially located (figs 5, 6, 32). C12 in these locations thickens distally from 3 m to 6 m. FA 1, FA 2, FA 3 and FA 4 are represented in the logged sections (W10 and W12) (fig. 37). The shale wedge separating C12 from C14 thickens basinward from 3 to 8 meters. Three amalgamated, FA 4, sections of BT 12 are present in W12, separated by successions of FA2. In the more proximal W10, the lower 1.5 meters of C12 are comprised of BT 12 (FA 4) (fig. 36). Overlaying the amalgamated facies, are two lobe assemblages of FA 3, separated by FA 1. The fan at W10 has two sandy sections separated by three meters of basinal shales (FA 1). The deep sea fan of clinoform 12 begins to outcrop on Storvola (fig.4). Hyrnestabben represents the most distal exposed segment of C 12 (fig 4). W10 and W12 are roughly 500 m apart (figs. 38, 62) Individual bed thicknesses are greatest in W12. Thick normal graded sandstone beds (BT 12) comprise the majority of the FA 4 present in the two sections through C12 .Two beds of linked debrites are present in the uppermost portion of C12 at W12. The two data points cannot have beds reliably correlated, but the prevalence of FA 3 in the more proximal location, and its absence in favor of FA2 in W12 suggests the effects of lobe migration are more pronounced farther basinward.

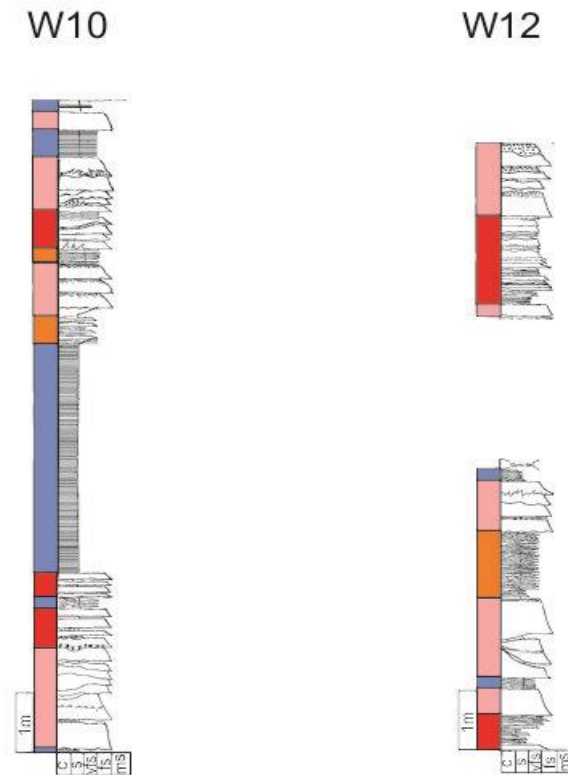


Figure 37: Correlation panel of C12, two lobes are separated by FA1

#### 4.3.2. Lobe Stacking Pattern of C14a:

Two logs pass through C14a; W10 and W12 (figs. 5, 6, 32) W10 (fig. 52) passes through 51 m of lobe deposits, W12 (fig. 54) passes through 34 m of C14a. C14a is the most prominent of the deep sea fan lobes on Hyrnestabben (Fig. 34). Facies associations FA 1, FA 2, FA 3, FA 4, and FA5 are represented. Amalgamation is high in the logged portion of C14a, with a 3m thick slump (BT 18) in the mid portion. The logs are mostly characterized as FA4 with thin intervening sections of FA 3 and FA 2 (figs 52, 54) BT 10(fig. 18), BT 13 (fig. 22), and BT 15 (fig. 24) occur regularly within the FA 4 assemblages. Beds however are predominately of BT

12. Medium sands occur in C14a. 10 to 15 cm beds of BT 14 occur on top of normally graded sandstones. The area studied of C14a represents the thickest sandstone outcrops of any submarine fan studied.

#### 4.3.3 Lobe stacking pattern of C14b:

C14b has the most lateral exposure of the submarine fans, subsequently it is the most logged unit of the study, with some portion of all logs, but W2, passing through the lobe. Figure 38 shows the entire correlation panel. A proximal portion of the lobe roughly 300 meters from W1. The thickest, medial section of the lobe occurs roughly between 300 m and 1800 m (fig. 38) the distal section of the fan body occurs beyond 1800 m. Most proximally, W1 (fig. 47) is dominated by FA 1. The lowermost portion of the logged unit, roughly two meters is characterized by distal lobe deposits. 80 m basin-ward, at W3, the assemblage is characterized as FA 4 overlying one meter of FA 1. C14b gradually thickens for 280 m basin-ward from W1. At W7, the thickness of the lobe increases more abruptly (fig.38). Proximal of W7, lobe deposits (FA 2, FA 3, and FA 4), are less than 8 m. Basin-ward of W7, the logs are characterized by intervals of FA 4 broken up by FA 2 or FA 3. At the thickest logged section, C14b is 25 m thick. Log W12 (fig. 54) location is characterized by 2–5 m intervals of FA 4 separated by units of FA 3 or FA 2. FA 5 is present in the medial (W10–W18) portion of the lobe. The fan thins gradually to W18, which is 18 m thick and located roughly 1780 m from W1. The bases of many of the outcrops are obscured by hillside scree. The most distal outcrops of C14b are less than 10 m thick, and separated from C15 by 3 m to 6 m of scree.

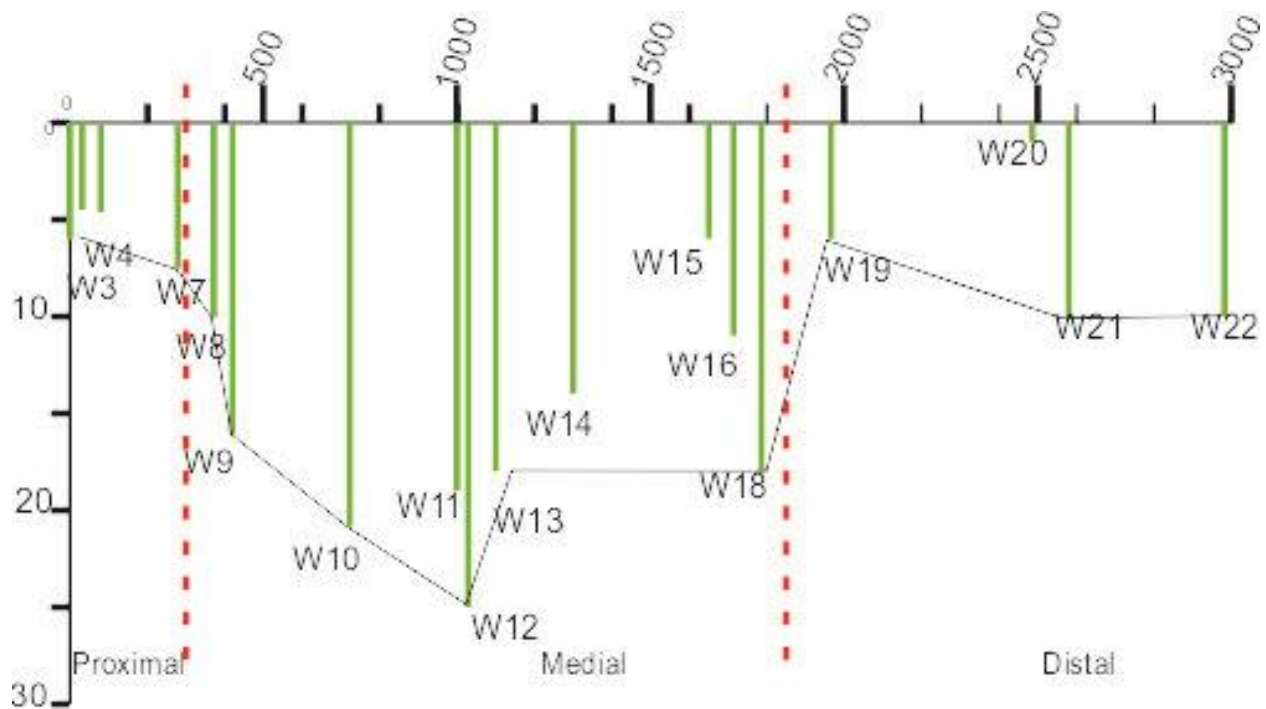


Figure 38: Correlation of log thicknesses of C14b, proximal, medial and distal refer to location, not environment. Horizontal and vertical scale are in meters. W1 starts at 0m. Log heights are measured from the top.

Normal graded beds occur with the greatest frequency in the proximal reaches of the fan, the most proximal portion of the fan where BT 10 (fig. 18) was encountered is at W7. The thickest portion of the fan, between W8 and W 18, contains reverse grading, and debris beds occur with the greatest frequency. Debris flow emplaced bed types (BT 8, BT 11, BT 14, and BT 17) (table 1) were frequently encountered overriding normal graded fine to medium grained sandstone beds (BT5, BT 6, and BT 12). BT 13 (fig. 22) and BT 15 (fig. 24) were also observed in the mid fan reaches.

Intervals of FA 3 in proximal sections consist mainly of BT 7 and BT 10 (fig. 18). Large scale erosion was not observed under FA 4, in the medial fan portions, between 700 m and 1800 m basinward from W1. More commonly, there were planar bases and meter scale scours at the

contacts between amalgamated beds (FA 4), and underlying thin beds (FA 1, FA 2, FA 3). The observation agrees with previous assertions by other workers of the deposit (Crabaugh and Steel, 2004; Petter and Steel, 2006). The proportion of heterolithic distal lobe deposits (FA 2) increases basinward. In the most distal logged outcrops, the deposits ranged from typical basinal mudstones (FA 1) to thin normally graded very fine-grained sandstones (FA 2). It is inferred that bypass was occurring at proximal locations while the submarine fan was being deposited, which is consistent with Mellere et al.(2002) (Crabaugh and Steel, 2004; Petter and Steel, 2006) who noted that deep water coarse grained deposits in the Battfjellet system are generally associated with shelf edge deltas, and a deeper shift of depocenter. Amalgamated paleoflows trended north of east, making an accurate count of lobe bodies problematic.

#### 4.3.4. Lobe Stacking Pattern of C15:

Logs W2 (fig. 47), W10 (fig.52), W20 (fig.60), W21, and W22 (fig.61) pass through the deep sea fan of clinoform 15 (fig. 39). The lobe is between 4 m and 6 m, with its thickest portion in the most distal logged sections location. Beds thicken distally in C15, the most proximal location logged is comprised of FA 2 and FA 1, showing parallel laminations, with some wavy bed boundaries and cm scale bedding. In the medial W10, the assemblage is thicker, however beds are still centimeter scale. They are assembled in meter scale fining upwards sequences, the bases of which underwent extensive soft sediment deformation. This same scale of sediment deformation noted in some beds of W10 (figs. 39, 52) was observed near W18, from the camp toilets, but not logged. The distal log W22 is a thick bedded slumping debris flow (BT 18). C15 dips more steeply than C14b, in proximal location as intervening mudstone thins basinward.

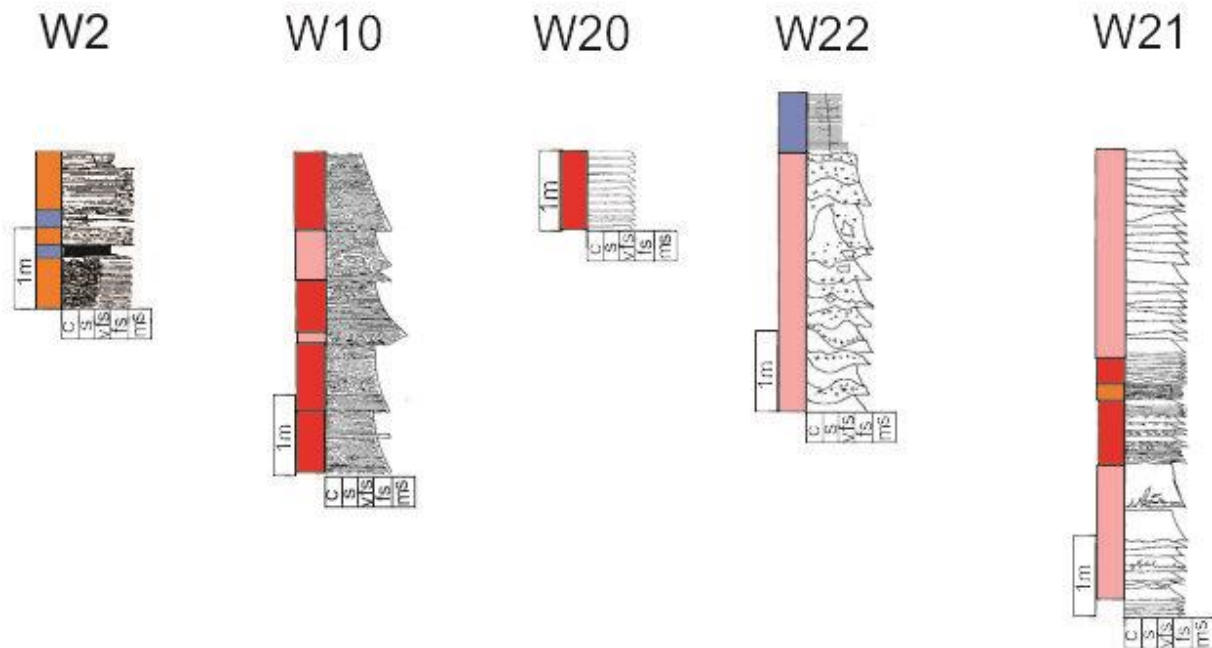


Figure 39: Correlation Panel of C15, W20 is interpreted to be an off axis deposit, thin bedded sandy deformation was present in C15 above W17 too.

#### 4.3.5. Comparison of the lobes C12, C14a, C14b, and C15:

Throughout the lobes, the degree of amalgamation is highest at the thickest points. The most bed types from FA 4 are also present in the thick medial section of the lower three lobes. The western outcrops are dominated by normal graded type turbidite sands (BT 2, BT 5, BT 6, BT 7, BT 9, BT 12, BT 16)(table 1) in all but C15. The thickness of FA 4 assemblages also increases in the thickest portions of the deep sea fans. C15 is least like any other lobe, the prevalence of FA 1 and FA 2 in the limited outcrops as well as the thinning basin-ward wedged geometry of the intervening shale between C14b and C15 supports the assertion that C15 on Hyrnestabben is depositionally more proximal, than the underlying deep sea fans C12, C14a, or C14b, the result of a prograding system. The western outcrops of C15 are depositionally more indicative of lower or base of slope deposits. Paleoflow directions in the system trend from a generally

eastward, in lower deposits portions of C14a, C14b, and C15, and shift farther northward in the upper sandier portions of the deposits. Trace fossils are more common in the proximal sections, and are comprised of *Planolites*, *Thalassinoides*, *Arenituba*, *Helminthopsis* and *Phycosiphon*. Trace fossils in the mudstones and most fine-grained bed types are predominately *Phycosiphon*.

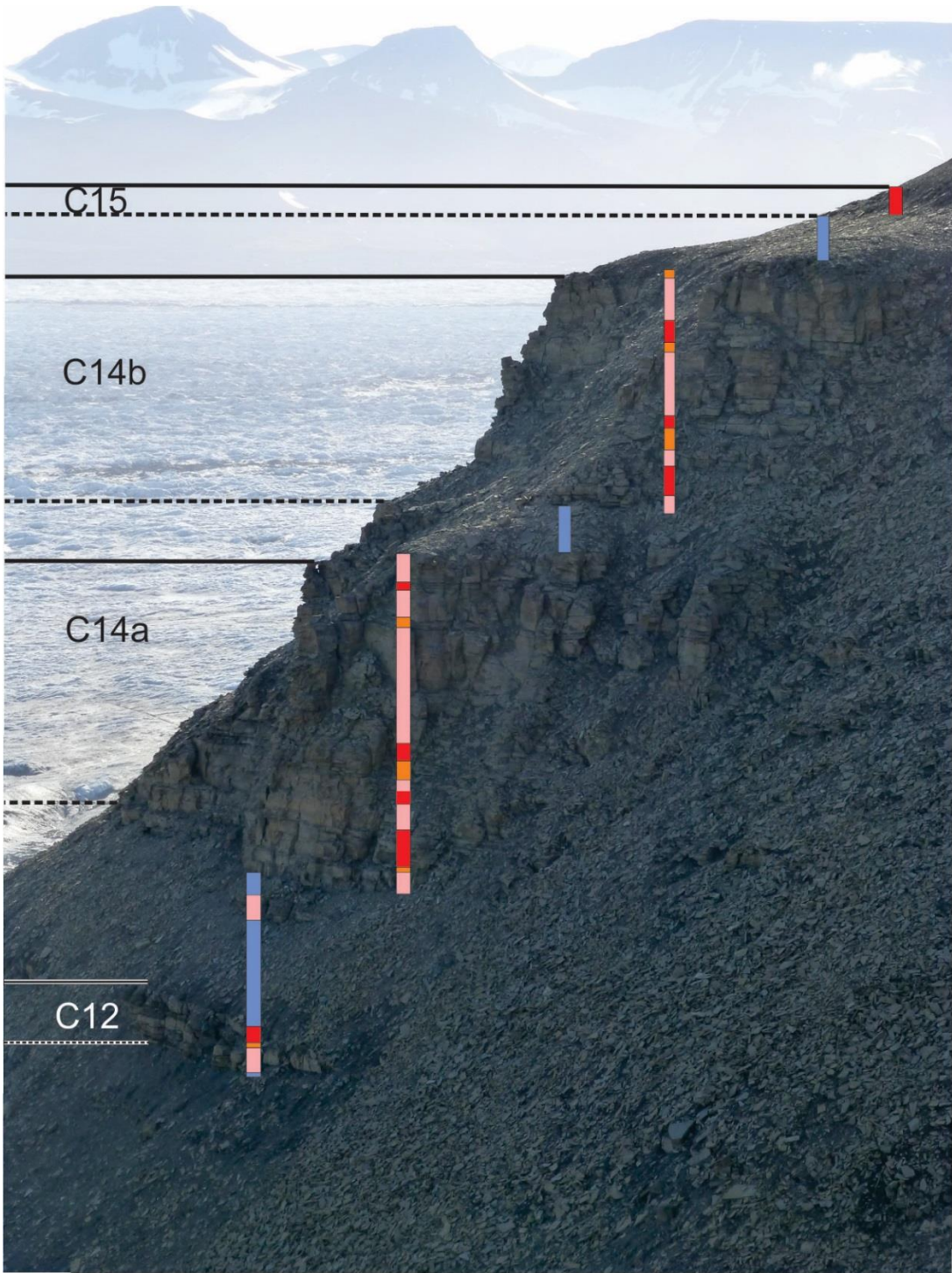


Figure 40: Top lobe of clinoform 14 with thin bedded lateral splay sandstones called out (FA 3) between thick amalgamated facies (FA 4)



## 5. Discussion

### 5.1. Origin of Bed Types

The relatively short shelf, and proximal location of the shore (Crabaugh and Steel, 2004, Petter and Steel, 2006), to the deep sea environment during the formation of C12, C14a, C14b and C15 led to the emplacement of beds from a diverse set of processes. The processes leading to the various bed types in the submarine fan, include surge type turbiditic flows, hyperpycnal underflows, slurry or hybrid flows, debris flows, and slumping. Outcrop evidence including structures, grading, geometries, boundaries, and grain size were used to determine the dominant process of flows leading to the individual bed types.

#### 5.1.1. Deposits emplaced by surge type turbidites

Bed types emplaced by surge type turbidites are BT 2, BT 5, BT 7, and BT 9 (table 1). Deposits resulting from surge type turbidites were established by their relative thinness, location, and normal grading. BT 2 conforms closely to Bouma T<sub>c</sub> and T<sub>d</sub> (Bouma, 1962) type deposits. BT 5 (fig. 13) resemble T<sub>a</sub> and T<sub>b</sub> beds (Bouma, 1962). They have associated silty tops, meaning a preserved reduction in flow energies, and likely lower sediment concentration in the flows (Shanmugam, 2000). These occur in FA 1, FA 2 or FA 3, and are inferred thus to be distal sediment gravity flows, and lobe fringe deposits. They are more than likely laterally linked to more proximal deposits.

# Classic Turbidites

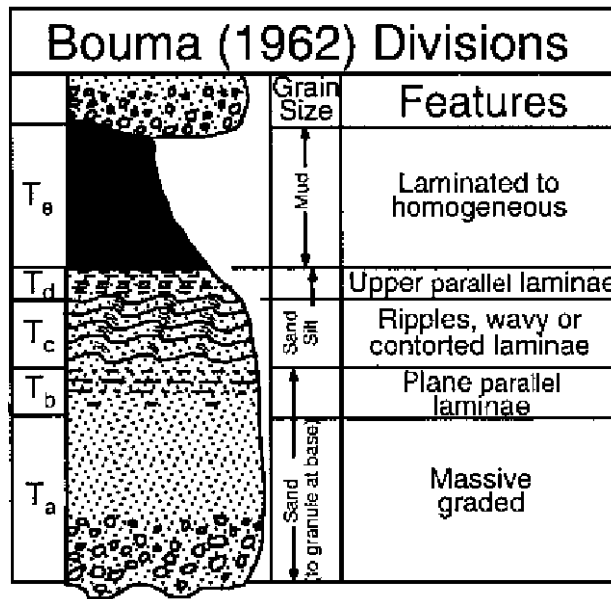


Figure 41: The Bouma Sequence for turbidites, adapted from Shanmugam (2000)

## 5.1.2. Deposits deposited by sustained flows or hyperpycnites

Bed types resulting from sustained hyperpycnal flows in are BT 13 (fig. 22) and BT 15 (fig. 24). The association of BT 10 (fig. 18) with an overlying bed of BT 15, could also be indicative of hyperpycnal underflow deposits. Hyperpycnites were somewhat difficult to establish in the deep sea fan. Shelf and slope deposits in the system were identified as hyperpycnal by their physical connection to fluvial channels, abundant coal clasts, low abundance of slumped material, thick individual sandy turbidite beds with pinch out geometries, and their location in accreted shelves (Plink-Björklund and Steel, 2004). Means for determining hyperpycnal deposits in the deep sea fans were coarsening upwards sandy beds, abundant organic material, and structures not generally linked with turbidite deposits (e.g... low angle cross bedding, climbing ripples, faint

laminar bedding, and pronounced laminar lamination). Coarsening upwards facies sequences with sedimentary structures generated by progressively higher energy flows, truncated by an erosional surface and subsequently overlain by a fining upward facies sequence containing structures attributable to waning flow is suggested to be indicative of hyperpycnal flows (Zavala et al., 2006). Petter and Steel (2006) however, noted that hyperpycnites in the Battfjellet Formation shelf-edge and slope systems do not follow flood hydrographs. Low-angle cross stratification is a structure associated with traction deposits (Zavala et al., 2006). The occurrence of low angle cross bedding in the current study is, determined to be from long lived flows of fluctuating energy.

The thick amalgamated sandstone beds (BT 12) could result from upslope hyperpycnal processes igniting turbidite flows that reach submarine fan. Hyperpycnal flows generated from the shelf-edge are likely to continue farther downslope by inertia (Petter and Steel, 2006). The thickness of the submarine fans, and sandy slope of clinoform 14, as well as bed types have been invoked to demonstrate the prevalence of quasi-steady hyperpycnites in the system (Crabaugh and Steel 2004; Clark and Steel, 2006). Thick sand rich beds are indicative of thick flows, or long lived thinner flows, depositing sediment over a long time frame. Hyperpycnal flow deposits, being functions of flow duration as well as sediment input, deposit thick sandy deposits if they are long lived. Additionally they have very long runout distances over shallow slope angles (Zavala et al., 2006) Sustained turbidity flows, at river mouths are maintained as long as high density fluvial discharge continues (Prior et al., 1987). Hyperpycnal currents can initiate turbidity flows, termed hyperpycnal flows (Bates, 1953; Crabaugh and Steel 2004).



*Figure 42: Low angle crossbedding, truncating parallel laminated amalgamated sands, with 15 cm reindeer hip bone for scale the overlying bed displays dewatering structures.*

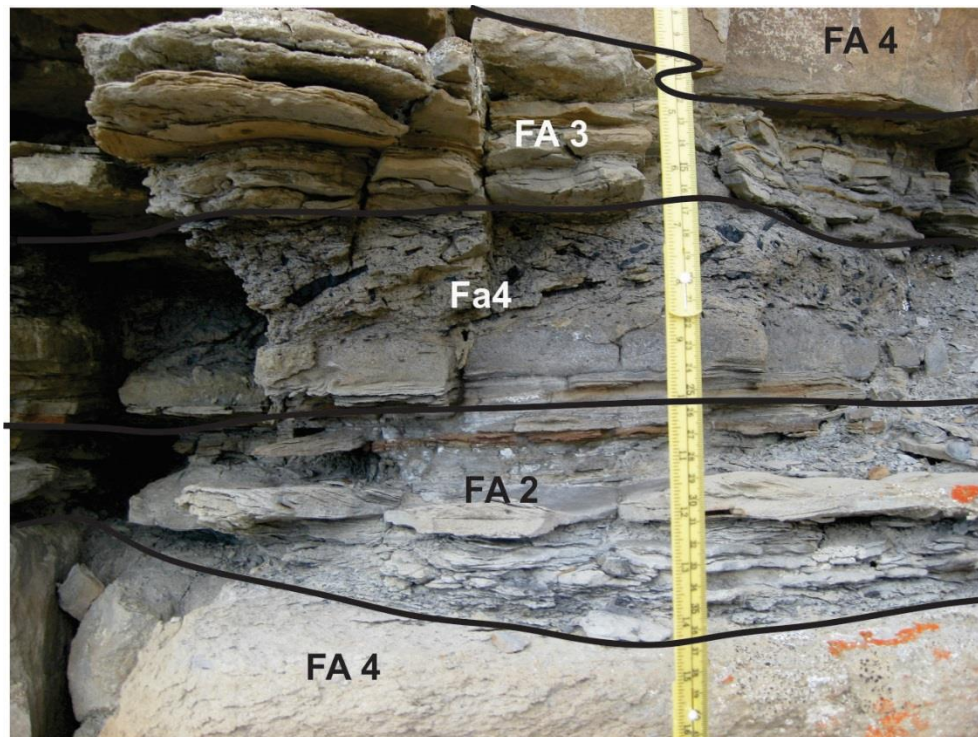
### 5.1.3. Beds deposited by Debris Flows and Slumps:

BT8 (fig. 16) , BT 11 (fig. 19), BT 14 (fig. 23), and BT 17 (fig. 26) are all massive to occasionally normally graded beds with high mud content and organic clasts throughout the flow that were deposited by a flow type with poor flow partitioning (table 1). Outsized clasts throughout and poor grading reflect deposition by debris flow processes. BT 18 (figs. 27, 28) is the only bed type inferred in the area to be deposited by slumping, its bedding is convolute, but original bedding is discernible, signifying short transport distances, and making it differentiable from linked or co-genetic debrites (in sensu Haughton et al., 2009).

#### 5.1.4. Beds deposited by Hybrid Flows

Bed types resulting from hybrid flows were established using more complex criteria. The determination between linked debrites, hybrid flows and turbidite deposits is confused by differing terminologies and classifying flows based on sediment concentration or dominant process (Shanmugam, 2002; 2006; Lowe, 1982). There has been a strong focus on non-turbiditic flow processes within turbidite flows, flow transformations, whether they are based on sediment support mechanisms, sediment concentration, flow velocities, or end member types (Haughton et al., 2003; Amy et al., 2004; Amy and Talling, 2006; Talling et al., 2007; Haughton et al., 2009). Fluid turbulence, hindered settling, dispersive pressure and matrix strength interact to influence the characteristics of submarine gravity flows and their resulting deposits (Shanmugam, 2000).

*Figure 43: Linked debrite and co-genetic turbidite, contained in middle FA4 body. Other FA 4 call outs are BT 12. Amalgamated units separated by off axis lobe (FA3) deposits and distal lobe (FA2) deposits.*



Hybrid flows change flow regime (i.e. flow transformations) either gradually or suddenly within the same event. They can emplace distal beds which may accumulate and serve as petroleum traps or caps. Hybrid beds are recognized by distinct bi-partite facies motif; typically a lower turbidite capped by a debrite (i.e. co-genetic turbidites-debrites, where the debrite is referred to as a “linked debrite”) (Haughton et al., 2009). Bed types which may be inferred as linked debrites include BT 8, BT 11, BT 14, and BT 17 (table 1).

BT 11 (fig. 19), grading from clean sandstone through planar bedding into chaotically structured silt and clay rich ‘dirty’ sandstone occurs predominately in proximal to medial outcrops. While conventionally recognized turbidite deposits have discreet mud and carbonaceous matter contents: the upper linked debrite division commonly show; a high clay content, outsized clasts and carbonaceous material, with vertical fractionation, mixed within the upper bed that suggests changing energy deposition (Haughton et al., 2009). In many cores and outcrops, this can be recognized as beds with a cleaner sandier lower portion and a darker dirtier upper portion of the bed, generally a chaotically structured muddier sand or sandy mud (Haughton et al., 2009). Geometries of BT 11, showed steep bases, cutting into underlying laminated sandstone. These hybrid beds were inferred as a result of up-dip flow transformations. BT 11 occurs in proximal locations, so flow bulking is inferred to have occurred on slope, and flow collapse at the toe of slope, where the reduction in angle would result in lower flow velocities, and competency leading to the progressive deposition of larger grains to smaller grains (Kneller, 1995). The preferential settling of coarse sand grains would increase the bulk fine particle portion suppressing turbulence. Haughton et al. (2009) suggested that beds could result from flow bulking forced transformations of previously fractionated flows, whereby mud eroded by the

head of the flow increases its density. An extensive study of the Marnoso Arenacea formation, which contain linked debrite beds concluded flow transformations to be a likely source of turbidite to debrite transitions (Amy & Talling, 2006). Linked debrite beds have been noted in proximal fan locations, where the reduction in slope transformed mud rich turbidity currents into debris flows (Patacci et al., 2014). Increased amounts of clay, in experimental flows have been shown to reduce flow turbulence resulting in more chaotically structured units as grain on grain action becomes more prevalent than settling. (Baas et al., 2011)

The basin floor fans of C14 and C15 are notably sand dominated, with Crabaugh and Steel (2004) estimating 90% sand content. While finer particles are more likely to be entrained further in submarine gravity flows; simple short duration depletive turbidity currents rarely have higher clay contents than 10% (Shanmugam, 2000). The prevalence of well-developed linked debrite beds in lobe deposits at medial to distal localities within the clinoform system supports the hypothesis that the reduction slope angle at the basin floor, preferentially deposited sand, fining the flow and contributing to the formation of linked debrite beds. When a reduction in slope angle or decrease in flow confinement removes the driving force, natural high density flows will often quickly lose their sediment load. The blunt terminations of debris flows, with internal massive or structureless organization (Stow and Johansson, 2000) are evidence of flow freezing (Talling et al., 2012) after rapid deposition (Amy et al., 2004; Amy & Talling, 2006).

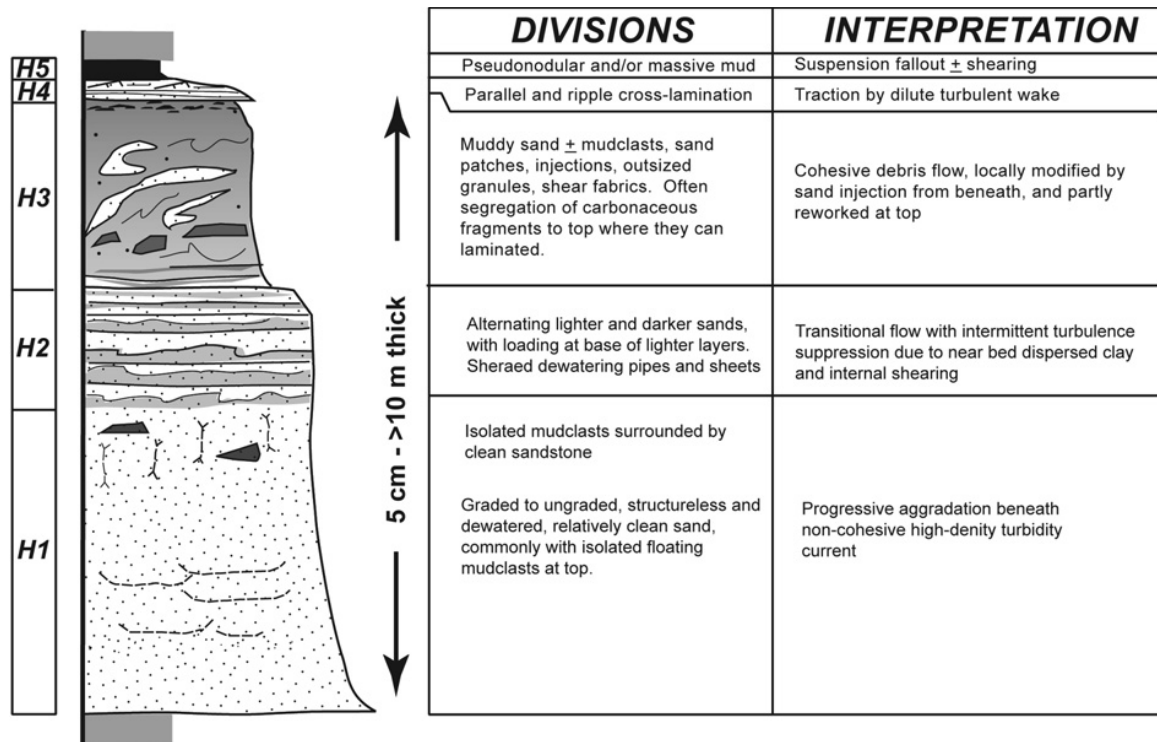


Figure 44: Idealized divisions of debris flows from Haughton et al. (2009)

Deposits from flow transformations are grouped into several categories by Haughton et al. (2009) (summarized in fig 42). Of pertinence to the submarine fans in the present study are: the muddy sandstones and sandy mudstones that notably lack injections or mud clasts, of the H3 division and the H4 division, defined as “a structured finer grained sandstone, often with dark laminae containing mud chip... and plant matter segregations...” (Haughton et. Al., 2009). Beds conforming most closely to the H1, H3 and H4 divisions (Haughton et al., 2003), are more common in the study area.

## 5.2 Depositional elements in Sand Rich submarine fans

The deep sea fans studied herein, span only a few kilometers from the base of the slope to their terminus, and the basin to which they were deposited was also small (Helland-Hansen, 2010)

The sediment supply was high (Helland-Hansen, 2010; Grundvåg et al., 2014a), and channelization of flows is not common or not preserved. Thin bedded sandstones with silty caps, are common between sets of thick bedded amalgamated sandstones, and interpreted as lateral splays. Lobes C12, C14a, C14b and C15 of this study are relatively small, on the order of several kilometers long. Paleoflow directions inferred in the system trend generally north eastward. Previous authors have noted a change in paleoflow directions northward within the investigated submarine fans on Hyrnestabben (Steel and Olsen, 2002; Johannessen and Steel, 2005). Paleo flow measurements within this study are in accordance with previous workers. Ripples in lower heterolithic units trend generally eastward, while those in the upper sandier portions of clinoform 14 and clinoform 15, have a more northward trend. It has been proposed that the fan deposition rotated more distally to be closer to slope parallel due to merging thrust faults on the sea floor (Crabaugh and Steel, 2004 ), or had a general north of east depositional trajectory (Petter and Steel, 2006). The assertion is further confirmed, by comparing the easternmost outcrop, W20 with W21, which (Henriksen et al., 2010) proposed as channel deposits. Evidence of extensive channelization was not apparent in W21 but slumping was. The northernmost deposits contained in log W21 showed thick bedded amalgamated lobe deposits. W20 on the far eastern face of Hyrnestabben, is comprised primarily of thin lobe fringe deposits, and the lobes have a much thinner apparent thickness (fig. 60). The outcrops exposed on Hyrnestabben offer only a one dimensional view of the submarine fans, making inferences of three dimensional shape dubious.

The system feeding C12, C14a, C14b, and C15 could be wholly or mostly driven by a high sediment supply. This assumption is based on the proximity to the growing orogenic WSFTB (Steel and Olsen, 2002) and the warm and wet Eocene climate on Svalbard (Schweitzer, 1980). Another factor speaking against relative sea-level falls as a main driver for clinoform growth is the tectonic subsidence of the basin, and overall ascending clinoform trajectories of 1.2° to 0.88°, reflecting a long term rise in relative sea-level which possibly prevented shelf-break exposure (Crabaugh and Steel, 2004; Plink-Björklund and Steel, 2004; Helland-Hansen 2009; Grundvåg et al., 2014a). Deltas rapidly prograded onto the shelf after transgressions, frequently all the way to the shelf edge, as evidenced by flat tabular delta sequences on the shelf (Helland-Hansen, 2010). Shelf edge deltas advanced the shelf when they prograded to the shelf edge (Helland-Hansen, 2010) The submarine fans also record progradation, with distal lobe deposits overridden by lobe, lobe proximal, and channelized deposits from both the slope proximal (western), and basinward outcrops (eastern). Hybrid event beds occur interspersed with conventional turbidite sandy beds in conditions of fan aggradation or fan decay. Very commonly they are in the lower portions of fans in growth (Haughton et al., 2009).

#### 5.2.1. Lateral and Frontal Splays

FA 2 and FA 3 are indicative of splay deposits. Relatively small volume channels are ideal candidates for lateral splaying, in short lived cut and fill scenarios. Frontal splays tend to occur with reduced flow confinement, when channel levees heights have sufficiently been reduced distally to allow the sandier bodies of sediment gravity flows to overtop them, sand deposition increases in the levees down system (Kolla and Coumes, 1987; Hiscott et al., 1997). Successions of FA2, sandwiched between successions of FA 4 and FA 5 are interpreted to be lateral splays.

Crevasse splay deposits interpreted by Crabaugh and Steel (2004) in the sandy deep sea fans clinofolds were thinner bedded sandy turbidites. In this study, distinctive levees were not encountered, so the term lateral splay is used.

### 5.2.2. Distributary Channels

Channel features encountered in the present study (FA 5), were limited, but most complete in the upper and medial portions of the fan (W12, W13, and W14). The most apparent (fig. 30) was roughly 3m in height, with steep sides, filled with 20-50 cm normal graded sandy beds contain lagging clasts (BT 16) (fig. 25). Channels in C12, C14a, C14b and C15 are rare. When they do occur they are in the upper sandy amalgamated sequences, and are likely part of a braided system. The stratigraphically elevated position of the channel features, suggests that towards the end of fan deposition, the gradient or flow confinements were well enough developed to result in fan progradation. Well developed levee deposits (in sensu Posamentier and Kola, 2003) were not encountered. Clinofold 14, sand prone to the basin floor (Plink-Björklund and Steel, 2004), with thick sandy deposits in the submarine fan, was a high sediment supply system. Prélat et al. (2010) note frequent lobe switching in short, thick submarine fan systems, where rapid aggradation occurs. Bourget et al., (2009) note that high sediment load systems often do not have well developed channels apparent in bathymetry.

### 5.3. Controls on Submarine fans and Lobe Hierarchy:

Internally submarine fans are built of individual packages of sediment, termed beds, which represent single flow events. Successive beds can form lobe elements, which together make up

composite lobes (Deptuck et. al., 2008). The largest unit in the hierarchy of lobes are amalgamations of composite lobes, called lobe complexes (Deptuck et. al., 2008; Prélat et. al., 2009) These represent pathways that are activated and abandoned based on local slope differences and sediment supply (Prélat et. al., 2009; Hodgson et. al., 2006) in submarine fan systems, that build the overall sediment package (Walker, 1978; Deptuck et al., 2008). This can be tens of kilometers long, thousands of meters wide (Walker, 1978; Talling et al, 2012) and generally contain one to two km<sup>3</sup> of volume (Prélat et. al., 2009). The overall shape of lobes changes with varying topography; low relief settings, often distal, tend toward thin lobes with complex architecture (Deptuck et. al., 2008) Submarine settings with higher relief, such as slope toes, slope gullies or channels with poorly developed levees (Deptuck et. al., 2008) have thicker lobe deposits. The composition and structures of lobes vary along their length and width (Prélat et al., 2009). Lobe architecture variations are influenced by the volume, duration, concentration and grainsize of their parent flows. The flow frequency and variation through time, as well as the gradient change at the mouth of the feeder conduit, lifespan prior to avulsion, channel geometry and channel stability also effect final architecture (Deptuck et. al., 2008).

The bipartite structure of C14a, C14b, and distal C15 deposit is suggestive of progradational fan emplacement. Sets of clinofolds in the Battfjellet and Frysjaodden formations show large scale progradational patterns in shelf edge delta development, reflecting changes in sediment supply (Grundvåg et al. 2014a) and/or relative sea-level (Steel and Olsen, 2002). The stacked clinofolds contained within the Van Keulenfjorden transect, show a trend of eastward progradation and aggradation (Steel and Olsen, 2002; Helland-Hansen, 2010). At a basinal scale, the easternmost clinofolds are shingled and lack any slope segments, while the western examples display a

classic sigmoidal shape with sandy slope segments, having been deposited directly on basinal sediments (Helland-Hansen, 2010). The advancement of deltas across the shelf to the shelf break was either due to high sediment supply (Helland-Hansen, 2010; Grundvåg et al., 2014) or changes in sea-level (Johannessen and Steel, 2005; Porębski and Steel, 2006) or a combination of both.

### 5.3.1. Fan Trends

The depositional architecture of a basin floor fan is determined in large part by flow discharge, sand-to-mud ratio, slope length, slope gradient, and seafloor rugosity (Posamentier and Kola, 2003, Deptuck et al., 2008; Prélat et al., 2009; Prélat et al., 2010). Thus, depositional elements can change by location and through time as environmental parameters change (Prélat et al., 2010). The Eocene system feeding the CB was determined to be 100 to 400 m from terrestrial deposits to basin floor (Plink-Björklund and Steel, 2004; Helland-Hansen, 2010). The slope of clinoform 14 is 3–4 degrees (Steel and Olsen, 2002). C12, C14a, C14b, and C15 can be broadly characterized as having lower portions of individual fans comprised of FA2, that are overlain by amalgamated and more lobe proximal deposits (FA 3, FA 4). C12, C14a C14b, and C15 were in a system largely controlled by sediment input (Helland-Hansen, 2010), and prograded with the overall system, evidenced by the pattern distal heterolithics (FA 2) and basinal sediments (FA 1) overlain by facies associations FA 3, FA 4, and/or FA 5. with the more distal and early deposits (FA 2 and FA 3 in the present study) occurring as the thin bedded and beds rich in emplaced coaly fragments, the upper reaches of each cliff show evidence of rapid sedimentation (FA 4). Rapid sedimentation can suppress the formation of particle fabrics (Duller et al., 2010), faint

laminar bedding, rare instances of rippled bases in amalgamated portions of the fan, are indicative of rapid deposition as well. High discharge fan systems (Bourget et al., 2009) are prone to aggradation, progradation, and lobe switching to preferred sediment pathways. Prélat et al. (2010) noted, in submarine fan systems with short runouts and thick lobes, frequent pathway switches where lobe aggradation results in steep lateral gradients. Condensed sections contained within submarine fans of clinoforms 12, 14, and 15, are influenced by shifting distributaries in shelf edge deltas, as well as preferential tracking of flows on the basin floor into topographic lows established by previous flow paths. Condensed sections that are the result of large scale sea level change (Posamentier and Kola, 2003) could not be established from outcrop evidence within composite lobes.

Relative sea level change, and shoreline position, has been noted to shift sedimentary depositional centers along the source to sink fairway (Helland-Hansen, 2010). Direct gravity flow deposits to the basin floor often occur often when relative sea level places the shoreline on the shelf edge, with shelf edge deltas making ideal sediment staging areas for deep-water deposition (Posamentier and Kola, 2003; Helland-Hansen, 2010; Grundvåg et al., 2014a; Mellere et al., 2002). C14b is best characterized as thick amalgamated turbidites with inter-nested linked debrites and hyperpycnites, prograding basinward directly onto basin floor sediments, rather than a turbidite system with debris flows resulting from over steepening of the slope resting on top. The active uplift that occurred in the WSFTB, in conjunction with a deepening basin (Grundvåg et al., 2014b), and a transit distance of 30 km from the overthrusting zone to the basinal sink (Crabaugh and Steel, 2004) suggest rapid infilling of nearshore accommodation space. Tabular deltaic parasequences in the topset of the Battfjellet Formation clinoforms also support

progradation of nearshore sediments across the shelf, allowing for coarser grains to reach deeper sinks (Helland-Hansen, 2010).

#### 5.4. Occurrences of and mechanisms for linked debrites in the study area

Beds displaying structures consistent with debris flows, occur in conjunction with underlying sandy beds, resembling Bouma (1962) T<sub>a</sub> or T<sub>b</sub> divisions (fig. 21), in the thicker medial-to distal outcrops of W16(fig. 57), W17 (fig. 58), and W18 (Fig. fig. 59). BT 17 (Table 1, Fig 26), occurs in distal amalgamated outcrops, with cryptic bedding, and grainsizes ranging from silt to fine sand, and wedge shaped geometries, the result of deposition by a debris flow induced by gradual flow bulking. Beds deposited from debris flows are uncommon in western outcrops within the study area. In basal sections of logs taken where C14a and C14b thicken rapidly, BT 8 and BT 14 occur. This suggests that during the early phase of basin floor fan growth, flows traversed and eroded an out-of-grade slope. BT 8 and BT 17 both show coarsening upwards trends from siltier bases, to sandy mid sections and tops. They may represent well developed and poorly developed end-members of a similar bed type. BT 8 however, are predominately recorded in more slope proximal, but stratigraphically lower reaches of the submarine fans and are more sandy. Much work on the outcropping submarine fans in Hyrnestabben has focused on allogenic forcing factors influencing deposition (Johannessen and Steel, 2005; Clark and Steel, 2006). However, autogenic factors also played a role in the types and positions of basin floor deposits. Beds deposited by flows that underwent flow transformations and by flows of intermediate rheological characteristics BT 8 (fig 16), BT 11 (fig 19), BT 14 (fig 23), and BT 17 fig (26) are notable in the mid-fan to distal sections logged in the study (fig 38).

The continued debris flow runout after a partial transformation into a forerunner turbidity current, aided by the input of fluid into the flow has been proposed as a mechanism leading to hybrid beds (Haughton et al., 2009). This mechanism may require the contribution of a dewatered sand to dilute the initial flow (Amy & Talling, 2006). Coarse grains settling through a low coherency debris flow is proposed in Jackson et al., (2009) as a possible mechanism for the generation of hybrid beds. Incorporation of eroded sediment, down dip, into a flow causing bulking and eventual freezing is another proposed mechanism for hybrid flow formation (Haughton et al., 2009): whereby the decrease in large grains by deposition, results in a flow transforming from turbulent to a muddy debris flow (Jackson, et al.,2009). Simultaneous retrogressive slope failure was finally proposed by Haughton et al. (2009), indicating a link between out-of-grade slopes and hybrid event beds. An implication of hybrid beds is that submarine flows' energies do not only deplete in energy nor are they the result of a single type of submarine gravity flow, but rather the expression of out of grade slopes.

High density flow dynamics behave differently from low density turbidity flows, or clear water flows (Baas et al., 2011). They noted settling velocity differences accounted for the bi-partite structure of linked debrites (Baas et al., 2011). Increasing clay contents resulted in thicker upper muddy beds, and thinner clean sand beds. The debrite portions (BT 14 and BT 17 in particular) of the linked debrites become thicker the further the travel, this is in accordance with Barker et al. (2008) who noted a prevalence of linked debrites occurring in fan fringe environments. Change in flow velocity are most likely the mechanisms for the emplacement of debrite beds in medial to distal fan locations. Linked debrites studied in Borneo (Jackson et al., 2009) were common in distal lobes. Linked debrites thicken from the more confined proximal sheet, to the

medial sheet where they are less constrained. Loss of flow velocity either due to the change in confinement or a reduction in slope is the likely culprit for most mid-fan linked debrites (Jackson et al., 2009). Slumping debris flows, are rare in C12, C14a, C14b, and C15. Siltstone or mudstone interbeds occur infrequently in proximity to the linked debrite assemblages in the fan, so erosion of substrate is a possibility. The debrites develop in under 3 km of travel, and large erosive structures are not common. The debrites in the more distal fringe fan settings are interpreted occur due to preferential settling of larger grains between the toe of the slope, and the eventual freezing point of the given flows. Distal linked debrites are laterally equivalent to mid fan sandy successions (Haughton et al., 2003). While larger fans have more segregated upper and lower successions in linked debrites, smaller fans, like those outcropping on Hyrnestabben, have less space for the portions to segregate (Haughton et al., 2009). Clark and Steel (2006) observed the submarine fan in clinoform 14 to occur where the slope transitioned into the basin floor. The transition to the basin floor is the common environment to see a reduction in slope or decrease in flow confinement. In this locale, natural high density flows will often quickly lose their coarser sediment load (Petter and Steel, 2006).

The rare highly amalgamated bed of BT 12, will have mud clasts and current ripples above a basal structureless sandy section, some several centimeters in thickness then overlain by more structureless sandstone. Hindered settling is inferred to have played a role in the emplacement of those beds. A large down flux of grains in the lowermost section of a flow or highest concentrated portion of a flow, is characterized by grain interactions rather than turbulence. Grains deposited at the base of the flow are continuously replenished from above, creating a sustained liquefied zone spanning the flow boundary (Kneller and Branney, 1995), or traction

carpet (Talling et al., 2012). If the interface of the settling boundary is diffuse, traction may occur as a transient phenomenon related to temporary reductions in flow concentration, while hindered settling, grain interactions are dominant. Unlike classical turbidity flows, the thickness of the deposits resulting from quasi steady currents are functions of the duration and flow characteristics. Deposits can thus be thicker than the current that formed it (Kneller and Branney, 1995).

#### 5.5. Importance of hyperpycnal flows in the study area:

With shelf edge deltas present in the system (fig. 4) hyperpycnal beds ought to be encountered. Other authors have noted a prevalence of hyperpycnal deposits throughout the system (Crabaugh and Steel, 2004; Plink-Björklund and Steel, 2004; Petter and Steel, 2006, Henriksen et al, 2010). Within the deep sea fan, evidence of direct hyperpycnal deposits is sparse. BT 13 (fig. 22) a thick, coarsening upward sandy bed type and BT 15 (fig. 24), a thick fining upward bed type with low angle cross lamination in the base are presented as examples of hyperpycnal flow within the submarine fan system (table 1). The abundance of coal fragments in the submarine fans, including woody debris (figure 43) indicate terrestrial sediment sourcing. The presence of coal fragments has been used by others to denote terrestrially sourced gravity deposits (Mulder et al., 2003; Plink Björklund and Steel, 2004; Zavala et al., 2006; Nakajima, 2006). The relative infrequency of BT 13 (fig. 22) and BT 15 (fig. 24) occurring in the submarine fans, denotes the rarity of hyperpycnal underflows flows within the submarine fan environment.

BT 15, shows bases with low angle cross bedding, truncating on rippled bases, transitioning upward into progressively lower energy structures; weak planar bedding, and/or asymmetric

ripples. Traction plus fallout structures are commonplace in hyperpycnal deposits in the waning flood stage (Bourget, 2009) as climbing ripples, planar lamination, and low angle cross stratification, are emplaced on top of what remains of the accelerating phase structures (Zavala et al., 2006) BT 15 deposits are encountered in mid to distal fan environments, in FA 4 in lobe C14b, overlying eroded scoured coarsening upwards beds. Coarsening upwards sandstone beds, such as BT 13, occur in the thick sandy deposits of C14a and C14 b at W10, within larger assemblages of BT 12, and overlain by coarser grained normally graded sandy beds separated by erosional contacts. Inverse grading can reflect, in some beds, sandy debris flow deposition (Shanmugam and Moiola, 1995; Shanmugam, 1996), however BT 13 beds are found in section in the mid to lower reaches of C14a and C14b, nested in heavily amalgamated BT 12, where other signs of debris flows are not present. Super critical flow erosion, as well as longitudinal and temporal flow variations, present problems for the preservation potential of hyperpycnal deposits. Previous workers have noted that hyperpycnal flow beds within the Spitsbergen Eocene system, show a complex downslope flow pattern that does not necessarily show a single waxing then waning event (Mellere et al., 2002; Plink-Björklund and Steel, 2004). Plink-Björklund and Steel (2004) note that the confinement of hyperpycnal flows are removed by delta mouth bars, creating unconfined jet-flows (Crabaugh and Steel, 2004). Hyperpycnal deposits can have upwards coarsening to fining characteristics in one place, but have intervals upslope or down slope with an opposite grading character or no structure at all (Plink-Björklund and Steel, 2004).

Cliniform 14 and cliniform 15 show evidence of slope bypass (Plink-Björklund and Steel, 2004). In the case of cliniform 14, sandy channels cut into the slope, feeding thick sandy deep sea fan. Sandy channel deposits in slope canyons observed by Crabaugh and Steel (2004) point

towards a significant sandy source, deposited by river effluent. In the case of clinoform 15, an unconnected coarse-grained deep sea fan (Steel and Olsen, 2002). Sandy hyperpycnal flows are a significant means for sediment delivery into the submarine fans of clinoforms 14 and 15, however, their deposits are difficult to definitively determine in the submarine fan environment alone, due to classical criteria in their discernment relying on larger scale linkages. Sedimentological evidence in outcrop is sparse.

A further explanation for the rarity of deposits from hyperpycnal underflow deposits is shelf over steepening. As shelf edge deltas positioned foresets on the upper slope, short run out turbidites were observed in mid-slope environments of clinoform 14 (Petter and Steel, 2006) that can serve as deep sea sediment staging areas. The fronts of shingled deltas are turbidite (gravity flow process) prone (Porębski and Steel, 2006; Crabaugh and Steel, 2006). The thick sandy submarine fans could result from slumping of over steepened shelf edge deltas initializing mass gravity flows that bypass the slope, emplacing the thick coarse grained lobe deposits of BT 12. Within the submarine fan, BT 12 beds are noted to have limited lateral extents, evidenced by frequent pinch-outs. Large scale slumping of the shelf is not a likely means for the emplacement of BT 12, however localized gravity flow processes, where delta lobes had steepened the shelf beyond a sustainable angle of repose is plausible. Crabaugh and Steel (2004) interpreted thick laminated sandstone beds, on the slope, that fined basin-wards over long distances, while losing only 1 meter of thickness over the run of 2–3 km, as hyperpycnally derived. These beds then pinched out abruptly. The pinch-outs display water escape structures, and occasional dish and ball structures. In deeper settings, the beds displayed almost no parallel bedding, but rather structureless graded or ungraded bedding, with occasional ripples. The collapse of hyperpycnally

ignited turbidites is a plausible explanation for some normal graded amalgamated beds (BT 12) in the basin floor fans.

## 5.6 Offshore analogues

The uplifted Eocene Battfjellet succession represents a potential analogue to still drowned basins on the Barents Sea and Norwegian continental margins. Cenozoic sea floor spreading of the Norwegian-Greenland Sea, affected the continental margins from Svalbard to the Mid-Norwegian continental margin (Faleide et al., 1984), resulting in the formation of large clinoformal clastic wedges (Safronova et al., 2014) along the whole margin. The Greenland shelf displays similar fault bounded basins, of Paleozoic and Mesozoic age overlain by newer shelf deposits (Ryseth et al., 2003).

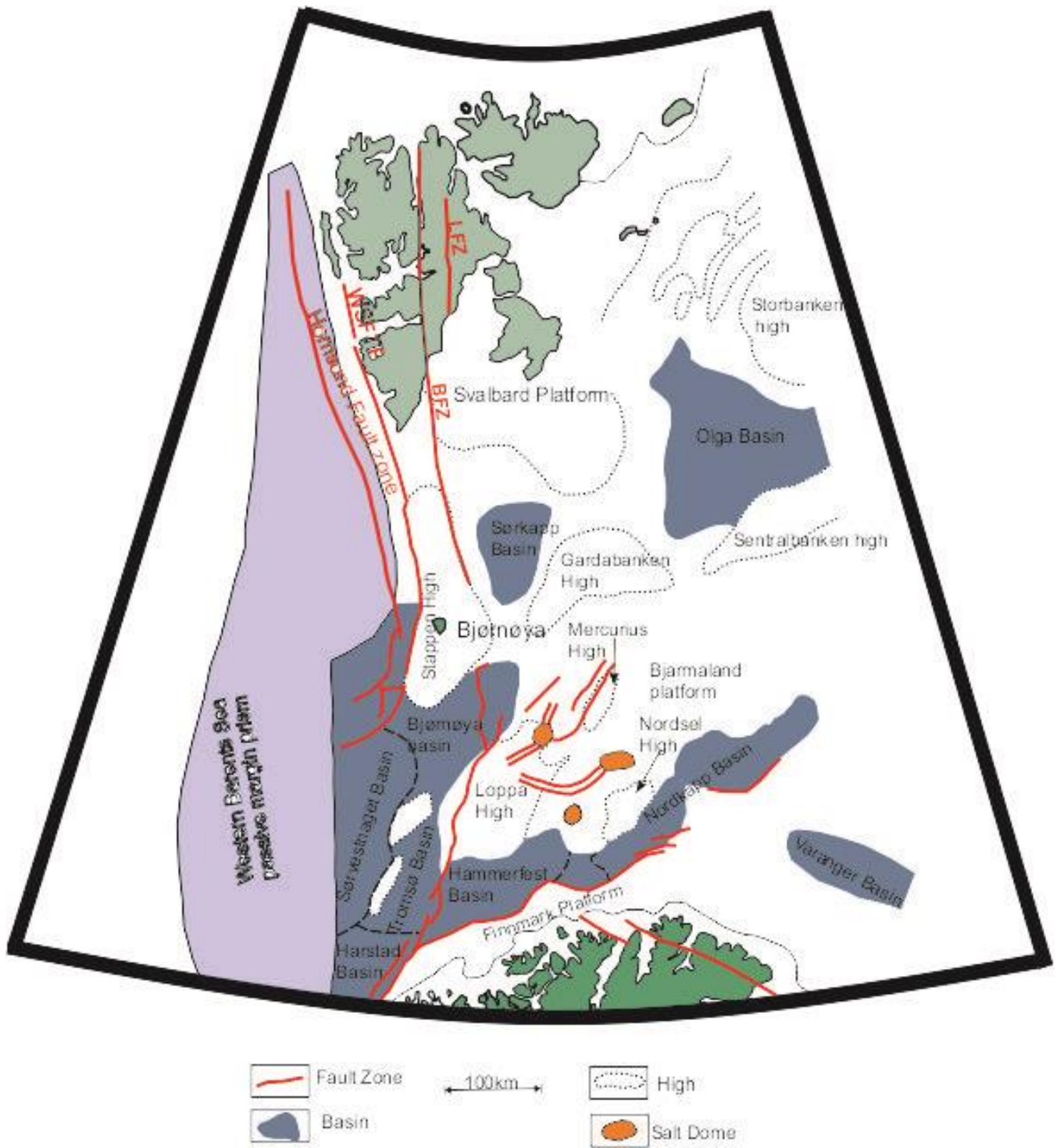


Figure 45: Barents Sea Area adopted from Nøttvedt et al. (1988)

Ryseth et al. (2003) and Safronova et al. (2014) studied the sedimentary fill of the Sørvestnaget Basin, a contemporaneous structural element to the CTB on Spitsbergen. The Cenozoic

sedimentary succession in the basin is approximately 4 km (Breivik et al., 1998), and predominately contains deep water sediments deposited in anoxic conditions (Ryseth et al., 2003). The basin underwent gradual basin infilling from the north in the Eocene, influenced by southward-prograding shelf margin clinoforms. The Sørvestnaget Basin (fig. 43) saw the contemporaneous increase in accommodation space in the middle Eocene due to the associated crustal subsidence to the opening of the Norwegian Greenland Sea. Ryseth et al. (2003) noted an axially located 135 m thick amalgamated sandy reservoir unit with total sandstone content of 30%, in the Eocene section. It was inferred to result from the stacking of high density turbidites (Ryseth et al., 2003). The base of the sandy unit displays an irregular character, further supporting a rapid deposition hypothesis. The Sørvestnaget basin was fed from the west by a prograding shoreline; the result of Paleogene uplift of the Stappen and Løppa highs (Ryseth et al., 2003). The clinoforms of the Van Kuelenfjorden transect represents a slightly older (early Eocene) but architecturally similar system to the Sørvestnaget Basin, and is thus an accessible analogue for a potentially petroleum rich province. Understanding the partitioning of flow processes throughout the submarine fans exposed in the Van Keulenfjorden transect may yield dividends in future deep ocean petroleum exploration, in areas such as the Sørvestnaget basin.



## 6. Conclusions:

C12, C14a, C14b and C15 display similar overall stacking patterns, with distal, lobe fringe deposits, overlain by lobe deposits (FA 3, FA 4, and FA 5). The highly amalgamated units of FA 4, do not show large scale system wide stacking trends; rather, they are representative of localized lobe shifts, due to lateral variations in slope, in the prograding fan system. The cliffs on Hyrnestabben expose the thickest portions of C14a and C14b (figs. 32, 33, 34) on the south face. C12, underlying them, has more environmentally distal deposits, with sandy deposits separated by several meters of mudstones (fig. 40). C15 by contrast to the two underlying submarine fans, was deposited in a more proximal situation, with predominately lobe fringe deposits in the western out crops. Only in the easternmost recorded logs (W21 and W22) (fig. 61) does the pattern of amalgamated facies overlying distal ones occur in C15.

Bed types indicative of linked debrites occur in medial to proximal locations, as BT 11 (fig. 19, table 1), and are inferred to be the result of primed turbidites transitioning into debrite flows. In medial to distal environments debris flow beds overlying normally graded beds are BT 14 (fig. 23, table 1) and BT 17 (fig. 26, table 1). BT 12 (fig. 20, table 1), comprises the largest population, by volume, of sandy beds. The debrites that occur throughout the medial portions of the fan do not represent a stage of a systems tract, but rather a variable flow character within the turbidite dominated system. Their proximity to the shelf edge indicates that long runouts are not necessary for the development of linked debrites.

Channel deposits comprising FA 5 (BT 16, BT 18) (figs. 25, 27, table 1) are found rarely as thin, poorly preserved scours, in stratigraphically lower portions of the fan lobes. They are more complete in the upper and medial portions of C14a and C14b (figs. 30, 52, 54), indicating that channels were transient features on the fan. Thinner turbidite sand beds within the amalgamated portion are interpreted as lateral splays, stemming from flows whose sediment load overwhelmed the cut and fill channels. The thick well developed sand rich submarine fans occur at the slope to basin floor fan transition in the system. The high sedimentation rate, erosive bases, and rapidly shifting sediment pathways resulted in few, widespread fine grained barriers in the thickest portions of the submarine lobes. While hyperpycnally derived turbidite flows, from perched shelf edge deltas likely emplaced thick sandy beds, evidence of hyperpycnal underflows acting in the submarine fan is not widespread.

## 7. References

- Amy, L. A., McCaffrey, W. D., & Kneller, B. C.** (2004). The influence of a lateral basin-slope on the depositional patterns of natural and experimental turbidity currents. *Geological Society, London, Special Publications*, 221(1), 311-330.
- Amy, L. A., & Talling, P. J.** (2006). Anatomy of turbidites and linked debrites based on long distance (120× 30 km) bed correlation, Marnoso Arenacea Formation, Northern Apennines, Italy. *Sedimentology*, 53(1), 161-212.
- Baas, J. H., Best, J. L., & Peakall, J.** (2011). Depositional processes, bedform development and hybrid bed formation in rapidly decelerated cohesive (mud–sand) sediment flows. *Sedimentology*, 58(7), 1953-1987.
- Baas, J. H., & Best, J. L.** (2002). Turbulence modulation in clay-rich sediment-laden flows and some implications for sediment deposition. *Journal of Sedimentary Research*, 72(3), 336-340.
- Bates, C. C.** (1953). A rational theory of delta formation as exemplified by the present-day Mississippi delta. *Journal of Sedimentary Research*, 23(2).
- Blythe, A. E., & Kleinspehn, K. L.** (1998). Tectonically versus climatically driven Cenozoic exhumation of the Eurasian plate margin, Svalbard: Fission track analyses. *Tectonics*, 17(4), 621-639.
- Bouma, A. H., Kuenen, P. H., & Shepard, F. P.** (1962). *Sedimentology of some flysch deposits: a graphic approach to facies interpretation* (Vol. 168). Amsterdam: Elsevier.
- Bourget, J., Zaragosi, S., Mulder, T., Schneider, J. L., Garlan, T., Van Toer, A., ... & Ellouz-Zimmermann, N.** (2010). Hyperpycnal-fed turbidite lobe architecture and recent sedimentary processes: A case study from the Al Batha turbidite system, Oman margin. *Sedimentary Geology*, 229(3), 144-159.
- Braathen, A., Bergh, S. G., & Maher, H. D.** (1999). Application of a critical wedge taper model to the Tertiary transpressional fold-thrust belt on Spitsbergen, Svalbard. *Geological Society of America Bulletin*, 111(10), 1468-1485.
- Braathen, A., & Bergh, S. G.** (1995). Kinematics of Tertiary deformation in the basement-involved fold-thrust complex, western Nordenskiöld Land, Svalbard: tectonic implications based on fault-slip data analysis. *Tectonophysics*, 249(1-2), 1-29.
- Bruhn, R., & Steel, R.** (2003). High-resolution sequence stratigraphy of a clastic foredeep succession (Paleocene, Spitsbergen): An example of peripheral-bulge-controlled depositional architecture. *Journal of Sedimentary Research*, 73(5), 745-755.

- Burgess, P. M., & Hovius, N.** (1998). Rates of delta progradation during highstands: consequences for timing of deposition in deep-marine systems. *Journal of the Geological Society*, 155(2), 217-222.
- Clark, B. E., & Steel, R. J.** (2006). Eocene turbidite-population statistics from shelf edge to basin floor, Spitsbergen, Svalbard. *Journal of Sedimentary Research*, 76(6), 903-918.
- Crabaugh, J. P., & Steel, R. J.** (2004). Basin-floor fans of the Central Tertiary Basin, Spitsbergen: relationship of basin-floor sand-bodies to prograding clinoforms in a structurally active basin. *Geological Society, London, Special Publications*, 222(1), 187-208.
- Dalland, A.** (1976). Erratic clasts in the lower Tertiary deposits of Svalbard—evidence of transport by winter ice. *Norsk Polarinstitutt Årbok 1976*, 151-165.
- Deptuck, M. E., Piper, D. J., Savoye, B., & Gervais, A.** (2008). Dimensions and architecture of late Pleistocene submarine lobes off the northern margin of East Corsica. *Sedimentology*, 55(4), 869-898.
- Duller, R. A., Mountney, N. P., & Russell, A. J.** (2010). Particle fabric and sedimentation of structureless sand, Southern Iceland. *Journal of Sedimentary Research*, 80(6), 562-577.
- Dypvik, H., Riber, L., Burca, F., Rùther, D., Jargvoll, D., Nagy, J., & Jochmann, M.** (2011). The Paleocene–Eocene thermal maximum (PETM) in Svalbard—clay mineral and geochemical signals. *Palaeogeography, Palaeoclimatology, Palaeoecology*, 302(3), 156-169.
- Faleide, J. I., Vågnes, E., & Gudlaugsson, S. T.** (1993). Late Mesozoic-Cenozoic evolution of the south-western Barents Sea in a regional rift-shear tectonic setting. *Marine and Petroleum Geology*, 10(3), 186-214.
- Faleide, J. I., Gudlaugsson, S. T., & Jacquart, G.** (1984). Evolution of the western Barents Sea. *Marine and Petroleum Geology*, 1(2), 123IN1129IN5137-128IN4136IN8150.
- Grecula, M., Flint, S. S., Wickens, H. D. V., & Johnson, S. D.** (2003). Upward-thickening patterns and lateral continuity of Permian sand-rich turbidite channel fills, Laingsburg Karoo, South Africa. *Sedimentology*, 50(5), 831-853.
- Grundvåg, S. A., Helland-Hansen, W., Johannessen, E. P., Olsen, A. H., & Stene, S. A.** (2014). The depositional architecture and facies variability of shelf deltas in the Eocene Battfjellet Formation, Nathorst Land, Spitsbergen. *Sedimentology*, 61(7), 2172-2204.
- Grundvåg, S. A., Johannessen, E. P., Helland-Hansen, W., & Plink-Björklund, P.** (2014). Depositional architecture and evolution of progradationally stacked lobe complexes in the Eocene Central Basin of Spitsbergen. *Sedimentology*, 61(2), 535-569.

- Harland, W. B.** (1997). Part 1: Chapter 3 Svalbard's geological frame. *Geological Society, London, Memoirs*, 17(1), 23-46.
- Haughton, P. D., Barker, S. P., & McCaffrey, W. D.** (2003). 'Linked' debrites in sand-rich turbidite systems—origin and significance. *Sedimentology*, 50(3), 459-482.
- Haughton, P., Davis, C., McCaffrey, W., & Barker, S.** (2009). Hybrid sediment gravity flow deposits—classification, origin and significance. *Marine and petroleum geology*, 26(10), 1900-1918.
- Helland-Hansen, W.** (1990). Sedimentation in Paleogene Foreland Basin, Spitsbergen (1). *AAPG Bulletin*, 74(3), 260-272.
- Helland-Hansen, W.** (1992). Geometry and facies of Tertiary clinothems, Spitsbergen. *Sedimentology*, 39(6), 1013-1029.
- Helland-Hansen, W., & Martinsen, O. J.** (1996). Shoreline trajectories and sequences: description of variable depositional-dip scenarios. *Journal of Sedimentary Research*, 66(4).
- Helland-Hansen, W.** (2010). Facies and stacking patterns of shelf-deltas within the Palaeogene Battfjellet Formation, Nordenskiöld Land, Svalbard: implications for subsurface reservoir prediction. *Sedimentology*, 57(1), 190-208.
- Henriksen, S., A. Pontén, N. Janbu, and B. Paasch** (2010) The importance of sediment supply and sequence-stacking pattern in creating hyperpycnal flows, in R. M. Slatt and C. Zavala, eds., *Sediment transfer from shelf to deep water—Revisiting the delivery system: AAPG Studies in Geology* 61,1–24.
- Hiscott, R. N., Hall, F. R., & Pirmez, C.** (1997). Turbidity-current overspill from the Amazon Channel: texture of the silt/sand load, paleoflow from anisotropy of magnetic susceptibility, and implications for flow processes. In *PROCEEDINGS-OCEAN DRILLING PROGRAM SCIENTIFIC RESULTS* (pp. 53-78). NATIONAL SCIENCE FOUNDATION.
- Hodgson, D. M., Flint, S. S., Hodgetts, D., Drinkwater, N. J., Johannessen, E. P., & Luthi, S. M.** (2006). Stratigraphic evolution of fine-grained submarine fan systems, Tanqua depocenter, Karoo Basin, South Africa. *Journal of Sedimentary Research*, 76(1), 20-40.
- Hodgson, D. M.** (2009). Distribution and origin of hybrid beds in sand-rich submarine fans of the Tanqua depocentre, Karoo Basin, South Africa. *Marine and Petroleum Geology*, 26(10), 1940-1956.
- Ito, M.** (2008). Downfan transformation from turbidity currents to debris flows at a channel-to-lobe transitional zone: the Lower Pleistocene Otadai Formation, Boso Peninsula, Japan. *Journal of Sedimentary Research*, 78(10), 668-682.

- Jackson, C. A. L., Zakaria, A. A., Johnson, H. D., Tongkul, F., & Crevello, P. D.** (2009). Sedimentology, stratigraphic occurrence and origin of linked debrites in the West Crocker Formation (Oligo-Miocene), Sabah, NW Borneo. *Marine and Petroleum Geology*, 26(10), 1957-1973.
- Johannessen, E. P., Henningsen, T., Bakke, N. E., Johansen, T. A., Ruud, B. E., Riste, P., ... & Woldengen, M. S.** (2011). Palaeogene clinoform succession on Svalbard expressed in outcrops, seismic data, logs and cores. *First Break*, 29(2), 35-44.
- Johannessen, E. P., & Steel, R. J.** (2005). Shelf-margin clinoforms and prediction of deepwater sands. *Basin Research*, 17(4), 521-550.
- Kellogg, H.E.** (1975) Tertiary stratigraphy and tectonism in Svalbard and continental drift. *American Association of Petroleum Geologists Bulletin*, 59, 465-485.
- Keunen, P.H. and Migliorini, C.I.** (1950) Turbidity currents as a cause of graded bedding. *J. Geol.*, 58, 91-127.
- Kolla, V., & Coumes, F.** (1987). Morphology, internal structure, seismic stratigraphy, and sedimentation of Indus Fan. *AAPG Bulletin*, 71(6), 650-677.
- Kneller, B., & Buckee, C.** (2000). The structure and fluid mechanics of turbidity currents: a review of some recent studies and their geological implications. *Sedimentology*, 47(s1), 62-94.
- Kneller, B.** (1996). Beyond the turbidite paradigm: physical models for deposition of turbidites and their implications for reservoir prediction. *Oceanographic Literature Review*, 43, 10-28.
- Kneller, B. C., & Branney, M. J.** (1995). Sustained high-density turbidity currents and the deposition of thick massive sands. *Sedimentology*, 42(4), 607-616.
- Lang, J., & Winsemann, J.** (2013). Lateral and vertical facies relationships of bedforms deposited by aggrading supercritical flows: from cyclic steps to humpback dunes. *Sedimentary Geology*, 296, 36-54.
- Leever, K. A., Gabrielsen, R. H., Faleide, J. I., & Braathen, A.** (2011). A transpressional origin for the West Spitsbergen fold-and-thrust belt: Insight from analog modeling. *Tectonics*, 30(2).
- Lien, T., Walker, R. G., & Martinsen, O. J.** (2003). Turbidites in the Upper Carboniferous Ross Formation, western Ireland: reconstruction of a channel and spillover system. *Sedimentology*, 50(1), 113-148.
- Lowe, D. R.** (1982). Sediment gravity flows: II Depositional models with special reference to the deposits of high-density turbidity currents. *Journal of Sedimentary Research*, 52(1).

- Lundin, E., & Doré, A. G.** (2002). Mid-Cenozoic post-breakup deformation in the 'passive' margins bordering the Norwegian–Greenland Sea. *Marine and Petroleum Geology*, 19(1), 79-93.
- Løseth, T. M., Steel, R. J., Crabaugh, J. P., & Schellpeper, M.** (2006). Interplay between shoreline migration paths, architecture and pinchout distance for siliciclastic shoreline tongues: evidence from the rock record. *Sedimentology*, 53(4), 735-767.
- Maher, Jr, H. D.** (2001). Manifestations of the Cretaceous High Arctic large igneous province in Svalbard. *The Journal of Geology*, 109(1), 91-104.
- Manum, S. B., & Throndsen, T.** (1986). Age of Tertiary formations on Spitsbergen. *Polar Research*, 4(2), 103-131.
- Mellere, D., Plink-Björklund, P., & Steel, R.** (2002). Anatomy of shelf deltas at the edge of a prograding Eocene shelf margin, Spitsbergen. *Sedimentology*, 49(6), 1181-1206.
- Middleton, G. V., & Hampton, M. A.** (1973). Part I. Sediment gravity flows: mechanics of flow and deposition.
- Mulder, T., Syvitski, J. P., Migeon, S., Faugères, J. C., & Savoye, B.** (2003). Marine hyperpycnal flows: initiation, behavior and related deposits. A review. *Marine and Petroleum Geology*, 20(6), 861-882.
- Müller, R. D., & Spielhagen, R. F.** (1990). Evolution of the Central Tertiary Basin of Spitsbergen: towards a synthesis of sediment and plate tectonic history. *Palaeogeography, Palaeoclimatology, Palaeoecology*, 80(2), 153-172.
- Mutti, E., & Ricci Lucchi, F.** (1978). Turbidites of the northern Apennines: introduction to facies analysis. *International geology review*, 20(2), 125-166.
- Myhre, A. M., Eldholm, O., & Sundvor, E.** (1982). The margin between Senja and Spitsbergen fracture zones: implications from plate tectonics. *Tectonophysics*, 89(1-3), 33-50.
- Mørk, A., Dallmann, W. K., Dypvik, H., Johannessen, E. P., Larssen, G. B., Nagy, J., ... & Worsley, D.** (1999). Mesozoic lithostratigraphy. *Lithostratigraphic lexicon of Svalbard. Upper Palaeozoic to Quaternary bedrock. Review and recommendations for nomenclature use*, 127-214.
- Nakajima, T.** (2006). Hyperpycnites deposited 700 km away from river mouths in the central Japan Sea. *Journal of Sedimentary Research*, 76(1), 60-73.
- Normark, W. R.** (1970). Growth patterns of deep-sea fans. *AAPG bulletin*, 54(11), 2170-2195.

**Nøttvedt, A., L.T. Berglund, Rasmussen E., and Steel, R.J.** (1988) Some aspects of tertiary tectonics and sedimentation along the western Barents Shelf, *Geological Society of London spec. pubs.*, **39**, 421-425.

**Nøttvedt, A.** (1985). Askeladden Delta Sequence (Palaeocene) on Spitsbergen-sedimentation and controls on delta formation. *Polar Research*, **3**(1), 21-48.

**Petter, A. L., & Steel, R. J.** (2006). Hyperpycnal flow variability and slope organization on an Eocene shelf margin, Central Basin, Spitsbergen. *AAPG bulletin*, **90**(10), 1451-1472.

**Piepjohn, K., von Gosen, W., & Tessensohn, F.** (2016). The Eureka deformation in the Arctic: an outline. *Journal of the Geological Society*, **173**(6), 1007-1024.

**Plink-Björklund, P., & Steel, R. J.** (2004). Initiation of turbidity currents: outcrop evidence for Eocene hyperpycnal flow turbidites. *Sedimentary Geology*, **165**(1), 29-52.

**Plink-Björklund, P., Mellere, D., & Steel, R. J.** (2001). Turbidite variability and architecture of sand-prone, deep-water slopes: Eocene clinofolds in the Central Basin, Spitsbergen. *Journal of Sedimentary Research*, **71**(6), 895-912.

**Pontén, A., & Plink-Björklund, P.** (2009). Process regime changes across a regressive to transgressive turnaround in a shelf-slope basin, Eocene central Basin of Spitsbergen. *Journal of Sedimentary Research*, **79**(1), 2-23.

**Porębski, S. J., & Steel, R. J.** (2006). Deltas and sea-level change. *Journal of Sedimentary Research*, **76**(3), 390-403.

**Posamentier, H. W., & Kolla, V.** (2003). Seismic geomorphology and stratigraphy of depositional elements in deep-water settings. *Journal of sedimentary research*, **73**(3), 367-388.

**Postma, G., & Cartigny, M. J.** (2014). Supercritical and subcritical turbidity currents and their deposits—A synthesis. *Geology*, **42**(11), 987-990.

**Prélat, A., Covault, J. A., Hodgson, D. M., Fildani, A., & Flint, S. S.** (2010). Intrinsic controls on the range of volumes, morphologies, and dimensions of submarine lobes. *Sedimentary Geology*, **232**(1), 66-76.

**Prélat, A., Hodgson, D. M., & Flint, S. S.** (2009). Evolution, architecture and hierarchy of distributary deep-water deposits: a high-resolution outcrop investigation from the Permian Karoo Basin, South Africa. *Sedimentology*, **56**(7), 2132-2154.

**Prior, D. B., Bornhold, B. D., Wiseman Jr, W. J., & Lowe, D. R.** (1987). Turbidity current activity in a British Columbia fjord. *Science*, **237**, 1330-1334.

- Ryseth, A., Augustson, J. H., Charnock, M., Haugerud, O., Knutsen, S. M., Midbøe, P. S., ... & Sundsbø, G.** (2003). Cenozoic stratigraphy and evolution of the Sørvestsnaget Basin, southwestern Barents Sea. *Norwegian Journal of Geology/Norsk Geologisk Forening*, 83(2).
- Safronova, P. A., Henriksen, S., Andreassen, K., Laberg, J. S., & Vorren, T. O.** (2014). Evolution of shelf-margin clinoforms and deep-water fans during the middle Eocene in the Sorvestsnaget Basin, southwest Barents Sea. *AAPG bulletin*, 98(3), 515-544.
- Schweitzer, H. J.** (1980). Environment and climate in the early Tertiary of Spitsbergen. *Palaeogeography, Palaeoclimatology, Palaeoecology*, 30, 297-311.
- Shanmugam, G.** (2002). Ten turbidite myths. *Earth-Science Reviews*, 58(3), 311-341.
- Shanmugam, G.** (2000). 50 years of the turbidite paradigm (1950s—1990s): deep-water processes and facies models—a critical perspective. *Marine and petroleum Geology*, 17(2), 285-342.
- Shanmugam, G.** (1996). High-Density Turbidity Currents: Are They Sandy Debris Flows?: PERSPECTIVES. *Journal of sedimentary research*, 66(1).
- Shanmugam, G., & Moiola, R. J.** (1995). Reinterpretation of depositional processes in a classic flysch sequence (Pennsylvanian Jackfork Group), Ouachita Mountains, Arkansas and Oklahoma. *AAPG bulletin*, 79(5), 672-695.
- Sluijs, A., Schouten, S., Pagani, M., Woltering, M., Brinkhuis, H., Damsté, J. S. S., ... & Matthiessen, J.** (2006). Subtropical Arctic Ocean temperatures during the Palaeocene/Eocene thermal maximum. *Nature*, 441(7093), 610-613.
- Spencer, A. M., Home, P. C., & Berglund, L. T.** (1984). Tertiary structural development of the western Barents Shelf: Troms to Svalbard. In *Petroleum Geology of the North European Margin* (pp. 199-209). Springer Netherlands.
- Steel, R. J., & Olsen, T.** (2002, December). Clinoforms, clinoform trajectories and deepwater sands. In *Sequence-stratigraphic models for exploration and production: Evolving methodology, emerging models and application histories: Gulf Coast Section SEPM 22nd Research Conference, Houston, Texas* (pp. 367-381).
- Steel, R., Gjelberg, J., Helland-Hansen, W., Kleinspehn, K., Nøttvedt, A., & Rye-Larsen, M.** (1985). The Tertiary strike-slip basins and orogenic belt of Spitsbergen. *SEPM, Special Publication 37*, 339-359.
- Steel, R. J., & Worsley, D.** (1984). Svalbard's post-Caledonian strata—an atlas of sedimentational patterns and palaeogeographic evolution. In *Petroleum geology of the North European margin* (pp. 109-135). Springer Netherlands.

- Steel, R. J., Dalland, A., Kalgraff, K., & Larsen, V.** (1981). The Central Tertiary Basin of Spitsbergen: sedimentary development of a sheared-margin basin.
- Stow, D. A., & Johansson, M.** (2000). Deep-water massive sands: nature, origin and hydrocarbon implications. *Marine and Petroleum Geology*, 17(2), 145-174.
- Srivastava, S. P.** (1978). Evolution of the Labrador Sea and its bearing on the early evolution of the North Atlantic. *Geophysical Journal International*, 52(2), 313-357.
- Talling, P. J., Amy, L. A., & Wynn, R. B.** (2007). New insight into the evolution of large-volume turbidity currents: comparison of turbidite shape and previous modelling results. *Sedimentology*, 54(4), 737-769.
- Talling, P. J., Masson, D. G., Sumner, E. J., & Malgesini, G.** (2012). Subaqueous sediment density flows: depositional processes and deposit types. *Sedimentology*, 59(7), 1937-2003.
- Talling, P. J., Malgesini, G., & Felletti, F.** (2013). Can liquefied debris flows deposit clean sand over large areas of sea floor? Field evidence from the Marnoso-arenacea Formation, Italian Apennines. *Sedimentology*, 60(3), 720-762.
- Walker, R. G.** (1978). Deep-water sandstone facies and ancient submarine fans: models for exploration for stratigraphic traps. *AAPG Bulletin*, 62(6), 932-966.
- Zavala, C., Ponce, J. J., Arcuri, M., Drittanti, D., Freije, H., & Asensio, M.** (2006). Ancient lacustrine hyperpynites: a depositional model from a case study in the Rayoso Formation (Cretaceous) of west-central Argentina. *Journal of Sedimentary Research*, 76(1), 41-59.

## 8. Appendix

# Key to Presentation Figures

	Fa1		faint lamination
	Fa2		laminar bedding
	Fa3		organic clasts
	Fa4		dish structures
	Fa5		flame casts
	assymmetric ripple		low angle lamination
	climbing ripple		convolute bedding
	trace fossil		rip-up clasts
	planar boundary		wavy boundary

Figure 46: key to presentation logs

Figure 47: Presentation logs W1 and W2

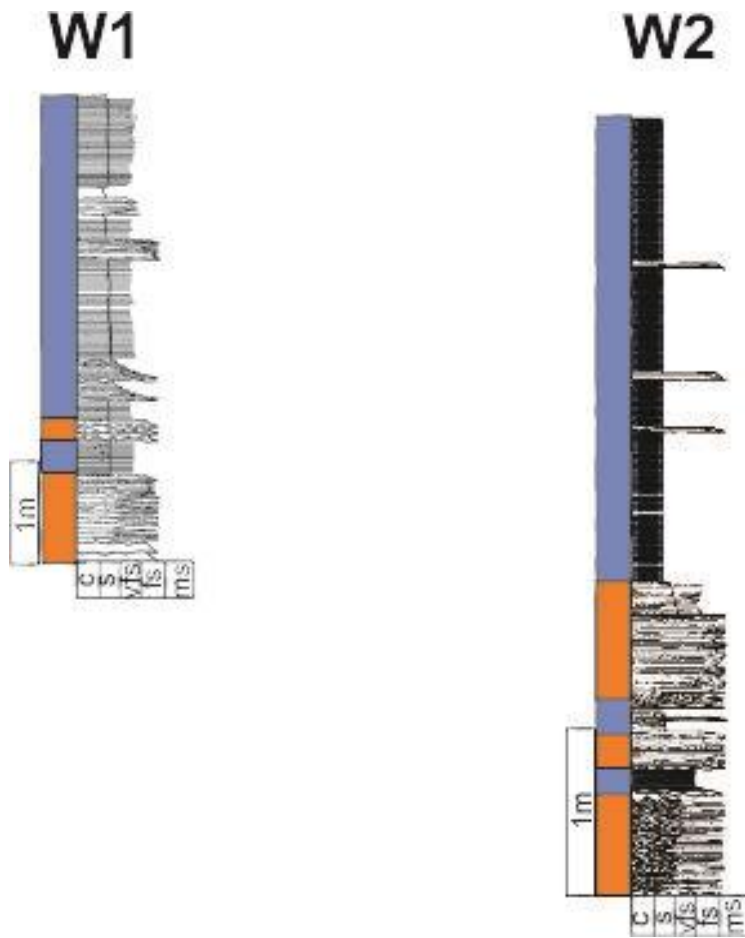


Figure 48: Presentation logs of W3 and W4

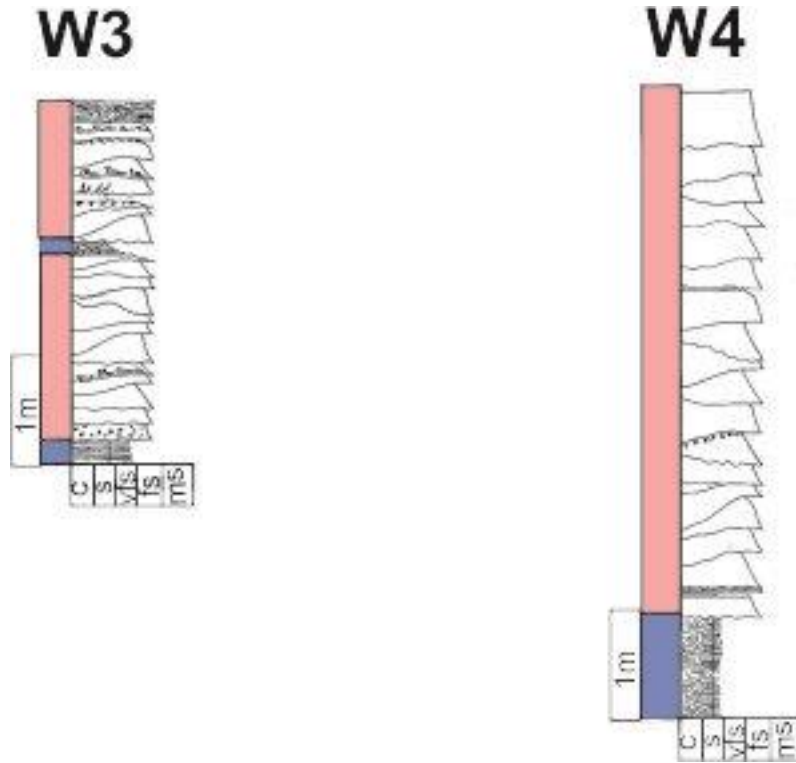


Figure 49: Presentation logs of W5 and W6

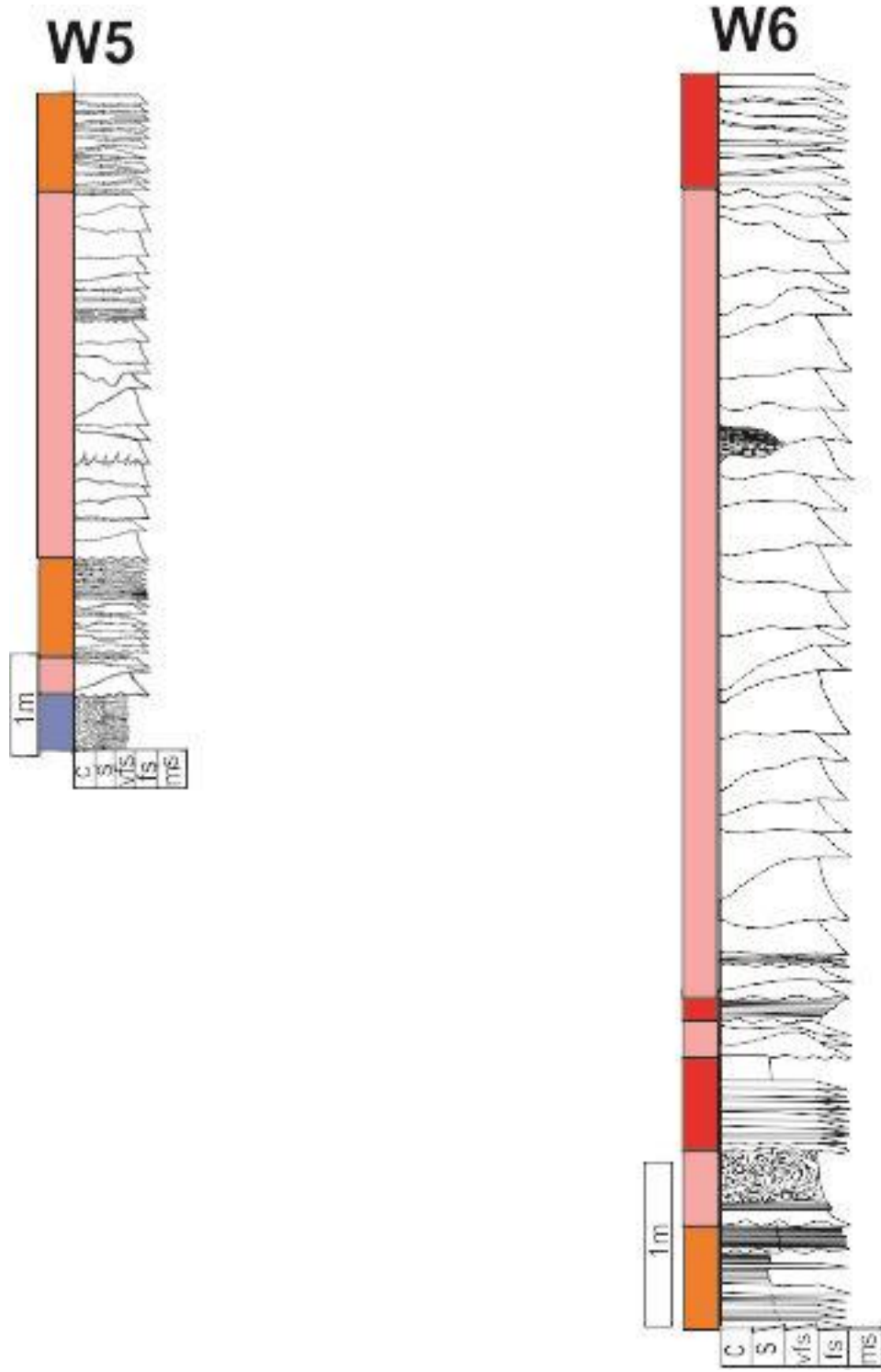


Figure 50: Presentation logs of W7 and W8

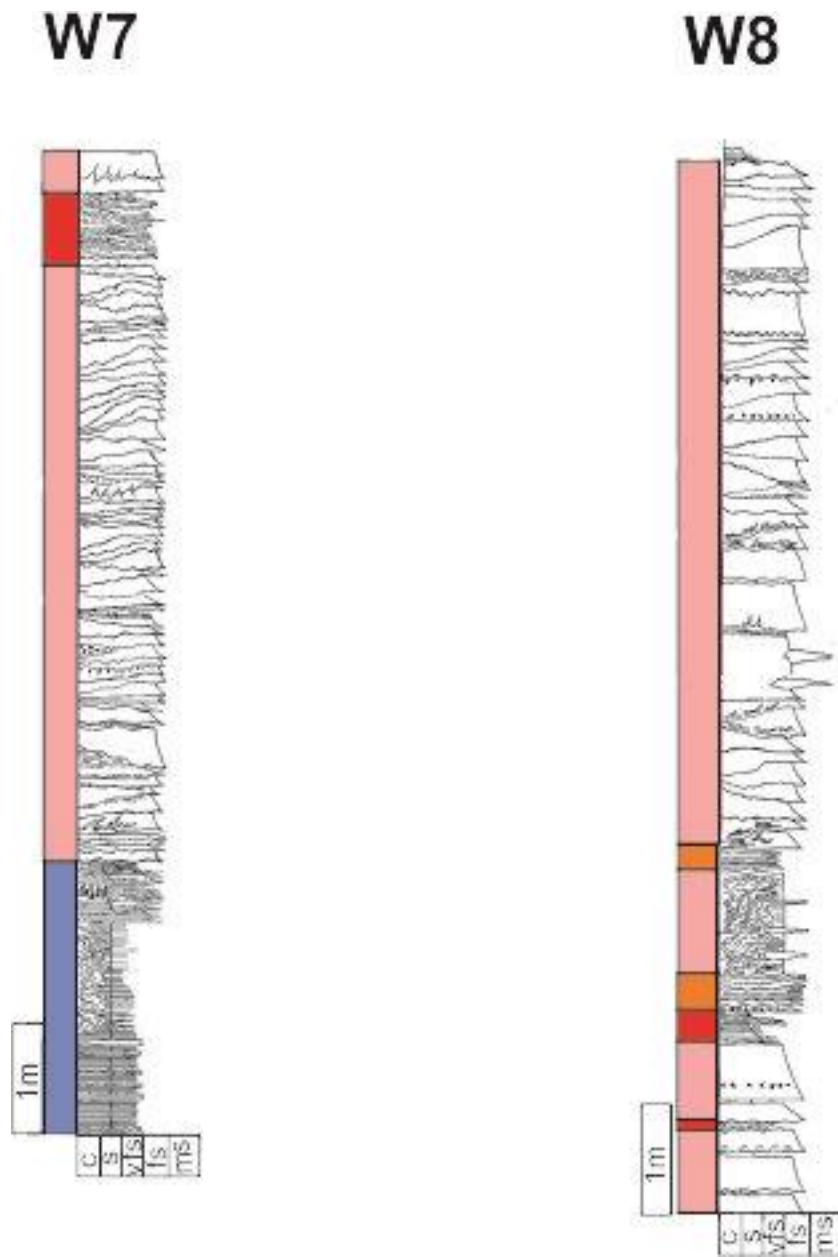


Figure 51: Presentation log of W9

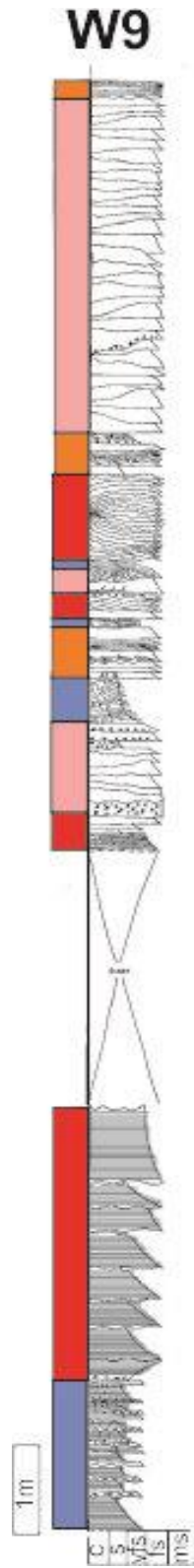
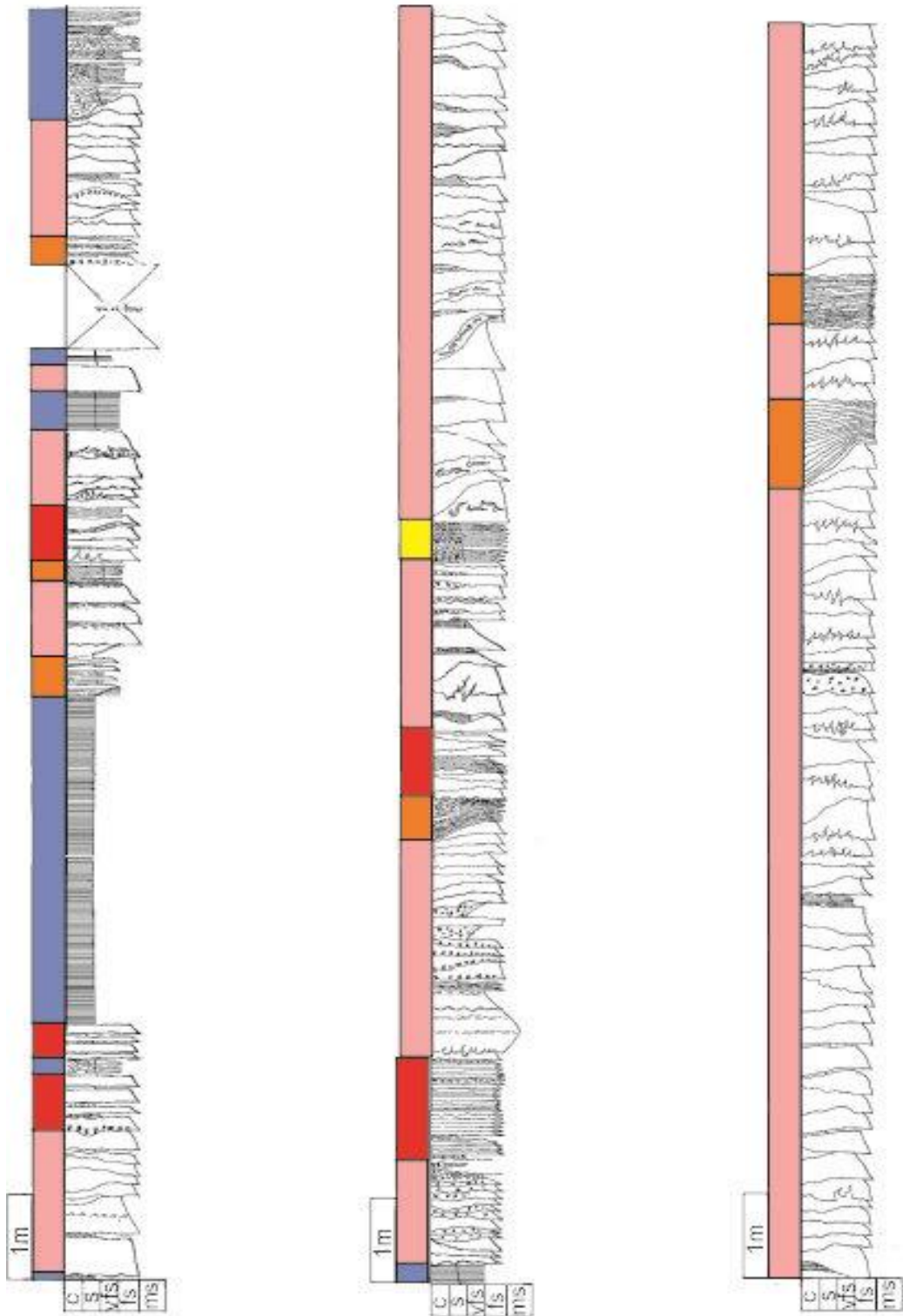


Figure 52: Presentation log of W10

# W10



# W10 ctd

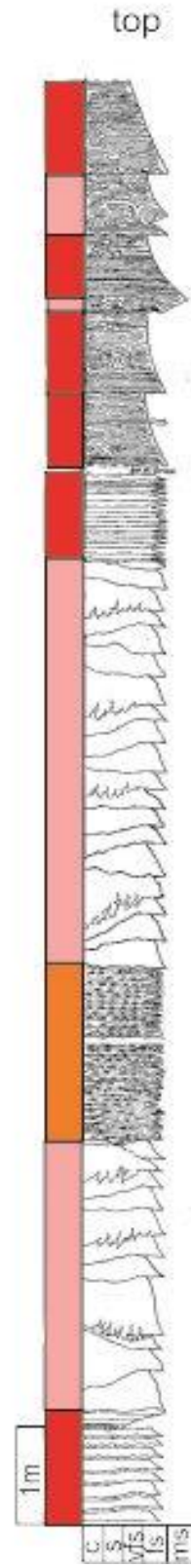
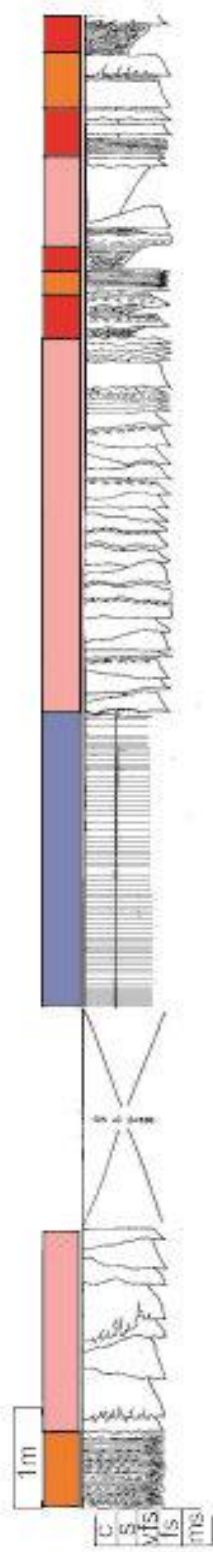
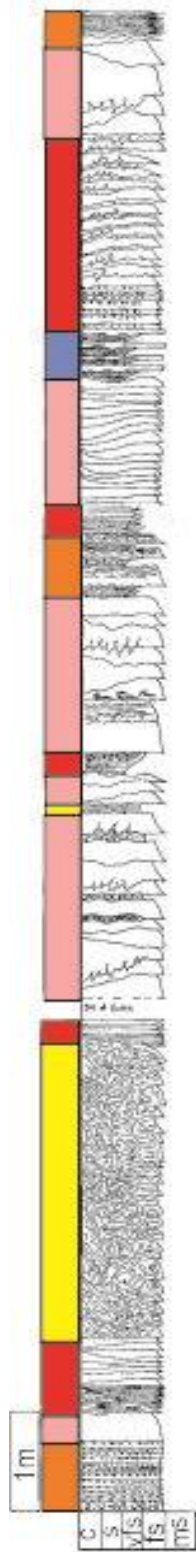


Figure 53: Presentation log of W11

# W11

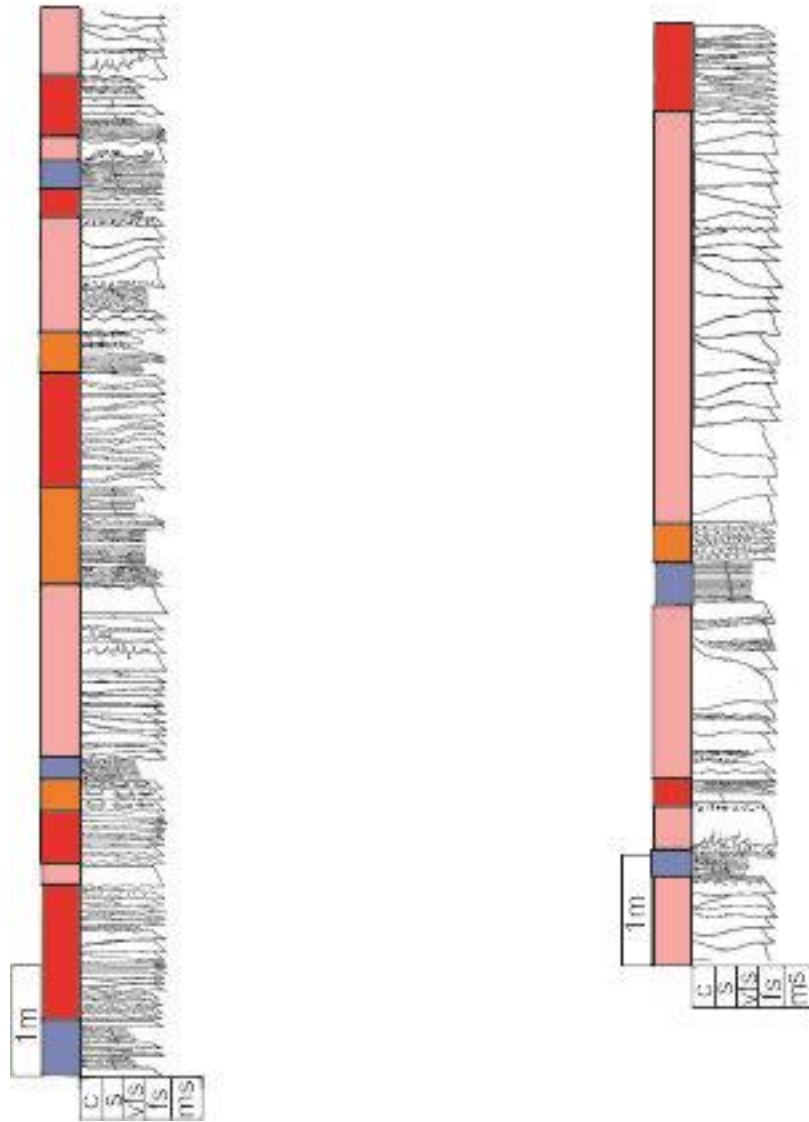


Figure 54: Presentation log of W12

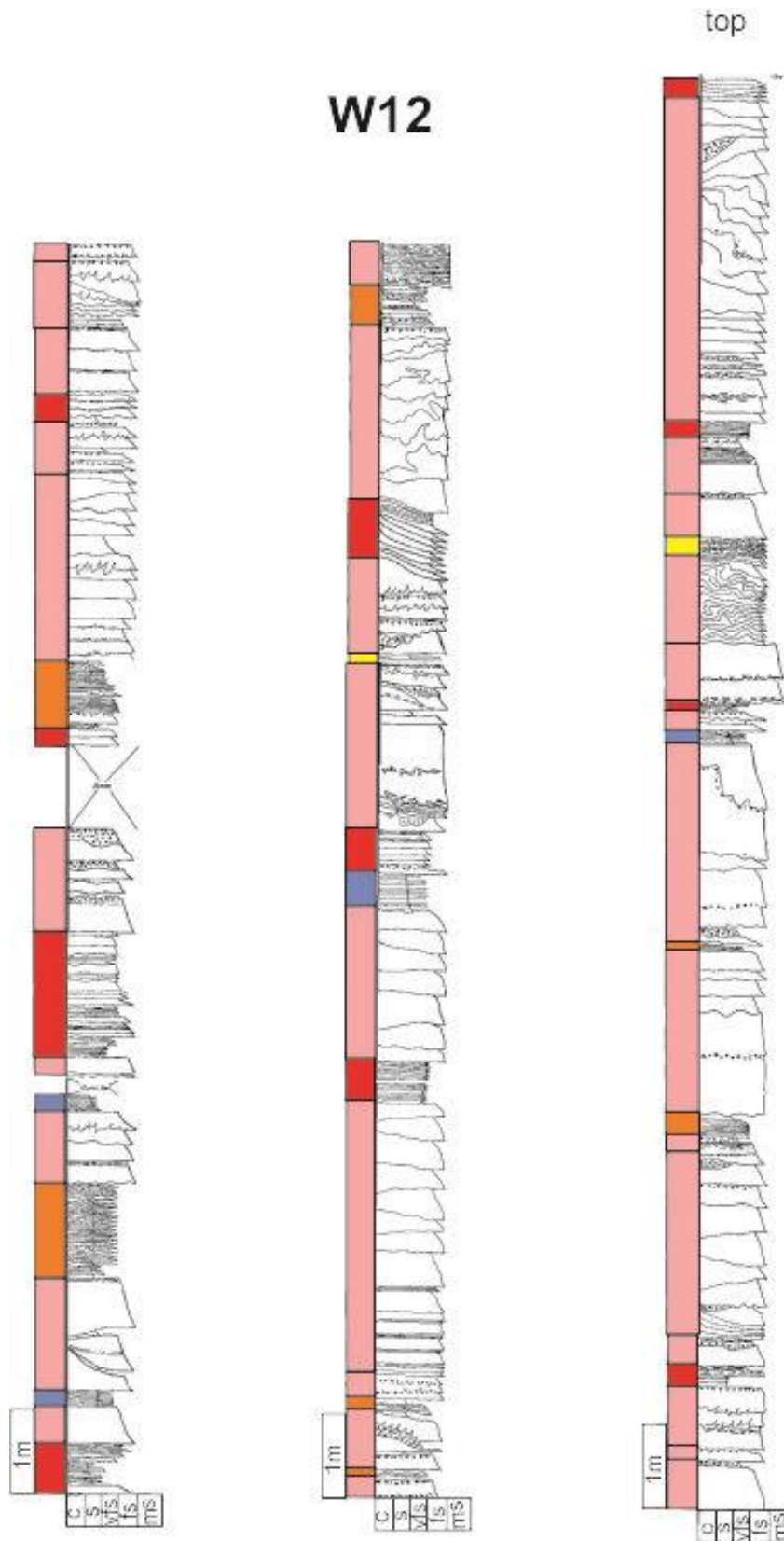


Figure 55: Presentation log of W13

# W13

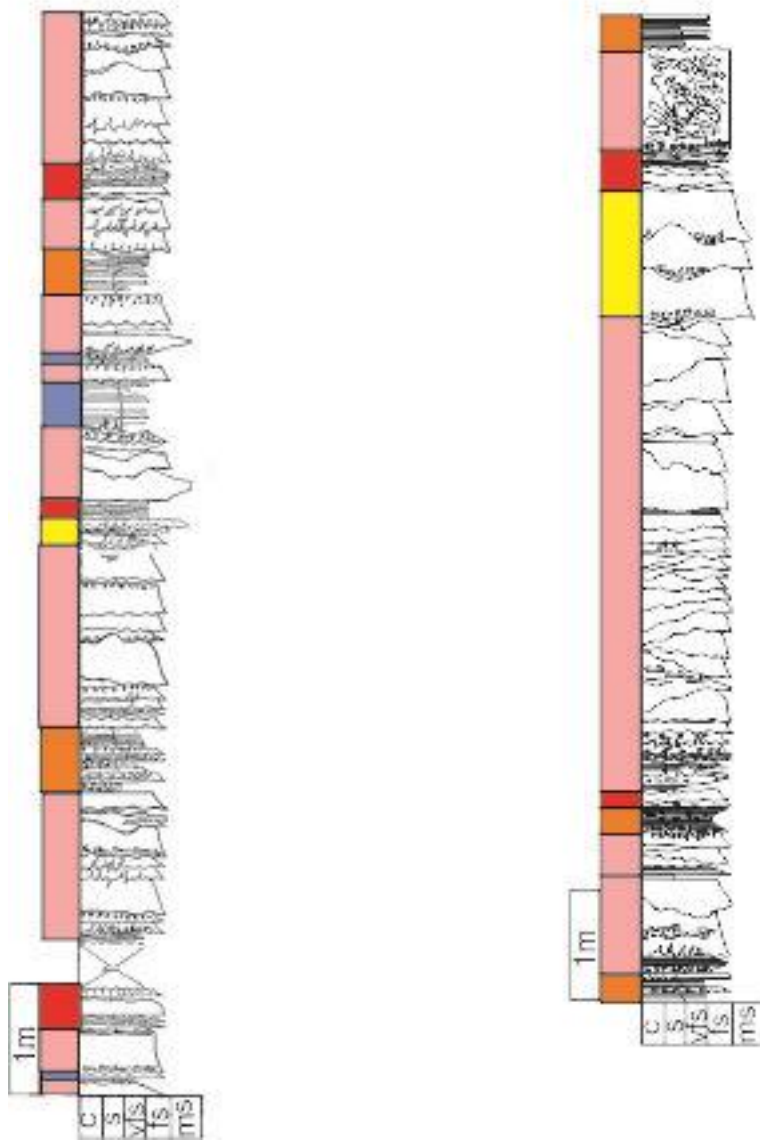


Figure 56: Presentation log of W14

# W14

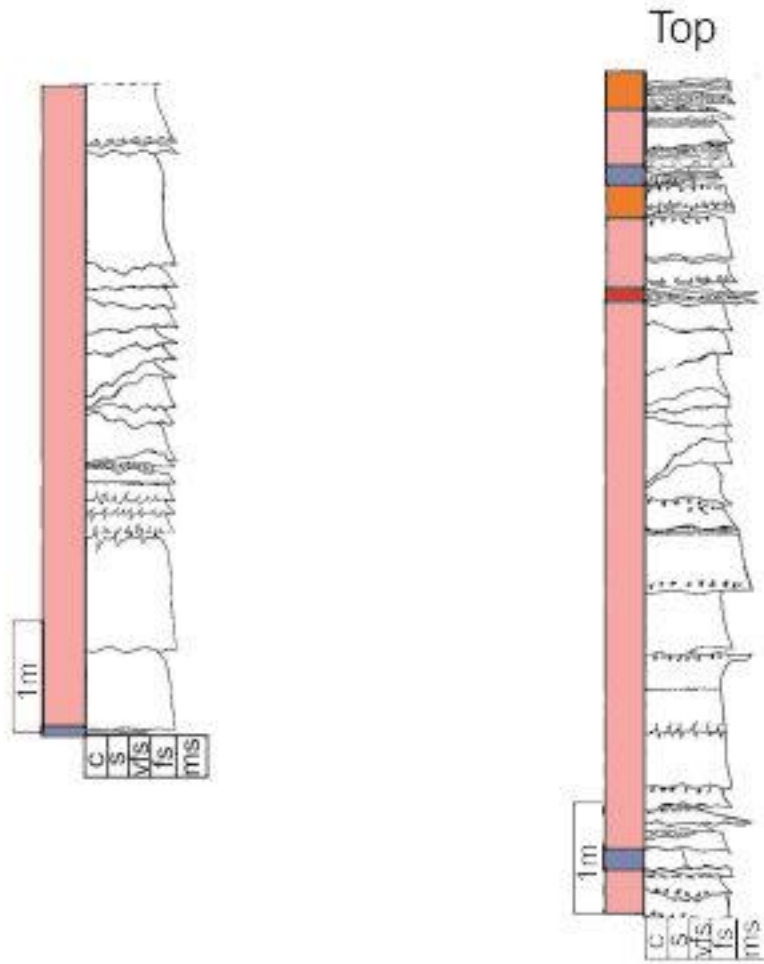


Figure 57: Presentation log of W15 and W16

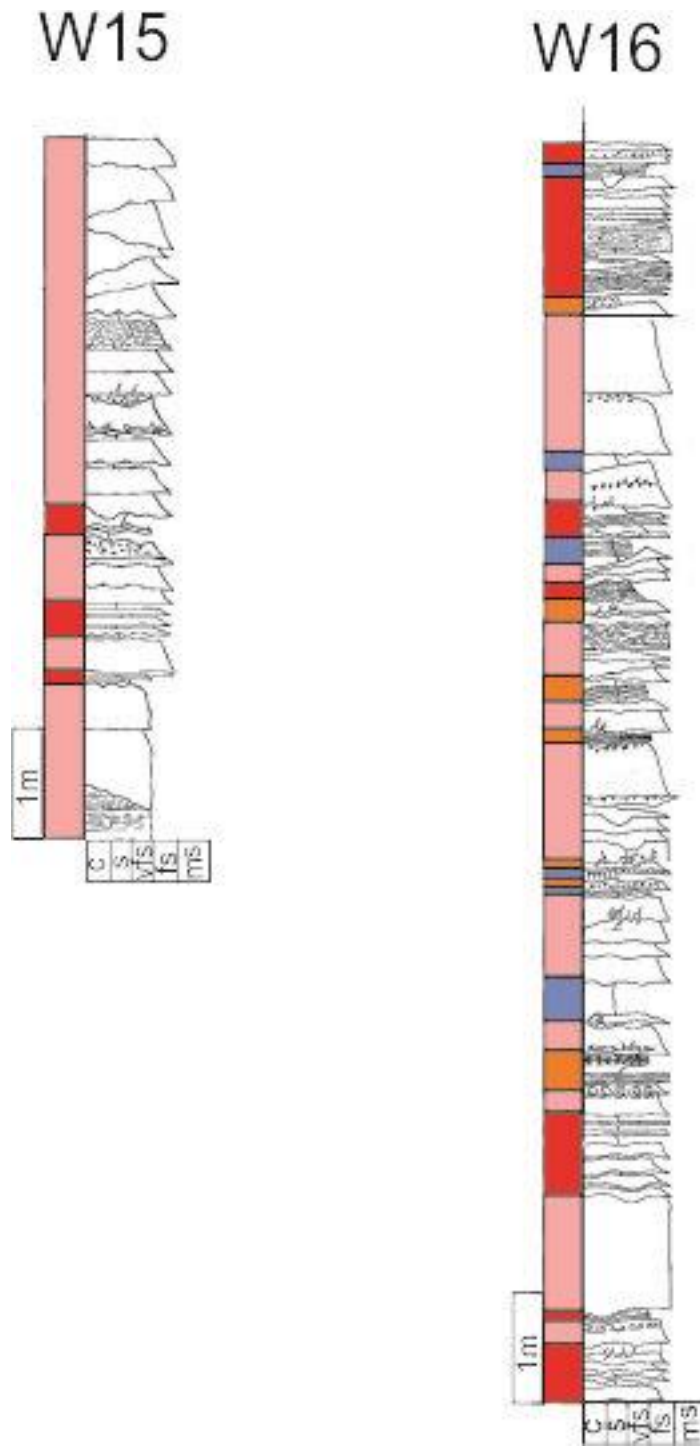


Figure 58: Presentation log of W17

# W17

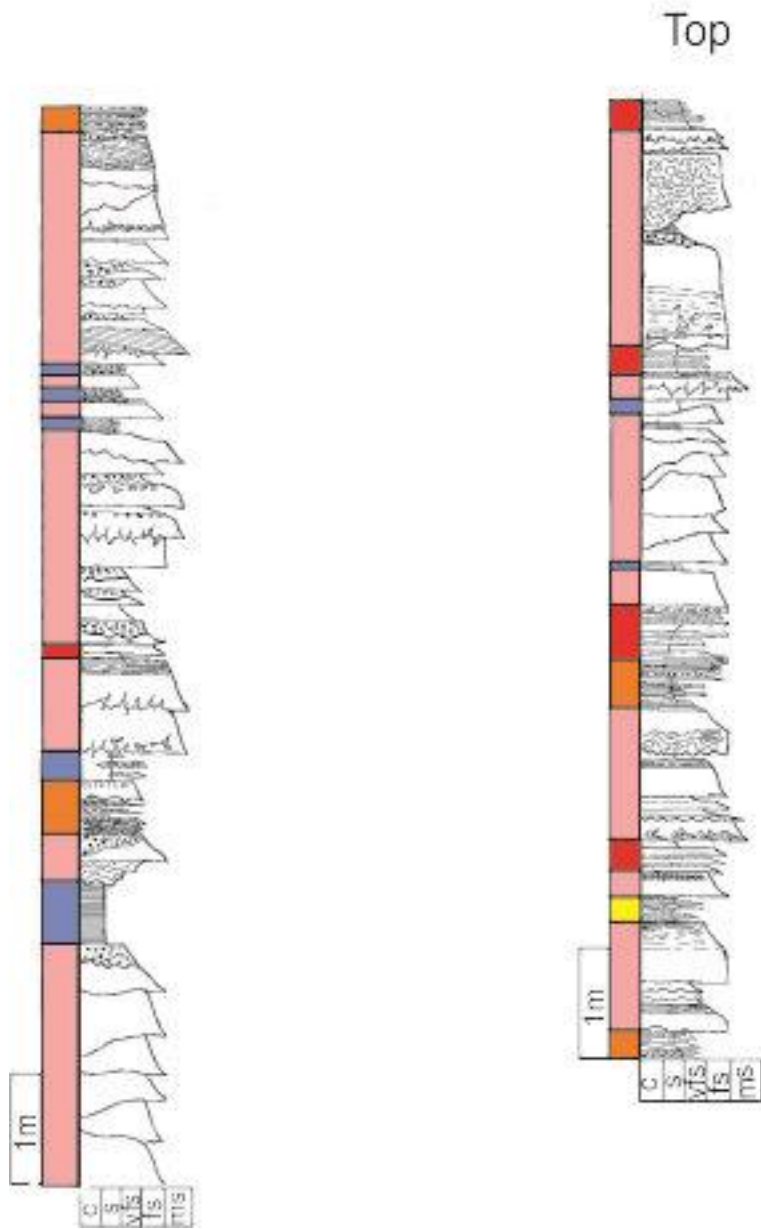


Figure 59: Presentation log of W18

# W18

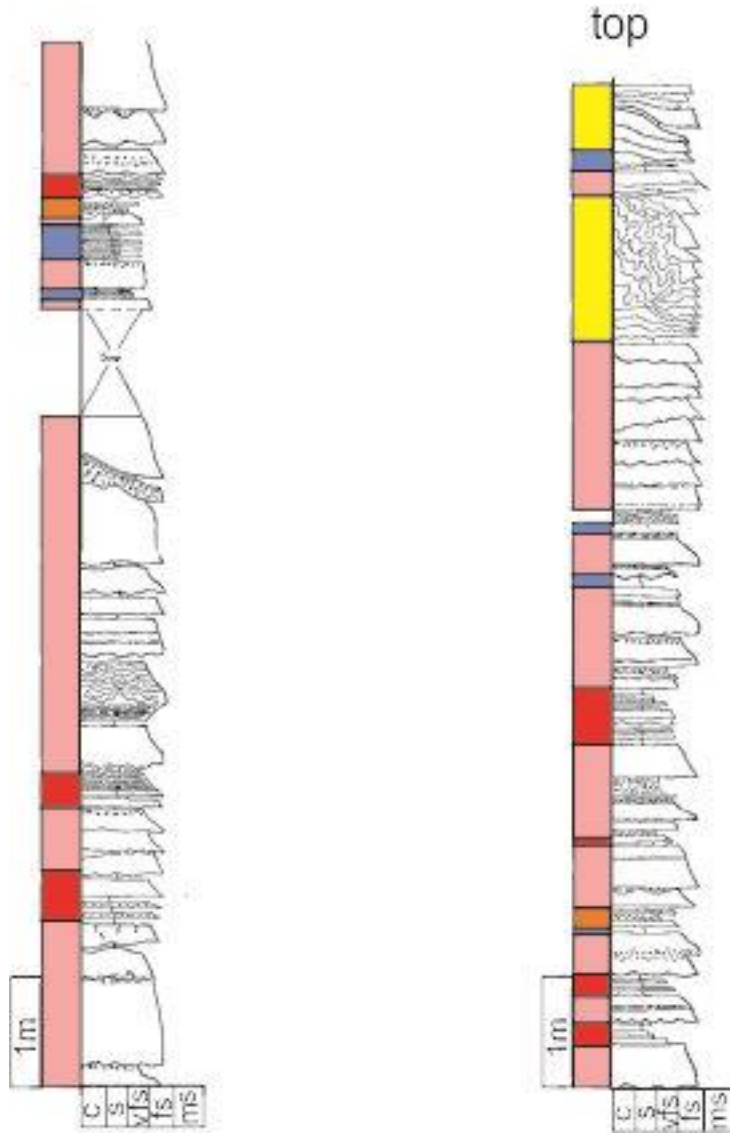
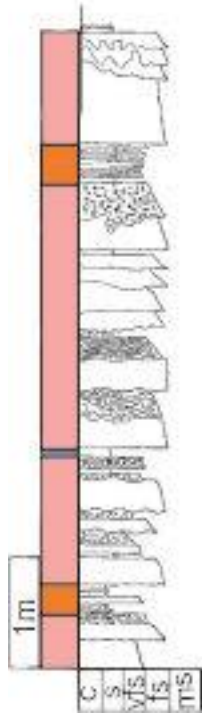


Figure 60: Presentation log of W19 and W20

**W19**



**W20**

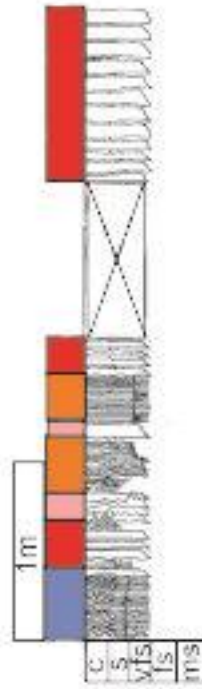
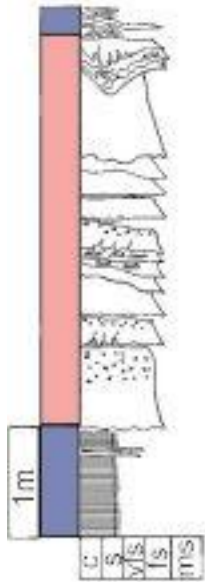
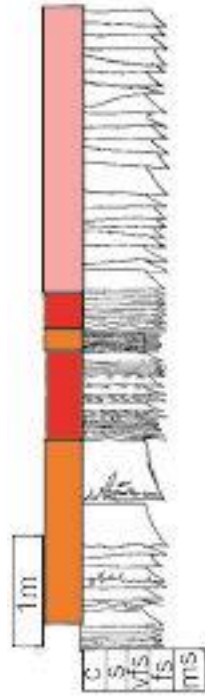


Figure 61: Presentation logs of W21 and W22

**W21**



**W22**

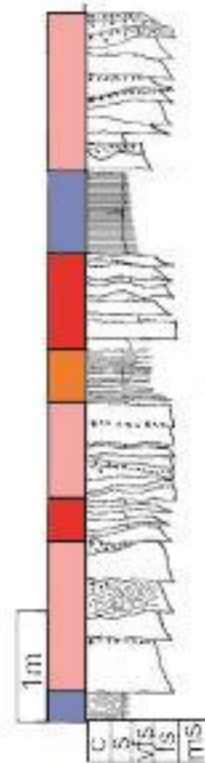
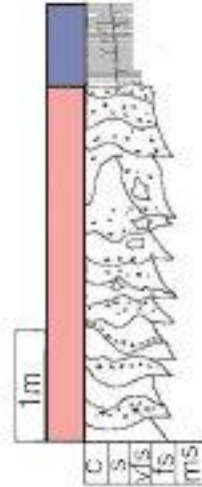


Figure 62: Correlation Panel of C14b

